

THE CATHOLIC UNIVERSITY OF AMERICA

Selective Regulation of Hepatic Protein Delivery:
Mechanisms and Binding Partners of MAL2

A DISSERTATION

Submitted to the Faculty of the

Department of Biology

School of Arts and Sciences

Of The Catholic University of America

In Partial Fulfillment of the Requirements

For the Degree

Doctor of Philosophy

By

Julie G. In

Washington, D.C.

2012

Selective Regulation of Hepatic Protein Delivery: Mechanisms and Binding Partners of MAL2

Julie G. In, Ph.D.

Director: Pamela L. Tuma, Ph.D.

Most classes of newly synthesized hepatic apical proteins take an indirect pathway to the cell surface. They are delivered from the TGN to the basolateral domain, selectively internalized then transcytosed to the apical surface. MAL2 has been implicated in regulating at least two steps in this pathway. MAL2 was first identified as a hepatic transcytotic regulator that mediates delivery from basolateral endosomes to the sub-apical compartment (SAC). However, overexpression of polymeric immunoglobulin A-receptor (pIgA-R) in polarized, hepatic WIF-B cells led to the dramatic redistribution of MAL2 into the Golgi and all the transcytotic intermediates occupied by the receptor. Although overexpressed hemagglutinin and dipeptidylpeptidase IV (DPPIV) distributed to the same compartments, MAL2 distributions did not change indicating the effect is selective. We found that DPPIV distributions were independent of MAL2, but surface delivery of pIgA-R was dependent on MAL2 expression. Thus, in addition to its role in transcytosis, MAL2 also regulates pIgA-R delivery from the Golgi to the basolateral membrane. Our studies have also shown that MAL2 and pIgA-R (but not DPP IV) selectively coimmunoprecipitate, but that their interactions are likely weak, transient, or indirect, suggesting other proteins are required to direct pIgA-R along its cellular itinerary. Because vesicle formation and delivery are driven by complex machineries, we predicted that MAL2 exists in large multi-protein complexes. To identify MAL2 interactors, we performed a split-ubiquitin yeast two hybrid screen using human MAL2 as bait. From a

human liver cDNA library, serine-threonine kinase 16 (STK16) was identified. This lipid-anchored kinase is enriched in liver and shown to regulate mammary gland development implicating it as a likely candidate for regulating polarized protein trafficking. While overexpression of STK16 did not disrupt normal trafficking processes, we found that expression of the mutant, kinase-dead form of STK16 (KD-STK16) rerouted the secretory proteins albumin and haptoglobin from the secretory pathway to the degradative lysosomal pathway. Knockdown of MAL2 caused the same defect, implicating the interaction of MAL2 and STK16 as regulators of the secretory pathway. Based on our previous research with MAL2, it is suggested that MAL2 is an essential component of multiple trafficking pathways in epithelial cells whose activity must be tightly controlled to ensure proper polarity maintenance and growth.


This dissertation by Julie G. In fulfills the dissertation requirement for the doctoral degree in the Department of Biology approved by Pamela L. Tuma, Ph.D., as Director, and by John E. Golin, Ph.D., and James M. Mullins, Ph.D. as Readers

A handwritten signature in cursive script, appearing to read 'Pamela L. Tuma', written over a horizontal line.

Pamela L. Tuma, Ph.D., Director

A handwritten signature in cursive script, appearing to read 'John E. Golin', written over a horizontal line.

John E. Golin, Ph.D., Reader

A handwritten signature in cursive script, appearing to read 'James M. Mullins', written over a horizontal line.

James M. Mullins, Ph.D., Reader

DEDICATION

I would like to dedicate this dissertation to...

....my family: dad, mom, and my immensely talented sister Joyce. Thank you for your support, your patience, and allowing me to cry when this just seemed too difficult. Your words of encouragement truly helped make this possible!

...my grandfather: Lee Min Mok. You have been my number one supporter since I was born and have always expressed how proud you are of me. Thank you for telling me to always persevere, just like your hero, General MacArthur!

TABLE OF CONTENTS

List of Illustrations	vi
List of Tables	viii
Abbreviations	ix
Acknowledgements	xiii
Introduction	
The liver	1
Epithelial polarity	6
Polarized trafficking	12
MARVEL domains	23
The MAL family	25
Implications of MAL and cancer	36
WIF-B cells: a model for polarized hepatic trafficking	38
Materials and Methods	
Reagents and antibodies	41
Preparation of antibodies to MAL2	42
Cell culture	43
Virus production and infection	43
Immunofluorescence microscopy and imaging	44
Antibody labeling of live cells	45
Recycling assays in Clone 9 cells	45
Immunoblotting	45
Immunoprecipitations	46
Surface biotinylation	46
Secretion assays in WIF-B cells	47
Differential centrifugation	47
Construction of bait yeast 2-hybrid (Y2H) plasmid	48
Split-ubiquitin Y2H screening	48
Part I: MAL2 selectively regulates polymeric IgA receptor delivery from the Golgi to the plasma membrane in WIF-B cells	50
MAL2 is an itinerant protein in WIF-B cells	51
MAL2 and overexpressed pIgA-R selectively colocalize and coimmunoprecipitate	55
MAL2 regulates delivery from the Golgi to the plasma membrane	62
Conclusions	74

Part II: Characterization of STK16, a novel MAL2 interactor, in WIF-B hepatic cells	75
A split-ubiquitin yeast 2-hybrid screen reveals 19 novel MAL2 interactors	77
MAL2 and STK16 selectively coimmunoprecipitate	82
KD-STK16 is present in an unidentified, post-Golgi compartment	87
STK16 is itinerant from the Golgi to the basolateral PM	89
KD-STK16 expression results in a decrease of albumin secretion	90
KD-STK16 expression results in albumin redirection to lysosomes	94
MAL2 regulates albumin secretion	97
Conclusions	100
Discussion	101
MAL2 and overexpressed pIgA-R selectively colocalize and coimmunoprecipitate	101
A new role for MAL2: selective regulation at the TGN	102
Novel MAL2 binding partners: a functional genomic approach	104
Serine/threonine kinase 16: a novel MAL2 interactor	106
A new role for MAL2: regulation of the secretory pathway	108
What is the basis of binding selectivity for MAL2?	110
MAL2: one protein, many functions	112
Possible mechanisms of MAL2-mediated sorting	113
Implications of MAL2 and cancer	115
References	116

LIST OF ILLUSTRATIONS

	Page Number
Figure 1	Hepatic plate of cells in the liver 6
Figure 2	Direct and indirect delivery of apical proteins 14
Figure 3	Sequence comparison of the MAL family members 26
Figure 4	Proposed sites for MAL2 function 33
Figure 5	WIF-B cells, our <i>in vitro</i> hepatic model 40
Figure 6	The peptide antibody specifically detects MAL2 52
Figure 7	Endogenous, untagged MAL2 is an itinerant protein, traversing the transcytotic pathway 55
Figure 8	MAL2 co-distributes with exogenously expressed pIgA-R, but not DPPIV 57
Figure 9	Immunoprecipitation controls 59
Figure 10	MAL2 and overexpressed pIgA-R are present in the biosynthetic pathway 61
Figure 11	Endogenous MAL2 is present in the “apical compartment” in nonpolarized WIF-B cells 63
Figure 12	In the absence of MAL2, DPPIV, but not pIgA-R, reaches the plasma membrane in Clone 9 cells 65
Figure 13	MAL2 expression in Clone 9 cells redistributes pIgA-R to the plasma membrane 67
Figure 14	MAL2 expression is required for pIgA-R delivery from the Golgi to the plasma membrane in Clone 9 cells 69
Figure 15	In WIF-B cells with MAL2 expression knocked down, pIgA-R, but not DPPIV, is present only in the Golgi 71
Figure 16	MAL2 knockdown in WIF-B cells inhibits basolateral delivery of pIgA-R, but not DPPIV, yet DPPIV transcytosis is impaired 73

Figure 17	Schematic of full-length STK16	81
Figure 18	MAL2 specifically immunoprecipitates STK16, but not KD-STK16	84
Figure 19	MAL2 minimally codistributes with STK16, but not KD-STK16	86
Figure 20	KD-STK16 is present in a post-Golgi compartment	90
Figure 21	Albumin and haptoglobin expression is decreased in KD-STK16 overexpressing cells	92
Figure 22	KD-STK16 expression results in decrease in albumin secretion	94
Figure 23	Albumin is rerouted to the lysosomes in KD-STK16 overexpressing cells	95
Figure 24	Lactacystin prevents KD-STK16 degradation, but promotes albumin degradation	97
Figure 25	MAL2 regulates albumin secretion	99
Figure 26	Our working model for MAL2-mediated protein sorting	113
Figure 27	Possible role of MAL2 in protein sorting	114

LIST OF TABLES

		Page Number
Table 1	Yeast 2-hybrid screens	78
Table 2	Novel MAL2 interactors	80
Table 3	Organelle markers for KD-STK16 colocalization	88

ABBREVIATIONS

5'NT	5'nucleotidase
ABC	ATP-binding cassette
AP2	adaptor protein 2
APN	aminopeptidase N
ARE	apical recycling endosome
ATP	adenosine triphosphate
BAPTA	1,2-bis(o-aminophenoxy)ethane-N,N,N',N'-tetraacetic acid
BC	bile canaliculus
BFA	brefeldin A
BL EE	basolateral early endosome
BSA	bovine serum albumin
CDC42	cell division control protein 42
CHX	Cycloheximide
CO-IP	co-immunoprecipitation
CUB	c-terminal ubiquitin
DMEM	Dulbecco's modified Eagle medium
DPPIV	dipeptidylpeptidase-IV
EDTA	ethylene diaminetetraacetic acid
EE	early endosome
EEA1	early endosomal antigen 1
EGTA	ethylene glycol tetraacetic acid
EMT	epithelial-mesenchymal transitions

ER	endoplasmic reticulum
ERGIC	ER-Golgi intermediate compartment
FBS	fetal bovine serum
GPI	glycophosphatidylinositol
GTP	guanosine triphosphate
HA	hemagglutinin
HNF	hepatocyte nuclear factors
HRP	horse radish peroxidase
IB	immunoblot
INF2	informin 2
JAM-A	junctional adhesion molecule-A
KD-STK16	kinase-dead serine/threonine kinase 16
LAC	lactacystin
Lat B	latrunculin B
LGP120	lysosomal glycoprotein 120
M6PR	mannose 6-phosphate receptor
MAL	myelin and lymphocyte protein
MAL2	myelin and lymphocyte protein 2
MANN II	mannosidase II
MARVEL	MAL and related proteins for vesicle trafficking and membrane link
m β CD	methyl-beta-cyclodextrin
MDCK	Madin-Darby canine kidney cells

MRP2	multidrug resistance protein 2
MUC1	mucin 1
NCBI	National Center for Biotechnology Information
NH ₄ Cl	ammonium chloride
NUB	n-terminal ubiquitin
Nz	nocodazole
PAGE	polyacrylamide gel electrophoresis
PAR-aPKC	partition defective - atypical protein kinase C
PBS	phosphate buffered saline
PBS-BT	PBS/BSA/Tween-20
PCR	polymerase chain reaction
PDZ	PSD95/Discs Large/ZO-1
PEM	Pipes/EGTA/MgSO ₄
PFA	paraformaldehyde
PM	plasma membrane
PMSF	phenylmethanesulfonylfluoride
pIgA-R	polymeric immunoglobulin A receptor
PKC	protein kinase C
PtdIns(4,5)P ₂	phosphatidylinositol-4,5-bisphosphate
PTEN	phosphatase and tensin
PVDF	polyvinylidene fluoride
RE	recycle endosome
SAC	subapical compartment

SDS	sodium dodecyl sulfate
SEM	standard error of the mean
STK16	serine/threonine kinase 16
TBS	tris buffered saline
TGN	<i>trans</i> -Golgi network
Tf-R	transferrin receptor
TJ	tight junction
TPD52	tumor protein D52
TX-100	Triton X-100
VSV-G	vesicular stomatitis virus glycoprotein G
WCE	whole cell extract
Y2H	yeast-2-hybrid
ZO-3	zona occludens-3

ACKNOWLEDGEMENTS

I am extremely grateful to...

...Dr. Pamela Tuma, my advisor. Thank you for constantly pushing me to work harder, think smarter, and not give up even after I make a million mistakes. Your discussions and advice have shaped me to become a better thinker, both scientifically and globally. I think it's fair to say that I owe you an ultimate pizza party!

...Dr. John Golin and Dr. J. Michael Mullins, my committee members. Thank you for your helpful discussions and taking the time out of your busy schedules to always be available.

...the friendly faces of all members of the Biology department; faculty, students and staff. To be on the safe side, I won't list everyone, that way I won't leave anyone out! The friendly hellos and the general collegiate atmosphere made this department a great place to come to everyday. I will greatly miss you all!

...last, but certainly not least, the Tuma Lab: Dr. Sai Prasad Ramnaryanan, Dr. Blythe Shepard, Dave Fernandez, Julia Omotade, Anneliese Striz, and Ben Kalu. We put the 'fun' in 'dysfunction.' Thank you all for being sounding boards for both scientific and personal problems. A successful experiment doesn't mean as much when you don't have anyone to share it with, and, thankfully, I was part of a lab that cheered you on and picked you up when things looked bad. You guys are awesome!

INTRODUCTION

The Liver

Understanding the mechanisms that regulate epithelial protein trafficking, specifically in hepatocytes, is the focus of our research. The organ of interest, the liver, will first be introduced. In this section, liver function will be briefly described. The different cell types which compose the sinusoidal component of the liver will be listed along with a brief synopsis of their respective functions. Finally, the functions and elegant architecture of the hepatocyte will be described in detail to provide context for the specific questions my research seeks to answer.

A. Functional properties

The liver is the largest internal and glandular organ of the body, developing around the portal vein, a major vein of the body. Due to this unique development, the adult liver maintains a close relationship with the blood. The venous blood from the portal vein converges in the liver, bringing nutrients and xenobiotics from a multitude of organs, namely the small intestine, pancreas, spleen and stomach (Alberts *et al*, 2002). The liver acts as a filtration unit, clearing out foreign particulates and toxins from the body. Additionally, it is the major metabolic center of the body, performing several fundamental and vital functions. In general, these functions include the metabolism and synthesis of various lipids, proteins and carbohydrates. The liver also directs secretory and excretory functions related to bile; namely, bile synthesis and secretion into the gut (Kuntz and Kuntz, 2008).

B. Cellular organization: sinusoidal cells

The intricate network of metabolic and biochemical functions in the liver is due to the unique structure and interactions of interconnected sheets of hepatocytes and sinusoidal cells (Alberts *et al.* 2002). The sinusoidal cells consist of four different mesenchymal cell types. They are the endothelial cells, Kupffer cells, Ito cells and pit cells. In total, they account for approximately 6% of total liver cell volume and 40% of cell number (Kuntz and Kuntz, 2008).

1. Endothelial cells

The endothelial cells form a continuous lining of the sinusoids (as depicted in Figure 1), yet also serve as regulators between the blood and hepatocytes. Additionally, the endothelial cells are essential for the correct balance of cholesterol, vitamin A and lipids in the liver. These tasks are accomplished by the fenestrae, or pores, interspersed among the cells. Taken from the Latin word for ‘windows’, the fenestrae allow for the exchange of molecules and metabolites between the blood and the hepatic cells through the space of Disse, or the perisinusoidal space (Fraser *et al.* 1995). The endothelial cells are often the initial targets of various hepatic stresses, such as toxins, hypoxia and alcohol. These stressors can damage or destroy the cells, resulting in the loss of the endothelium and unprotected or ‘naked’ hepatocytes (McCuskey, 2006; Kuntz and Kuntz, 2008).

2. Kupffer cells

Kupffer cells are macrophage-like stellate cells, so called due to their villiform (or fuzzy) surface and star-shaped structure. They are randomly distributed amongst the endothelial cells on the sinusoidal surface and constitute approximately 30% of the sinusoidal cells (Soto-Gutierrez *et al.* 2010). Primarily, Kupffer cells function in intravascular phagocytosis, clearing toxins and antigens from the blood. However, they also respond to cellular stresses and signals, resulting in the release of various cytokines, hepatic growth factors and eicosanoids (Gao *et al.* 2008; Kuntz and Kuntz, 2008).

3. Ito cells

Ito cells, also known as hepatic stellate cells, reside in the space of Disse and primarily function as storage units for fat droplets and retinol ester. Under healthy conditions, Ito cells constitute approximately 20% of the sinusoidal cells and are in a quiescent, inactive state (Soto-Gutierrez *et al.* 2010). However, upon liver injury or stress, they become activated and differentiate into myofibroblasts. This leads to enhanced secretion of collagen, laminin, desmin, fibronectin and loss of retinol esters. The secreted proteins accumulate and lead to fibrosis of the liver (Gao *et al.* 2008; Kuntz and Kuntz, 2008).

4. Pit cells

Pit cells, so called due to the presence of cytoplasmic granules that resemble pits in grapes, comprise approximately 1% of the sinusoidal cells. They are liver-specific natural killer cells. Like the well-characterized natural killer cells in the blood, pit cells

also function in spontaneous cytotoxic activity against a variety of tumors. They often adhere to the endothelial cells and have been shown to interact with Kupffer cells, possibly for differentiation and proliferation purposes (Luo *et al.* 2000; Braet *et al.* 2001).

C. Cellular organization: hepatocytes

The parenchymal cell of the liver, the hepatocyte, constitutes approximately 60% of total liver cells. These polygonal epithelial cells have six or more faces, dependent on each individual cells position relative to the overall structure. Overall, hepatocytes form single-cell anastomosing plates which extend from the portal vein to the central lobule, forming an extensive, three-dimensional structure (Parviz *et al.* 2003, Kuntz and Kuntz, 2008). As seen in Figure 1, the plate-like formation is arranged into interconnected and cord-like sheets which surround a system of bile caniliculi at one surface and sinusoids at a separate surface (Alberts *et al.*, 2002).

Hepatocytes have a unique architecture that is separate and distinct from other epithelial columnar cells. A functionally polarized hepatocyte consists of three plasma membrane domains: canalicular (apical), lateral and sinusoidal (basal), shown in Figure 1. The external area of hepatocytes comprises both the lateral and sinusoidal domains as continuous surfaces, thus combining the two into the basolateral surface. However, each domain has separate, unique functions. The lateral domain borders neighboring hepatocytes and acts as an intercellular crevice, separating the canalicular and sinusoidal domains. This is accomplished via the tight junctions, which seal off the lateral domain alongside the bile canaliculus to allow only the exchange of cations and water. Additionally, adherens and gap junctions are distributed along the lateral membrane,

promoting mechanical stability and communication between neighboring cells. (Kuntz and Kuntz, 2008; Soto-Gutierrez *et al.* 2010). The sinusoidal domain, as the name implies, faces into the sinusoids. This domain functions in both secretory and absorptive capacities with the blood. Its functions are increased exponentially by the numerous microvilli which extend from the surface into the space of Disse (Feracci *et al.* 1987).

The canalicular, or apical, domain forms the intricate bile canalicular network which transports bile and bile byproducts to the larger bile ducts. Many of the ATP-binding cassette (ABC) transporters function here, performing or assisting in the critical tasks of bile formation, detoxification, and bile or organic anion secretion (Kipp and Arias, 2002). The apical domain is characterized by the enrichment of cholesterol and glycosphingolipids, resulting in a thicker membrane bilayer (Zegers and Hoekstra, 1998). Few proteins reside in both the apical and basolateral domains. In general, each domain is characterized by specific subsets of proteins which function in either bile (canalicular) or blood (sinusoidal) –specific activities.

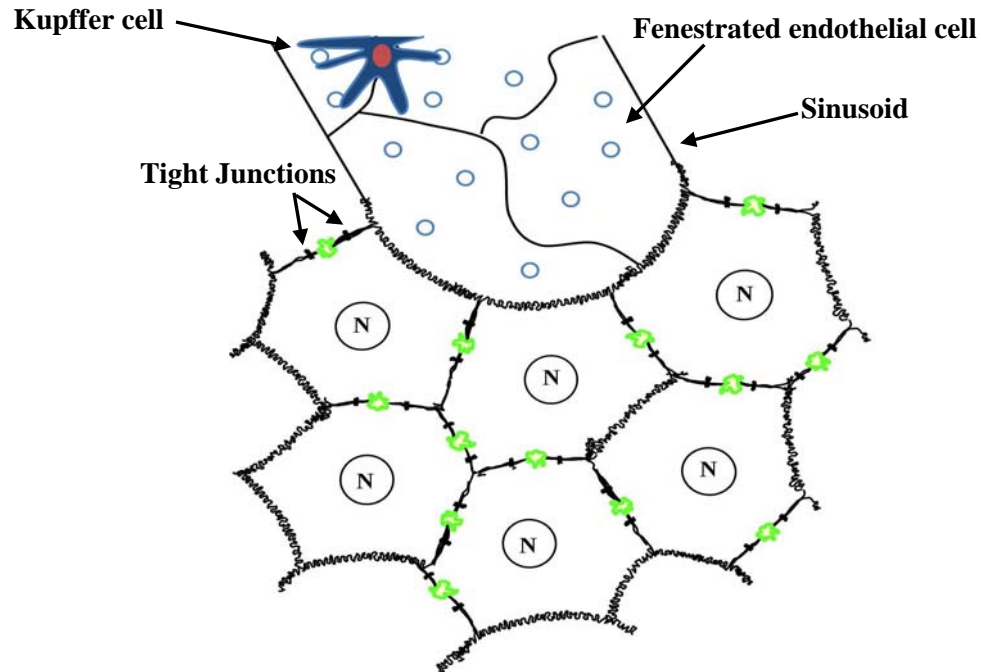


Figure 1. Hepatic plate of cells in the liver. Hepatocytes, the parenchymal liver cells, form interconnected plates surrounding bile canaliculi (BC) at the apical surface and the sinusoid at the basolateral surface. Note the presence of tight junctions which separate the apical and sinusoidal domains. Present within the sinusoid are fenestrated endothelial cells and macrophage-like Kupffer cells. The apical (BC) surface is depicted in green. N, nucleus.

Epithelial polarity

Hepatocytes form an elegant, polarized architecture upon full differentiation, with specific and separate functions at each polarized domain, as described above. However, it is important to consider the dynamic aspects of the domains. There is a continuous flux of proteins and membrane components actively moving between the domains (Braiterman and Hubbard, 2009). Therefore, a few questions remain: How do polarized cells maintain their polarity? What factor(s) determine or establish the polarized fate of hepatocytes?

A. Dynamic nature of polarity

The findings that endogenous membrane proteins specifically localized to distinct hepatic domains led to the hypothesis that there exists a distinct molecular correlation between the development of functional hepatic polarity and distribution (or trafficking) of membrane proteins (Bartles *et al.* 1985; Hubbard *et al.* 1985). Other results have expanded upon this hypothesis, showing that intact endosomal, recycling and transcytosis pathways are essential for proper development and maintenance of the polarized phenotype (Barr and Hubbard, 1993; Zegers and Hoekstra, 1998). In addition, epithelial cells often lose polarity or fail to gain polarity in disease states (known as epithelial-mesenchymal transitions, or EMT) and undergo structural reorganization as nonpolarized cells. This loss of polarity indicates the importance of dynamic membrane trafficking in the cell to maintain a polarized phenotype (Mellman and Nelson, 2008). While the confounding issue of epithelial polarity and trafficking has been extensively studied in simple epithelial cell types, such as kidney and intestinal cells; it still remains largely a mystery in hepatic cells. Therefore, the known complexes and proteins which direct simple epithelial polarity will be introduced to provide a better understanding of the many similarities and differences regulating hepatic polarity.

B. Molecular players in establishing polarity: simple epithelial cells

The currently accepted model for the development and maintenance of polarity involves a number of interdependent processes: 1) organization of the cytoskeleton, 2) spatial recognition and communication with neighboring cells and the extracellular environment, 3) asymmetric organization of the polarity complexes and 4) organized

membrane traffic (Bryant and Mostov, 2008; Braiterman and Hubbard, 2009). The chronological or sequential relationship among these processes during early development is still unknown. Extracellular cues and communication between neighboring cells via adherens and tight junctions have been shown to play essential roles in the development and maintenance of polarity. However, as more junction proteins are discovered and studied *in vitro* and *in vivo*, their exact role in polarity has become exceedingly complex. The absence of some junction proteins, such as β -catenin, claudin-1 and junctional adhesion molecule-A (JAM-A), leads to the loss of polarity. However, the absence of others, such as e-cadherin, occludin and zona occludens-3 (ZO-3), does not change polarity or alter the junctional complexes (Braiterman and Hubbard, 2009). The most surprising of these results was that for e-cadherin, which was previously described as the most important junctional protein for developing and maintaining cell-cell adhesion and polarization (Balkovetz *et al.* 1997; Nejsum and Nelson, 2007; Mellman and Nelson, 2008). While this finding was initially puzzling, it also supports the hypothesis that apico-basal polarity is governed by an ensemble cast, rather than soloists (Bryant and Mostov, 2008).

1. The PAR-aPKC complex

The emerging key players in establishing epithelial polarity are three groups of membrane-associated proteins known collectively as polarity complexes. They are segregated as: 1) PAR-aPKC (partition defective - atypical protein kinase C) complex, 2) Scribble/Discs Large/Lethal Giant Larvae complex and 3) Crumbs/Stardust/Discs Lost complex (Zegers *et al.* 2003; Braiterman and Hubbard, 2009). Please refer to these

excellent in-depth reviews for detailed descriptions of these complexes (Bryant and Mostov, 2008; Mellman and Nelson, 2008; van der Wouden *et al.* 2003; Braiterman and Hubbard, 2009) which are only briefly summarized below.

The PAR-aPKC complex is primarily composed of PAR3, PAR6, aPKC and cell division control protein 42 (Cdc42), a rho family GTPase. PAR3 and aPKC localize together to the tight junctions and recruits the lipid, phosphatase and tensin (PTEN). The recruitment of PTEN results in the enrichment of phosphatidylinositol-4,5-bisphosphate (PtdIns(4,5)P₂) at the apical domain (Martin-Belmonte *et al.* 2007; Martin-Belmonte and Mostov, 2008). This enrichment at the apical membrane results in the recruitment of Cdc42, PAR6 and aPKC (Bryant and Mostov, 2008; Mellman and Nelson, 2008). The full complex at the apical domain acts as a scaffold for proteins directly involved in both endocytosis and exocytosis. It is possible that through regulated membrane trafficking, the PAR complex efficiently generates apical polarity (Bryant *et al.* 2010; Golachowska *et al.* 2010; Shivas *et al.* 2010).

2. *The Crumbs complex*

Although described individually, the PAR complex functionally interacts with both the Scribble and Crumbs complexes. The Crumbs (Crumbs/Stardust/Discs Lost) and PAR complexes mutually regulate each other in a temporal manner. The PAR complex is needed to initially stabilize the Crumbs complex at the apical domain, where it then functions in maintaining apical polarity. The mechanism behind this maintenance is unknown, but it is thought that the Crumbs complex acts as a scaffold, recruiting other proteins via the PDZ (PSD95/Discs Large/ZO-1) domain. Later in development, the

Crumbs complex is needed to stabilize the PAR complex at tight junctions and the apical domain.

3. The Scribble complex

The Scribble complex (Scribble/Discs Large/Lethal Giant Larvae) localizes to the basolateral domain and is negatively regulated by the PAR complex. aPKC phosphorylates Lethal Giant Larvae, inhibiting it from localizing to the apical domain. The Scribble complex functions in maintaining basolateral polarity, though, like the Crumbs complex, the mechanism is unknown. Loss of any component of either the Scribble or Crumbs complex results in a loss of epithelial polarity (van der Wouden *et al.* 2003; Mellman and Nelson, 2008; Braiterman and Hubbard, 2009).

4. Polarity complexes and actin: a puzzle

Interestingly, multiple components of all three polarity complexes have been shown to interact functionally with the actin cytoskeleton. Disorganization of the actin cytoskeleton by latrunculin B results in displacement of the polarity complexes or a complete loss of polarity and misorientation of protein sorting (Stauffer *et al.* 1998; Low *et al.* 2000; van der Wouden *et al.* 2003; Mellman and Nelson, 2008). The exact role of the actin cytoskeleton in developing or maintaining polarity is unclear, however, it is possible that the actin meshwork acts as mechanical support for the polarity complexes.

C. Molecular players in polarity: hepatocytes

The described polarity complexes are not well understood in hepatocytes. Although some components of the complexes have been found to be expressed in

hepatocytes and hepatic-derived cell lines, their overall functional importance is unknown. For example, JAM-A binds PAR3 (of the PAR-aPKC complex) and anchors it at the tight junctions, abutting the apical domain. Scribble, on the other hand, has been shown to localize specifically and beautifully at the basolateral domain of hepatocytes (Braiterman and Hubbard, 2009). Considering the recent developments regarding the importance of the polarity complexes in kidney and intestinal cells (as described above), it is essential that further investigation of their role in hepatic polarity is needed. So then, what factors are known in controlling hepatic polarity?

Although a broad number of proteins and transcription factors have been implicated as playing a role in polarity, the effects are likely not direct. The best characterized are the hepatocyte nuclear factors (HNF). This family of transcription factors controls the gene expression of a number of hepatic-specific genes. Some members of the HNF family, such as HNF3 α , β and γ , do not affect hepatocyte development and polarization, but influence other epithelial cells (such as β -islet pancreatic cells). Others, such as HNF1 α and β , may regulate hepatic tubular formation, but the exact role and importance is not yet known (Tanimizu *et al.* 2009). However, HNF4 α has been shown to be essential for the development of hepatic polarity, both functionally and morphologically (Parviz *et al.* 2003; Duncan, 2003). Indeed, the over-expression of HNF4 α induced a cultured fibroblast cell line to differentiate to polarized cells, an embryonic carcinoma cell line to form functional junctional complexes, and most strikingly, an hepatocellular carcinoma to re-polarize, or make a mesenchymal-epithelial transition (Parviz *et al.* 2003; Lazarevich *et al.* 2004; Satohisa *et al.* 2005;

Braiterman and Hubbard, 2009). The transcriptional targets of HNF4 α and its probable relationship with the junctional complexes in hepatocytes is an area for further research.

Epithelial, particularly hepatic, polarity cannot be fully appreciated without understanding the elegant dynamics of polarized trafficking. As stated above, early work on localization of hepatic proteins established the hypothesis that cellular polarity and polarized trafficking are not sequential events, but rather, are occurring concurrently and are dependent on one other (Bartles *et al.* 1985; Hubbard *et al.* 1985). Therefore, to appreciate the intricacies of epithelial polarity, one must first understand polarized trafficking.

Polarized trafficking

Each cell surface domain is characterized by specific membrane components and functions. At the apical domain, functions include: transport of bile acids and bile components, transport of detoxification products and delivery of secretory immunoglobulin A for mucosal immunity. In contrast, functions at the basolateral domain include: transport and internalization of macromolecules to and from the blood, and secretion of blood proteins. To maintain the separate functions of the different domains, it is essential to maintain proper polarity. Thus, how do epithelial cells maintain their polarized phenotype such that their domain-specific activities are also maintained? We believe the answer to this question lies in understanding the mechanisms that regulate the delivery of newly synthesized proteins to the correct membrane domain. In epithelial cells, two major pathways to the apical surface have been identified: the direct route and

the indirect or transcytotic route (Carmosino *et al.* 2010a). In this section I will describe the trafficking compartments of each trafficking pathway, basolateral targeting and its known signals, apical targeting and its known signals and the transcytotic pathway.

A. Trafficking pathways: a review

As recently as 1990, it was thought that newly synthesized apical proteins were sorted at the TGN in MDCK cells (Madin Darby canine kidney cells, representing simple epithelial cells) and in the transcytotic intermediaries in hepatic cells. Delivery of all basolateral proteins was thought to be the ‘default’ pathway (Simons and Wandinger-Ness, 1990). However, in the past 20 years, our understanding of polarized trafficking has significantly increased. The apical and basolateral trafficking pathways are more complex than originally thought. Simple epithelial cells generally use the direct pathway to deliver both apical and basolateral proteins. The different subsets of proteins are directly delivered from the TGN to their respective destinations; the apical or basolateral surface. Hepatic cells use both the direct and indirect pathways (depicted in Figure 2). Basolateral proteins are directly trafficked from the TGN to the basolateral, but most apical proteins take a circuitous or transcytotic route to the canicular membrane. They are delivered to the basolateral surface, selectively endocytosed to the basolateral early endosome then transcytosed across the cell to the sub-apical compartment before delivery to their final destination, the apical surface.

Despite these generalizations, the polymeric immunoglobulin A receptor (pIgA-R) takes the indirect pathway in all epithelial cells and examination of its itinerary has led

to increased understanding of the transcytotic pathway (Tuma and Hubbard, 2003).

Also, the canalicular ABC transporters are directly delivered from the TGN to the apical membrane (Kipp and Arias, 2002). Given all these protein trafficking itineraries, how are proteins sorted to their respective polarized domains? What factor(s) determine which pathway they take? These questions are the fundamental basis of my research interests.

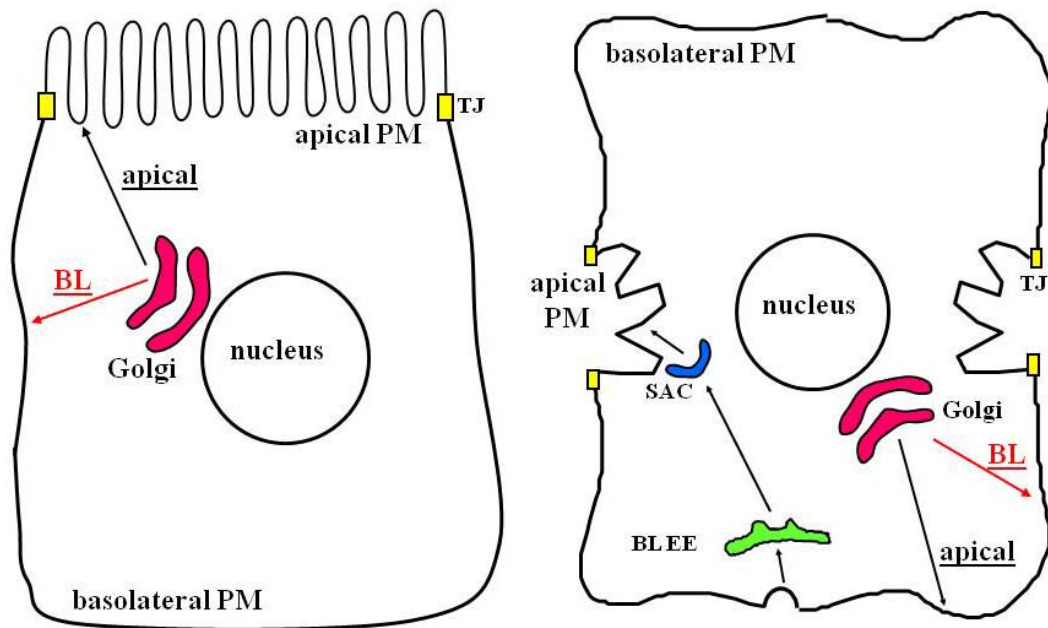


Figure 2. Direct and indirect delivery of apical proteins. Simple epithelial cells, such as intestinal and kidney cells, use the direct pathway for delivery of both apical (black arrow) and basolateral (red arrow) proteins (left panel). Hepatocytes use the direct pathway for delivery of basolateral proteins (red arrow), but the indirect pathway for delivery of most apical proteins (black arrow) (right panel). BL, basolateral; BL EE, basolateral early endosomes; SAC, sub-apical compartment; TJ, tight junction.

B. Trafficking compartments

All newly synthesized membrane proteins, regardless of pathway, begin their synthesis and trafficking in the endoplasmic reticulum (ER) and their sorting at the TGN. Intermediate endosomes, such as the basolateral early endosome, apical early endosome,

apical recycling endosome and common endosome, have been seen and described as intermediate stops for some proteins prior to direct delivery to the basolateral surface in simple epithelial cells (Ang *et al.* 2004; Cancino *et al.* 2007). Though it is clear that these intermediate compartments exist, the trafficking studies describing these compartments used vesicular stomatitis virus glycoprotein G (VSV-G), an exogenous viral protein.

Hepatic apical residents using the indirect pathway traverse at least two known intermediates en route to the apical domain: the basolateral early endosomes and the subapical compartment (SAC) (Barr *et al.* 1995; Ihrke *et al.* 1998) (Figure 2). The basolateral early endosome is the entry point for basolaterally internalized molecules and serves as a major sorting station into at least four other pathways: recycling, endocytic targeting to lysosomes, transport to recycling endosomes and transcytosis. In contrast, the SAC has the unique distinction of being a “one-way” sorting station to the apical surface. It was first identified in rat hepatocytes and was found to contain only newly synthesized apical proteins en route to the apical surface; no recycling populations were present (Barr *et al.* 1993, 1995). These results were confirmed in WIF-B cells (Ihrke *et al.* 1993) and extended in studies examining apical endocytosis of resident proteins (Tuma *et al.* 1999).

C. Basolateral targeting and signals

Basolateral targeting in both simple epithelial and hepatic cells has traditionally been described as direct delivery from the TGN to the basolateral surface. The conventional signals encoding basolateral targeting are tyrosine (Y) and di-leucine (LL) based motifs located in cytoplasmic regions of proteins. Specifically, the motifs are:

YxxΦ (x = any amino acid, Φ = bulky hydrophobic residue), NPxY and DExxxLLI (Gonzalez and Rodriguez-Boulán, 2009; Carmosino *et al.* 2010a). There are other unconventional motifs, such as a single leucine adjacent to acidic patches (as seen with CD147) and completely unique motifs that do not resemble any known basolateral sorting signal (as seen with pIgA-R, gp80 and transferrin receptor, Tf-R).

The Y- and LL-based sorting signals have been well-characterized as recognition sites for binding to clathrin adaptor proteins. However, these analyses described endocytic sorting, or internalization from the basolateral surface. Although the basolateral sorting signals and endocytic signals are markedly similar, mutational analyses have shown that they are independent of one another (Aroeti *et al.* 1993; Gonzalez and Rodriguez-Boulán, 2009). It is only recently that *direct* evidence of clathrin-dependent sorting from the TGN to the basolateral surface has been shown (Deborde *et al.* 2008).

D. Transcytosis

Because hepatocytes rely more heavily on the transcytotic pathway, more work has been done in hepatic systems to examine this pathway. However, it is a universal mechanism of apical delivery used by all polarized epithelial cells.

1. pIgA-R: a model for transcytosis

The best characterized model for transcytotic delivery in epithelial cells is pIgA-R (Apodaca *et al.* 1991). It follows nearly the same pathway in the varied polarized epithelial cell types studied (Tuma and Hubbard, 2003). It is first targeted to the basolateral surface from the TGN where it binds circulating polymeric immunoglobulin

A (pIgA). Although pIgA-R can transcytose without binding pIgA, the ligand binding increases both the efficiency and rate of transcytosis. Ligand binding stimulates protein kinase C (PKC) and increases the concentration of intracellular calcium (Ca^{2+}) (Cardone *et al.* 1996). Correlating with the increase in Ca^{2+} seen upon stimulation of transcytosis, interplay between calmodulin and PKC is also essential in regulating transcytosis of pIgA-R (Apodaca *et al.* 1994; Enrich *et al.* 1996; Tyteca *et al.* 2005). The intricate steps involved in this mechanism are not yet understood.

After delivery to the basolateral, phosphorylation of pIgA-R and its downstream targets is required for efficient transcytosis. This is mediated by a protein tyrosine kinase of the Src family, p62Yes (Casanova *et al.* 1990; Luton *et al.* 1998; Luton *et al.* 1999). Upon stimulation, pIgA-R transcytoses through several compartments prior to reaching the apical surface. In MDCK cells, it is internalized from the basolateral to the BEE, delivered to a common endosome, then the apical recycling endosome (ARE) before delivery to the apical surface (Song *et al.* 1994; Tuma and Hubbard, 2003). In hepatocytes, pIgA-R is internalized at the basolateral and sent to the basolateral early endosomes (BL EE), but makes one stop at the subapical compartment (SAC). This compartment is functionally and physiologically distinct from the ARE of MDCK cells. It lacks recycling apical membrane proteins, indicating it is a one-way compartment to the apical surface (Ihrke *et al.* 1998; Hoekstra *et al.* 2004).

E. Apical targeting and signals

Apical sorting and delivery of newly synthesized proteins is less well understood than basolateral sorting. As described above, apical proteins can be delivered directly

from the TGN to the apical PM (simple epithelial cells, canilicular ABC-transporters) and indirectly via the transcytotic pathway (hepatic apical proteins, pIgA-R). What confers trafficking specificity for apical protein delivery? A number of hypotheses have emerged to answer this fundamental question: **1)** coalescence into lipid rafts (Weimbs *et al.* 1997; Ikonen and Simons, 1998), **2)** N- or O-linked glycosylation of the cargo protein (Rodriguez-Boulau and Gonzalez, 1999), **3)** cytoplasmic or transmembrane motifs which act as sorting signals (Luton *et al.* 2009; Carmosino *et al.* 2010b). Most likely, it is a combination of these which confers specific sorting.

The numerous postulated sorting signals implies that there are either a variety of distinct carriers or several export pathways from the TGN. Thus far, this theory has been tested by comparing the export of raft-associated and raft-independent cargo. Export of the two types of cargo showed differential regulation (Jacob and Naim, 2001; Guerriero *et al.* 2008), possibly due to selective sorting from a separate regulator (In and Tuma, 2010). Although most apical proteins in hepatocytes undertake the same general route through the biosynthetic and transcytotic pathways; it is our hypothesis that specific regulators or post-translational modifications determine selective separation of the proteins into different transport carriers at the TGN and/or at the basolateral early BL EE in the transcytotic pathway.

1. Lipid rafts and GPI-anchors

The first established apical sorting signal was the GPI (glycophosphatidylinositol)-anchor (Brown *et al.* 1989; Lisanti *et al.* 1989). It has been shown (in various cell types) that GPI-anchored proteins are resistant to detergent extraction, indicating their presence

in lipid rafts or cholesterol-rich microdomains (Simons and Ikonen, 1997; Ikonen and Simons, 1998). Since the apical surface is enriched in glycosphingolipids and cholesterol, the “raft hypothesis” for apical targeting emerged.

According to the original “raft hypothesis” for apical protein sorting, glycosphingolipid and cholesterol-enriched membrane domains form in the biosynthetic pathway where they recruit apically-destined proteins (mainly GPI-anchored) due to their biophysical properties (Simons and Ikonen, 1997). The lipids rafts and their cargo are packaged into vesicles and delivered directly to the glycosphingolipid and cholesterol-rich apical surface.

However, the targeting role of the GPI-anchor may be much more complicated than originally thought. For example, although in MDCK cells, GPI-anchored proteins directly traffic to the apical domain (Hua *et al.* 2006; Paladino *et al.* 2006); in Fisher rat thyroid cells, endogenous GPI-anchored proteins traffic to the basolateral surface. Addition of a GPI-anchor onto a soluble protein does not change its targeting to the apical domain (Carmosino *et al.* 2010). Since GPI-anchors alone are not sufficient to direct apical trafficking, it is possible that they are needed to cluster other GPI-anchored proteins, initiating an ‘apical sorting platform’ which partitions the membrane into lipid rafts (Paladino *et al.* 2004). This is consistent with the updated “raft hypothesis.” The lipid raft domains may be too small or transient to mediate sorting, thus other proteins have been implicated to regulate lipid domain coalescence and stabilization (Paladino *et al.* 2004; Rodriguez-Boulan *et al.* 2005). Furthermore, in hepatic cells where all apical

proteins are delivered to the basolateral surface first, raft sorting has been found to occur in the BEE (Nyasae *et al.* 2003).

Interestingly, apical delivery of all cohorts of proteins is dependent on cholesterol and glycosphinglipids (Nyasae *et al.* 2003; Leyt *et al.* 2007). While this result lends credence to the lipid raft hypothesis, it was surprising in that not all apically targeted proteins are in lipid raft domains. A likely scenario is that there is a general regulator of apical delivery whose activity is cholesterol and glycosphingolipid dependent (described below).

2. *Post-translational glycosylation*

Glycosylation, an extracellular protein modification, has been shown to preferentially direct apical sorting of both soluble and membrane proteins. The two types of glycosylation (N- and O-) act as apical targeting signals in an unknown manner. O-linked glycosylation occurs in the Golgi complex with the addition of N-acetylgalactosamine (GalNAc) to serine or threonine (S/T) residues on the protein (Potter *et al.* 2006). Two heavily O-glycosylated proteins, p75NTR (neurotrophin receptor p75) and hydrolase SI (sucrose isomaltase), which typically localize to the apical domain in MDCK and Caco-2 cells (polarized intestinal cells), were mislocalized to both surface domains when O-glycosylation sites were deleted (Delacour and Jacob, 2006). In addition, the trafficking of apically-localized proteins DPPIV (dipeptidylpeptidase-IV), MUC1 (mucin 1) and CEA (carcinoembryonic early antigen) is disrupted when treated with O-glycosylation inhibitory reagents. The proteins accumulated intracellularly in

MDCK and Caco-2 cells, notably due to their inability to associate with lipid rafts (Delacour and Jacob, 2006).

For N-linked glycosylation, the core glycan structure is transferred *en bloc* to a specific consensus site, Asn-X-Ser/Thr (with X as any amino acid except proline), during cotranslational translocation of proteins into the endoplasmic reticulum (Potter *et al.* 2006). Studies performed in MDCK and LLC-PK1 cells found that mutagenic removal of N-glycosylation sites from H⁺/K⁺-ATPase, BSEP (bile salt export pump), erythropoietin, GLYT2 (glycine transporter 2) and endolyn resulted in loss of apical targeting. Interestingly, terminal glycosylation, not core glycosylation, is postulated to be the essential determinant for N-glycosylation mediated apical sorting (Potter *et al.* 2004; Vagin *et al.* 2009; Carmosino *et al.* 2010).

Recent studies hypothesize that there is a strong dependence on lectins, specifically of the galectin family, to cluster apical cargo for delivery. Galectin-4 has a high affinity interaction with specific glycosphingolipids, which are enriched in lipid rafts. Knockdown of galectin-4 resulted in loss of raft formation and impaired apical trafficking (Delacour *et al.* 2005). It is possible that association with galectin-4 clusters the apical cargo into lipid rafts, allowing them to be apically delivered via rafts. In contrast, galectin-3 directly interacts with selected apical cargo and transports them to the apical domain in a raft-independent manner in MDCK cells (Delacour *et al.* 2007). It remains to be determined whether the function of the glycans is to stabilize the proteins at the apical domain, incorporate the protein into lipid raft domains or whether they are directly involved in apical targeting.

3. *Cytoplasmic and transmembrane sorting motifs*

Another group of apical sorting signals lies within specific motifs in cytoplasmic or transmembrane domains. These signals can range from a few amino acids to 30 residue stretches (Rodriguez-Boulan and Gonzalez, 1999; Nelson and Yeaman, 2001; Mostov *et al.* 2003). Thus far, apical sorting signals of varied composition have been found in the cytosolic tails of ATP7B copper-ATPase, megalin, M2 muscarinic receptors, pIgA-R, receptor guanylyl cyclases and rhodopsin (Delacour and Jacob, 2006; Luton *et al.* 2009; Carmosino *et al.* 2010) and in the transmembrane regions of neuraminidase (NA) and hemagglutinin (HA) (Delacour and Jacob 2006).

The commonality among these sorting signals is the conformational determinants. It has been suggested that the amino acid stretches are essential to induce conformational sorting motifs that allow for incorporation into lipid raft domains or interactions with regulatory proteins (Carmosino *et al.* 2010). Interestingly, the short amino acid motif in the cytosolic tail of pIgA-R only directed basolateral to apical transcytosis; deletion of the motif did not affect biosynthetic delivery from the TGN to the basolateral in MDCK cells (Luton *et al.* 2009). Since there is still a significant number of apically-directed proteins with unknown sorting information, an interesting route of research would be to look at the levels of protein structure (primary, secondary, tertiary and quaternary) for signal variants.

While lacking in direct evidence, there may be a role for PDZ-domain containing proteins in apical localization of interacting partners. The CFTR and Na⁺/H⁺ exchanger proteins preferentially interact with and require the protein NHERF-1 (Na⁺/H⁺-exchanger

regulatory factor 1) to maintain apical localization via their PDZ domains (Carmosino *et al.* 2010). The apical conjugate efflux pump, MRP2 (multidrug resistance protein 2) also has a PDZ-domain located proximal to its C-termini. While MRP2 does bind to other PDZ-domain containing proteins, deletion studies have found that it does not rely solely on this motif for its apical localization (Nies and Keppler, 2007). Rather, it is likely the combination of the PDZ domain as well as other structural motifs that dictate its proper apical localization. Thus, it is not clear whether the PDZ domain influences apical sorting at the biosynthetic pathway or if it stabilizes apical localization after the proteins have already been delivered.

MARVEL domains

The focal point of my research has been the role of MAL2 in regulating apical protein delivery. MAL2 belongs to a family of proteins (known as the MAL family, described below) which belong to a larger family of MARVEL domain containing proteins. This domain was named after MAL and related proteins for vesicle trafficking and membrane link (Sanchez-Pulido *et al.* 2002). All proteins with MARVEL domains have an M-shaped architecture consisting of four transmembrane helices with cytosolic N- and C- terminal tails. The shared MARVEL domain is located in the transmembrane regions with a conserved acidic residue at the start of the third transmembrane domain (Figure 3). This domain does not have a strict consensus sequence, but is characterized by a statistically significant similarity in the sequences of several distinct families of proteins.

Protein families which share the MARVEL domain include (but are not limited to): MAL, physin, gylin, chemokine-like factor superfamily and occludin. Based on the functional analyses of the known members of these families, it is suggested that MARVEL-domain proteins are essential for membrane apposition events, including membrane fusion (Marazuela *et al.* 2004; Hatta *et al.* 2004). The physin and gylin families consist of proteins which are components of transport vesicles. In the mammalian system, the physin family consists of synaptophysin, synaptoporin, pathophysin and mitsugumin 29, while the gylin family consists of synaptogyrins 1-4 (Sanchez-Pulido *et al.* 2002). Though definitive proof has not been shown to accurately conclude the specific functions of the physins and gyrins, the structural model of synaptophysin (the first synaptic vesicle protein to be identified and cloned) suggests a direct role in vesicle fusion and recycling, mediated by the MARVEL domain (Arthur and Stowell, 2007).

The occludin family, along with newer members, marvelD3 and tricellulin, belong to the tight junction-associated MARVEL protein family (TAMP). They are integral membrane proteins localized at the tight junctions whose functions remain uncertain. *In vitro* studies have shown that disruption of any of these family members results in the loss of tight junction barriers (Shen and Turner, 2005). However, occludin knockout mice do not show any abnormalities with their epithelial barriers. Therefore, it is likely that these family members function as a group, rather than individual proteins, with redundant functions at the epithelial lateral membrane and regulation of tight junctions (Raleigh *et al.* 2010). Though it is unknown if the TAMP family functions in

membrane apposition; the MARVEL domain suggests the proteins may influence vesicle or membrane fusion to maintain the tight junction barrier (Shen *et al.* 2011).

The chemokine-like factor superfamily (CKLFSF) consists of nine known members, CKLFSF1-9. The best characterized member is chemokine-like factor superfamily 8 (CKLFSF8). CKLFSF8 is structurally similar to a MAL family member, plasmolipin, suggesting it may also function in membrane sorting and trafficking. To date, CKLFSF8 has been identified as a regulator of EGFR (epidermal growth factor receptor) endocytosis and desensitization.

The MARVEL domain is conserved across species, including *Caenorhabditis elegans* and *Drosophila melanogaster*, suggesting it is not a newly evolved domain. Interestingly, a novel *Drosophila* protein, singles bar, encodes the MARVEL domain and is an essential component of the pre-fusion complex in myoblasts where it contributes to membrane fusion (Estrada *et al.* 2007). Characterization of the proteins which contain a MARVEL domain has led to a common biochemical feature; the proteins associate with cholesterol. Therefore, it is possible that the MARVEL domain is necessary for organization of cholesterol-rich microdomains which function in membrane apposition events.

The MAL family

A. The MAL family: similarities and differences

The myelin and lymphocyte (MAL) family consists of four tetraspanning proteins that were originally found as highly expressing proteins in myelinating oligodendrocytes

and Schwann cells. They are MAL (also called VIP17, vesicle integral protein of 17 kDa), MAL2, BENE and plasmolipin. The sequence alignment of the family members (Figure 3) shows that the overall sequence identities is fairly low at 29-37%. However, they share a conserved motif of (Q/Y)GWVM(F/Y)V between the first extracellular loop and the second transmembrane domain (Magyar *et al.* 1997) which may act as a molecular fingerprint for all MAL family members. Due to their common association with glycosphingolipids, the family of proteins may be involved in maintenance of glycosphingolipid-enriched domains (Frank *et al.* 2000). All four proteins are widely expressed in a variety of tissues, implicating the family as having a basic and related role throughout the mammalian system.

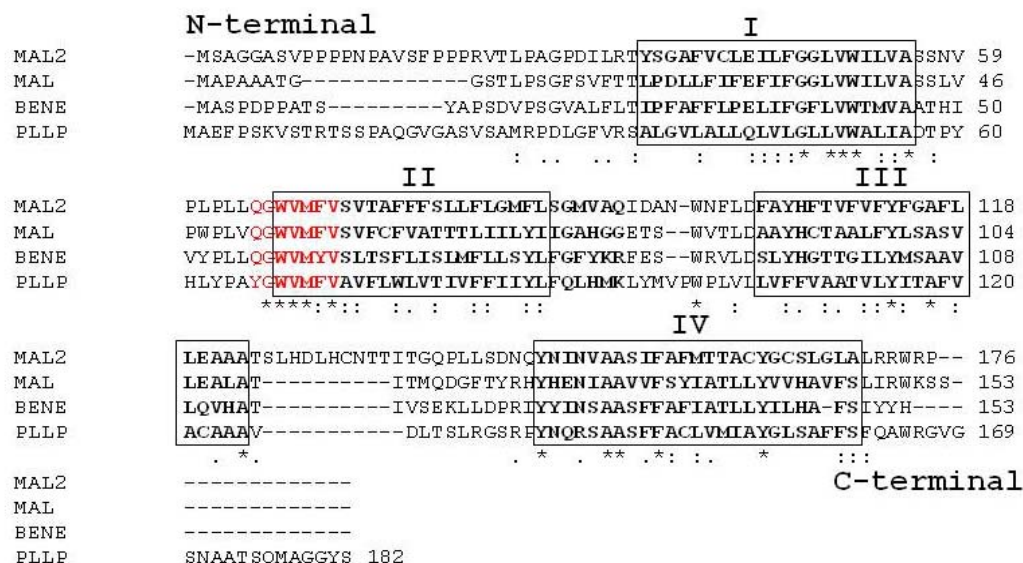


Figure 3. Sequence comparison of the MAL family members. Sequence alignment of the MAL family members reveals low identity (29-37%) but a highly conserved motif of (Q/Y)GWVM(F/Y)V (depicted in red). The four transmembrane regions, comprising the MARVEL domain, are boxed and listed as I-IV. *, conserved residues; :, conserved substitutions; ., semi-conserved substitutions

B. Plasmolipin

Plasmolipin, a 17 kDa protein, was initially isolated in the plasma membranes of kidney, but has been found to be most highly expressed in myelinating Schwann cells and oligodendrocytes (Cochary *et al.* 1990; Gillen *et al.* 1996; Bosse *et al.* 2003). Since the glycosphingolipid and cholesterol-enriched domains of polarized apical membranes resembles myelin-domains; myelin-producing cells (such as oligodendrocytes and Schwann cells) are also considered to be polarized cells. This is of particular interest because phosphorylated plasmolipin is a component of the ‘myelin lipid rafts’ (Frank *et al.* 2000; Bosse *et al.* 2003). Although the signaling or binding determinants for directional, polarized targeting of myelin proteins are unknown, research performed by Bosse *et al.* (2003) suggests phosphorylation of plasmolipin directs the formation and compaction of myelin in a polarized manner. Further research on this MAL family member will help elucidate the trafficking properties of all MAL proteins.

C. BENE

BENE, also a lipid-raft dependent protein, has a high level of expression in endothelial cells of the colon, heart, prostate and lung but is undetectable in many epithelial cells, such as the kidney and liver (de Marco *et al.* 2001). It shares high amino acid identity with MAL (39%) and an unusually high conservation of aromatic residues (Perez *et al.* 1997). However, the function of BENE is not yet known. Its similarities to MAL and plasmolipin, in both sequence alignment and association with lipid rafts, suggest that BENE also has a role in polarized trafficking. To support this hypothesis, BENE has been found to interact and co-localize with the protein caveolin-1 (cav-1) in

endothelial like ECV304 cells and human prostrate carcinoma PC-3 cells (de Marco *et al.* 2001; Llorente *et al.* 2004). Cav-1, a component of the caveolar architecture at the plasma membrane and Golgi, forms a scaffold where numerous signaling complexes are recruited to direct lipid raft domains into caveolae vesicles.

While the role of BENE in this endocytic pathway is unknown, it is possible that BENE is recruited as part of the signaling scaffold to either maintain the vesicles or direct them in a polarized manner. Interestingly, prostasomes (vesicles secreted by prostate cells to the prostatic fluid) secreted by the PC-3 cells excluded both BENE and MAL2, but contained MAL and cav-1 (de Marco *et al.* 2001). Since prostasomes are known to be enriched in lipid-raft components, it was not surprising to find both MAL and cav-1. However, the absence of BENE suggests that, like plasmolipin, its function will be related yet unique from that of MAL.

D. MAL

The founder protein of this family, the 17 kDa MAL, was originally isolated while searching for genes that are expressed differentially in T-cell development (Alonso and Weissman, 1987). Biochemical analyses of the T-cell specific MAL found that it behaved as a proteolipid, being highly soluble in organic solvents used to extract cellular lipids (Rancaño *et al.* 1994).

1. Localization of MAL

MAL has been found in a wide variety of specialized cell types and tissues. For example, parietal cells (stomach), acinar cells (pancreas), ductal cells (prostate), type 2 pneumocytes (lung), T cells (lymph node) and Leydig cells (testis) express MAL, specifically due to their specialized transport functions. For a comprehensive list of all cell types which express MAL, please refer to the review written by Marazuela and Alonso, 2004.

In human T-cells, MAL is restricted to the endoplasmic reticulum (ER), an observation which is not consistent with its localization in other cell types (Rancano *et al.* 1994; Millan and Alonso, 1998). Indeed, the two terminal serines at the carboxyl-tail have been shown to prevent ER-retention (Puertollano and Alonso, 1999a). Recently, further analysis of MAL in T-cells has shown that it is present in intracellular vesicles and at the plasma membrane (Anton *et al.* 2008). In many other cell types, including kidney and myelinating cells, MAL is found in sub-apical vesicles or at the apical surface (Kim *et al.* 1995; Cheong *et al.* 1999; Puertollano *et al.* 1999). The differing localizations seen in different cell types is not yet understood.

2. Function of MAL

MAL has been well-characterized in simple epithelial cells, where it is highly expressed. In functional studies, deletion or knockdown of MAL in MDCK and FRT cells resulted in reduced transport of secretory, GPI-anchored and single transmembrane domain (TMD) proteins to the apical surface, implicating the importance of MAL in direct apical delivery (Cheong *et al.* 1999; Martin-Belmonte *et al.* 2000, 2001). The

observed proteins included thyroglobulin and clusterin (secretory), alkaline phosphatase (GPI-anchored) and hemaagglutinin and dipeptidyl peptidase IV (single TMD). MAL has also been implicated in clathrin-mediated endocytosis at the apical surface of MDCK cells (Martin-Belmonte *et al.* 2003). These researchers also found that depletion of MAL led to reduced apical internalization of pIgA-R, giving a new role to MAL. Additionally, over-expression of MAL in MDCK cells results in amplification of the apical surface and the formation of tubular cysts (Frank, 2000). These interesting studies have broadened the hypothesis that MAL is essential in direct delivery and recycling of apical proteins (Magal *et al.* 2009; Carmosino *et al.* 2010b).

Universally, MAL has been shown to selectively reside in lipid raft domains of all cell types in which it is expressed (Kim *et al.* 1995; Martin-Belmonte *et al.* 1998; Cheong *et al.* 1999; Frank, 2000; Caduff *et al.* 2001; Tall *et al.* 2003; Ramnarayanan *et al.* 2007). Consistent with these observations, Puertollano *et al.* (1997) showed that recombinant expression of MAL in Sf21 insect cells, which lack endogenous MAL, induced the *de novo* formation of large vesicles with glycosphingolipid-enriched membranes. Recently, Magal *et al.* (2009) found that MAL self assembled into large homo-oligomers which recruited components of apical sorting raft domains. Based on their findings, they proposed the following functional model: MAL clustering is driven by positive hydrophobic mismatching between the long MAL transmembrane helices (23-25 amino acids) and the shorter hydrophobic chains of the membrane lipids. Once the cluster of MAL and apical proteins are delivered to the apical surface, which is rich in cholesterol and glycosphingolipids, therefore thicker and more able to support the long

transmembrane domains, the hydrophobic mismatch is relieved and the complexes dissociate (Magal *et al.* 2009).

E. MAL2

The 19 kDa, 176-residue protein, MAL2 is markedly similar to MAL with 50.6% conserved and 35.8% identical residues (Wilson *et al.* 2001). However, MAL2 differs from MAL in its N-terminal tail, both in length and residues, as shown in Figure 3. The significance of this difference is yet unknown and further research is needed to fully characterize these structural differences.

1. Localization of MAL2

The distributions of MAL and MAL2 are similar, with high expression levels of both in epithelial cells of a variety of tissues, such as breast, prostate, kidney, ovary and testis (Marazuela and Alonso, 2004; Byrne *et al.* 2010). However, MAL2 is highly expressed in hepatic cells while MAL is absent. Interestingly, Ramnarayanan *et al.* (2007) found that expression of MAL in WIF-B hepatic cells led to the rerouting of most apical proteins from the indirect to the direct pathway, indicating related yet unique functions for the two family members. Thus far, comprehensive studies on MAL2 have only been performed in hepatocytes and thyrocytes. In both cell types, MAL2 is found at the apical membrane (the bile canaliculi in hepatocytes) and at sub-apical structures (Marazuela *et al.* 2004; de Marco *et al.* 2006; In and Tuma, 2010).

Although it has been reported that MAL2 resides in lipid rafts in HepG2 hepatic cells (de Marco *et al.* 2002, 2006), results from our lab and others have shown that

MAL2 and several known binding partners are mostly soluble when extracted with the non-ionic detergent Triton X-100 (TX-100) in WIF-B hepatic cells, breast carcinoma and oligodendrocytes (Bello-Morales *et al.* 2009; Fanayan *et al.* 2009). However, some MAL2 was insoluble when extracted with a gentler, zwitterionic detergent, CHAPS, in oligodendrocytes (Bello-Morales *et al.* 2009). Instead, MAL2 may not be present in the classical raft domains (extracted with TX-100). However, the distributions and/or functions of MAL2 are dependent on cholesterol and glycosphingolipids,

2. Functional analysis of MAL2

MAL2 functions in selective basolateral delivery and transcytosis of apical proteins in hepatic cells (de Marco *et al.* 2002, 2006; In and Tuma, 2010) (Figure 4). Although the mechanism by which MAL2 sorts and delivers apical cargo is not yet known, its primary function as an apical regulator has been shown. De Marco *et al.* (2002) first observed a halt in transcytosis at the BL EE of both CD59 (GPI-anchored, raft-dependent) and IgA (ligand of pIgA-R, raft-independent), which was later confirmed by our lab in the hepatic WIF-B cells. This correlated with the theory that there is a general regulator of all subsets of apical proteins whose activity is dependent on cholesterol and glycosphingolipids (Nyasa *et al.* 2003). Expanding upon this exciting observation, our lab showed that MAL2 functions at an earlier step in trafficking as well, selectively sorting apical cargo at the TGN for delivery to the basolateral surface. The multifunctionality of MAL2 in the biosynthetic and transcytotic pathways as well as the specific itinerary in hepatic cells is discussed in Part I of this dissertation. The possibility of MAL2 in other pathways is discussed in Part II.

Unlike for MAL, MAL2 has been found to have numerous binding partners.

Based on the sequence comparison between the two proteins (Figure 3), our model predicts that the MAL2 cytoplasmic domains are important for mediating interactions.

The sequence-divergent, longer and proline-rich (which are important mediators of protein-protein interactions) N-terminal domain suggests that it is the essential component of MAL2 in mediating protein-protein interactions. Thus, to better characterize MAL2, our lab and others are actively examining the interactions between MAL2 and its binding partners.

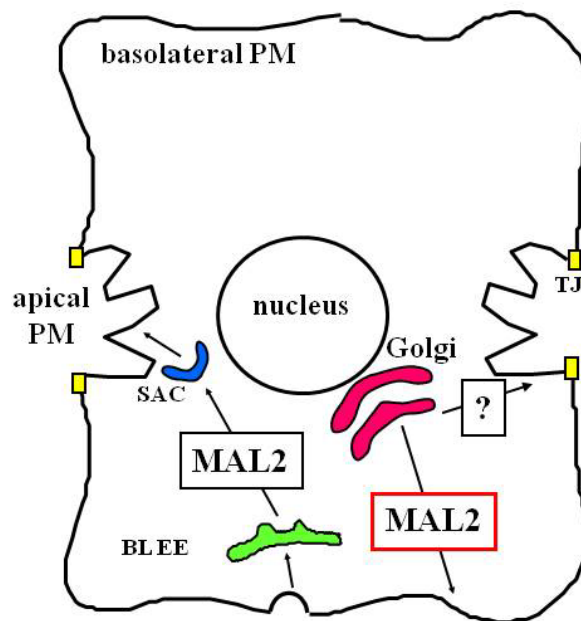


Figure 4. Proposed sites for MAL2 function. MAL2 selectively regulates the delivery of pIgA-R in the biosynthetic pathway to the basolateral PM (red box) and broadly regulates the delivery of a variety of apical proteins in the transcytotic pathway from the BL EE to the SAC (black box). MAL2 is also proposed to regulate polytopic transporters directly from the Golgi to the apical PM. BL EE, basolateral early endosome; PM, plasma membrane; SAC, sub-apical compartment; TJ, tight junction

3. *Characterizing MAL2: interaction with TPD52*

MAL2 was first identified by its interaction with tumor protein D52-like 2 (TPD52L2 or D54) in a yeast-2-hybrid (Y2H) screen of human breast carcinoma (Wilson *et al.* 2001). Subsequent analysis of MAL2 and the TPD family found that it interacts with three members (TPD52, D53 and D54). Interestingly, the number of preys obtained in each Y2H screen with MAL2 was low (between 1-6), indicating a weak or transient interaction between these proteins. This is comparable to the weak homo- and heterodimeric interactions seen among TPD family members (Byrne *et al.* 1998; Wilson *et al.* 2001). The interaction is mediated by the N-terminal tail of MAL2 (Fanayan *et al.* 2009) and the coiled-coiled motif present in the D52 family of proteins (Byrne *et al.* 1996) which was found to be essential for homo- and heterodimeric interactions (Sathasivam *et al.* 2001). The localization of D52 in gastric parietal and pancreatic acinar cells at supranuclear regions and surrounding the secretory granules led to the proposal that it functions in vesicle trafficking and exocytosis (Grolewski *et al.* 1999).

In pancreatic acinar cells, calcium-dependent phosphorylation of TPD52, via calmodulin-kinase II delta 6 (CaMKII δ 6), led to the secretagogue stimulation and rapid translocation of TPD52 from a supranuclear to subapical distribution (Kaspar *et al.* 2003; Thomas *et al.* 2004; Chew *et al.* 2008). Mutation of the phosphorylated serine results in the loss of TPD52 phosphorylation and decrease of secretion. TPD52 and secreted cargo did not translocate to the subapical but remained in a supranuclear distribution (Chew *et al.* 2008; Thomas *et al.* 2010). Because the translocation is reminiscent of the final step in apical delivery from the SAC to the apical domain in polarized epithelial cells and since

MAL2 is a known binding partner of TPD52 and its family members, its role in regulating apical delivery may also be Ca^{++} /calmodulin-dependent. The effect of Ca^{++} and calmodulin antagonists, Ca^{++} chelators and ionophores on the distributions and delivery of MAL2 and all subsets of apical proteins is an area for further research.

4. Characterizing MAL2: interaction with mucin1

MAL2 was also found to bind mucin1 (MUC1) in a human breast carcinoma Y2H. Although interaction with D52 is mediated via the N-terminal tail of MAL2; MUC1's interaction with MAL2 is mediated via the TM region (Fanayan *et al.* 2009). However, the physiological relationship between MAL2 and MUC1 remains unknown. Recent studies found that MUC1 traverses the apical endosome and is expressed at the apical surface in MDCK cells (Mattila *et al.* 2009). Although there is no direct evidence, this points to the hypothesis that MAL2 regulates MUC1 trafficking. It is also possible that MAL2 regulates MUC1 localization in cancerous cells (Fanayan *et al.* 2009). These and other implications of MAL2 in cancer will be discussed later.

5. Characterizing MAL2: interaction with informin 2

In the same human breast carcinoma Y2H screen, MAL2 also pulled down *inverted formin 2* (informin 2, INF2). INF2, as a member of the family of formins, associates with the fast growing end of actin filaments. While most formins function in polymerization of actin, INF2 promotes both polymerization and depolymerization of actin (Madrid *et al.* 2010). INF2 was found to regulate the dynamics of MAL2 in HepG2 cells. In tandem, INF2, MAL2 and the GTPase-Cdc42 regulate transcytosis and the formation of lateral and central lumens in HepG2 and MDCK cells, respectively (Madrid

et al. 2010). However, INF2 localizes to the endoplasmic reticulum, while MAL2 does not. It remains to be seen how they can interact in disparate compartments and in which stage of development they are actively forming these complexes. Also unknown is how the polymerization and subsequent depolymerization of actin by INF2 plays into this process. Interestingly, the N-terminal domain of MAL2 encodes an FPPP domain, a motif implicated in binding to a subset of EVH1 (Ena/VASP homology 1) domain-containing proteins (Renfranz and Beckerle, 2002). The specific FPPP motif has been seen in proteins which are involved in the assembly and disassembly of the actin cytoskeleton. Thus, MAL2's role in regulating apical transport may involve actin.

6. Characterizing MAL2: novel interactors

Because protein targeting is regulated by complex machineries and because MAL2 functions in at least two known steps in the itinerary of apical proteins, we postulate that MAL2 has other interactors that have yet to be discovered. Our studies to identify new MAL2 binding partners are described in Part II of this dissertation.

Implications of MAL and cancer

Nearly every member of the MAL family has been implicated in the progression of various carcinomas and tumors. For example, both BENE and MAL are overexpressed in prostate carcinoma, and with increased secretion of prostasomes, which is correlated to metastasis (Llorente *et al.* 2004). In contrast, levels of MAL and BENE are down-regulated in cervical squamous carcinomas (Hatta *et al.* 2004). Through genomic screening, MAL's promoter has been shown to be hypermethylated in a variety of

carcinomas: colorectal, esophageal, ovarian, cervical, T-cell lymphoma and Hodgkin's lymphoma (Tracey *et al.* 2002; Mimori *et al.* 2003; Hsi *et al.* 2006; Lind *et al.* 2008; Horne *et al.* 2009; Overmeer *et al.* 2009). Hypermethylation results in a drastic reduction or silencing of MAL expression. These results suggest that MAL functions as a tumor suppressor and must remain stable to maintain proper trafficking and polarity. Targeting MAL expression levels, perhaps with demethylating agents, at the first detection of cancers may be a useful therapeutic tool to prevent metastasis and a poor prognosis.

In contrast, MAL2 has been found to be overexpressed in a variety of carcinomas: pancreatic ductal adenocarcinoma, colorectal, renal cell, breast and ovarian carcinomas (Rohan *et al.* 2006; Chen *et al.* 2007; Shrout *et al.* 2008; Shehata *et al.* 2008; Byrne *et al.* 2010). Thus far, overexpression of MAL2 is seen as a genetic marker of poor prognosis and resistance to doxorubicin-based therapy in breast cancer (Folgueira *et al.* 2005; Adler *et al.* 2006). MUC1, a binding partner of MAL2, is also a tumor associated protein which redistributes from the cytosol (as seen in healthy cells) to the surface in cancerous cells. The surface localization of MUC1 results in the reduction of cellular adhesion to the extracellular matrix, allowing the previously stationary cell to migrate. This has been postulated as a precursor to cellular metastasis (Hollingsworth and Swanson, 2004). However, the molecular mechanisms causing mislocalization of MUC1 are unknown.

Additionally, both MAL2 and TPD52 are highly overexpressed in ovarian cancers. While MAL2 is mainly overexpressed in serous ovarian carcinomas (the most common ovarian cancer), TPD52 is mostly overexpressed in clear cell carcinomas (a rare form of ovarian cancer). Interestingly, patients with high expression levels of both

TPD52 and MAL2 in serous carcinomas showed improved patient survival (Byrne *et al.* 2010). This study postulates that while overexpression of MAL2 correlates with a poor prognosis in breast cancer, it may have different roles in different cancers.

Although further analysis is needed to directly determine MAL2's role in cancer progression, we hypothesize that MAL2 is an essential component of multiple trafficking pathways in epithelial cells that must be tightly controlled to ensure proper polarity maintenance and growth.

WIF-B cells: a model for polarized hepatic trafficking

Progress in understanding the molecular basis of transcytotic sorting in polarized hepatocytes has been hampered by the lack of good *in vitro* systems. Traditionally, animal models have been used to describe hepatic apical trafficking patterns. Although these studies have provided a wealth of information, there are disadvantages to using animal models. Not only is there considerable physiologic variation among animals, it is also difficult to quickly alter experimental parameters (e.g., addition or withdrawal of inhibitors, changes in temperature) that are required for mechanistic studies. Inhibitors or other experimental reagents are introduced to all organs of the animal's body where they may interfere with defining hepatic-specific responses or may produce severe side effects. Additionally, the fully-differentiated hepatocytes de-differentiate ~48 hours after growth *in vitro*, losing their liver-specific phenotype (Ihrke *et al.* 1993). Not only is their cell surface polarity lost, but also lost is the expression of many liver specific proteins.

The challenge here has been to maintain cells in culture that retain their hepatocyte-specific characteristics that are required for proper liver function.

Various hepatic cell lines, such as Fao, Clone 9 and Huh-7, are limited and not useful for *in vitro* studies. Similar to isolated hepatocytes, these hepatic cells have lost their cell surface polarity and expression of many liver specific proteins. The human-derived hepatic cell line, HepG2, is currently used for many hepatic membrane trafficking studies. However, these hepatic cells also have extensive limitations. The extent of polarity is only ~20%. Many of their liver functions have been lost and mislocalization of apical proteins and microvilli has been reported, precluding the use of biochemical approaches for measuring polarized trafficking (Decaens *et al.* 2008).

These problems have been resolved with the WIF-B cells; a fusion of two cell lines: rat hepatoma Fao and human fibroblast WI38. When cultured on plastic or glass coverslips without the aid of a coated matrix, the cells enter a terminal differentiation program. After 7-10 days in culture, 70-95% of WIF-B cells become fully differentiated and exhibit phase-lucent structures that are functionally and compositionally analogous to the bile canaliculi (BC). Domain-specific membrane proteins are localized in WIF-B cells as they are in hepatocytes *in situ*. Liver-specific functions are maintained, such as bile metabolism and secretion, cytochrome P450 expression, cholesterol synthesis, albumin production and secretion, glycogenolysis, and more (Ihrke *et al.* 1993; Bender *et al.* 1999; Decaens *et al.* 2008). The different polarity markers characterized by domain specific proteins and junctional proteins correctly express and localize to their respective domains (Bravo *et al.* 1998; Wakabayashi *et al.* 2004; Ramnarayanan *et al.* 2007). Figure

5 shows a depiction of WIF-B cells highlighted by the non-overlapping expression of basolateral and apical proteins. The high level of polarity allows us to perform the biochemical studies required to understand the mechanistic basis of apical protein sorting.

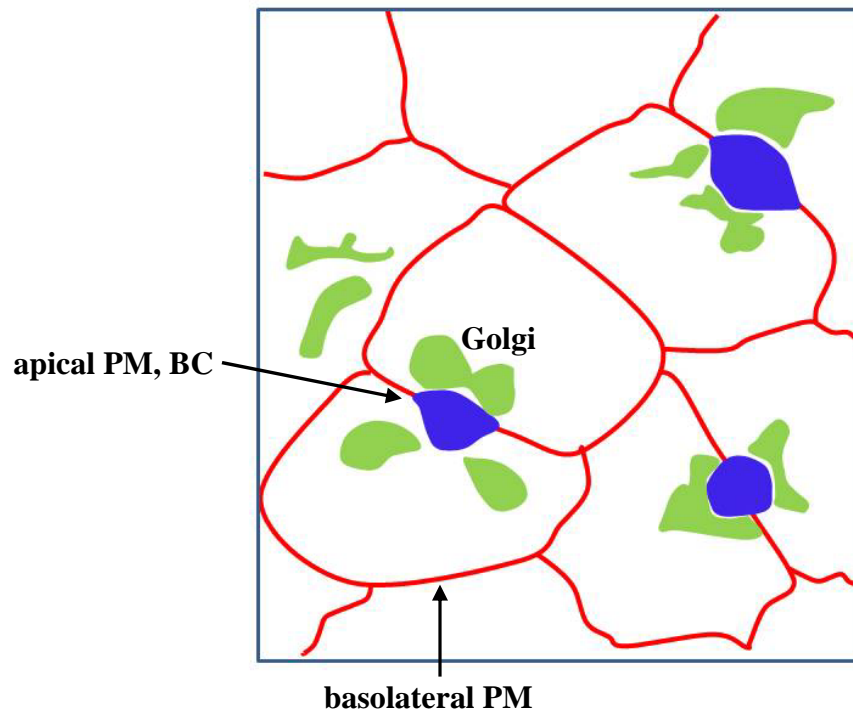


Figure 5. WIF-B cells, our *in vitro* hepatic model. WIF-B cells form functionally polarized membranes in culture with separate and distinct apical (depicted as phase translucent bile canaliculi) and basolateral membranes. Mock triple staining shows the basolateral PM in red, apical PM (BC) in blue and Golgi in green. BC, bile canaliculi; PM, plasma membrane

MATERIALS AND METHODS

Reagents and antibodies. Nocodazole, Triton X-100, F12 (Coon's modification) medium, methyl- β -cyclodextrin (m β CD), cycloheximide, latrunculin B (lat B), tunicamycin, calmodulin-agarose, vasopressin (AVP), brefeldin A (BFA), 1,2-bis(o-aminophenoxy)ethane-N,N,N',N'-tetraacetic acid (BAPTA), ionomycin, thapsigargin and streptavidin agarose were purchased from Sigma-Aldrich (St. Louis, MO). Nocodazole, lat B, tunicamycin, AVP, BFA, BAPTA, ionomycin and thapsigargin were stored at -20°C as 10 mM, 10 mM, 100 mg/mL, 10 nM, 10 mg/mL, 10 mM, 50 mM and 1mM in DMSO stock, respectively, while m β CD, 5 mM, and cycloheximide, 10 mg/mL, were made fresh in serum-free medium and 5% ethanol, respectively. N – Hydroxysulfosuccinimide (NHS)-biotin was purchased from Pierce (Rockford, IL). Bovine serum albumin (BSA) was purchased from VWR International (Radnor, PA). W-7 and monoclonal antibody against multi-drug resistance protein 2 (MRP2) were purchased from Enzo Life Sciences (Plymouth Meeting, PA). W-7 was stored at -20°C as 10 mM in DMSO stock. Fetal bovine serum (FBS) and newborn calf serum were purchased from Gemini Bio-Products (West Sacramento, CA). TaqSelect DNA polymerase was purchased from Lucigen (Middleton, WI). High speed plasmid mini kits were purchased from MidSci (St. Louis, MO). Horse radish peroxidase (HRP)-conjugated secondary antibodies and Western Lightning chemiluminescence reagent were purchased from Sigma-Aldrich and PerkinElmer (Crofton, MD), respectively. Monoclonal antibody against V5 tag was purchased from AbD Serotec. Alexa-conjugated

secondary antibodies and lactacystin were purchased from Invitrogen (Carlsbad, CA). Lactacystin was stored at -20°C as 5 mM in DMSO stock. Antibodies against TPD52 and TPD53 were purchased from Santa Cruz Biotechnologies (Santa Cruz, CA). Monoclonal antibody against mannosidase II (mann II) was purchased from Covance (Princeton, NJ). Polyclonal antibody against serine/threonine kinase 16 (STK16) was kindly provided by Dr. A. Bernad (Centro Nacional de Investigaciones Cardiovasculares, Madrid, Spain). Antibodies against pIgA-R, DPPIV, endolyn and 5'NT were generously provided by Dr. A. Hubbard (Johns Hopkins University, School of Medicine, Baltimore, MD). Recombinant adenoviruses encoding V5/His6 epitope-tagged full-length pIgA-R, V5/myc epitope-tagged full-length DPPIV and full-length HA were also provided by Dr. A. Hubbard and have been described in detail (Bastaki *et al.* 2002). Recombinant adenoviruses encoding V5 epitope-tagged full-length and antisense MAL2; full-length, antisense and kinase-dead STK16 were generated using the ViraPower Adenoviral Expression System from Invitrogen (Carlsbad, CA).

Preparation of antibodies to MAL2. Rabbit polyclonal antibodies were made against a peptide corresponding to amino acids 13-23 of rat MAL2 and affinity purified by Covance Research Products (Princeton, NJ). To verify specificity of the antibody, peptide competition experiments were performed. In a final volume of 100 μl of phosphate buffered saline (PBS) containing 1% BSA, 1 μg affinity purified antibody was incubated with a 10-fold molar excess of peptide. The mixture was incubated on ice for 2-4 h stirring occasionally by inverting and was used directly for immunofluorescence labeling or further diluted (1:4000) in PBS/BSA for immunoblotting.

Cell Culture. WIF-B cells were grown in a humidified 7% CO₂ incubator at 37⁰C as described (Shanks, 1994). Briefly, cells were grown in F12 medium (Coon's modification), pH 7.0, supplemented with 5% FBS, 10 μM hypoxanthine, 40 nM aminoterpin and 1.6 μM thymidine. In general, cells were seeded onto glass coverslips at 1.3×10^4 cells/cm² and grown for 8-12 days until they reached maximum density and polarity. Clone9 cells were grown in a humidified 5% CO₂ incubator at 37⁰C. Cells were grown under similar conditions to the WIF-B cells, but supplemented with 10% FBS. In general, cells were seeded into 6-well dishes at $0.25\text{-}0.5 \times 10^6$ cells/well and grown for 1-3 days until they reached maximum density. A293 cells were grown in a humidified 5% CO₂ incubator at 37⁰C. Cells were grown under similar conditions to Clone9 cells. In general, cells were seeded into 6-well dishes at 0.5×10^6 cells/well or 100 x 20 mM dishes at 2×10^6 cells/dish and grown for 1-3 days until they reached optimal transfection density.

Virus Production and Infection. Recombinant adenoviruses for pIgA-R, DPPIV and HA were generated using the Cre-Lox system as described (Bastaki et al. 2002). Recombinant adenoviruses for MAL2 and STK16 were generated using the ViraPower Adenoviral Expression System according to the manufacturer's instructions (Invitrogen). For the antisense constructs, MAL2 and STK16 were PCR-amplified with primers that have additional sequences that encode the recombination sites in the reverse order from how they appear in the Invitrogen Gateway® vector. Thus, when recombined, the fragment inserted in the opposite, antisense orientation, which was verified by plasmid sequencing. For the kinase-dead construct, STK16 was PCR-amplified with full-length

primers against a vector containing STK16 with a point mutation at amino acid 202 (E202A). The point mutation was verified by plasmid sequencing. The full-length and kinase-dead STK16 vectors were provided by Dr. A. Bernad (Centro Nacional de Investigaciones Cardiovasculares, Madrid, Spain). WIF-B or Clone9 cells were infected with recombinant adenovirus particles ($0.7\text{-}1.4 \times 10^{10}$ virus particles/ml) for 60 min at 37°C as described (Bastaki et al. 2002). Complete medium was added to the cells and incubated for an additional 16 - 20 h to allow expression.

Immunofluorescence Microscopy and Imaging. In general, control or infected cells were fixed on ice with chilled PBS containing 4% paraformaldehyde (PFA) for 1 min and permeabilized with ice-cold methanol for 10 min. Cells were processed for indirect immunofluorescence as previously described (Ihrke et al. 1993). Alexa 488- or 568-conjugated secondary antibodies were used at 3-5 µg/ml. To visualize STK16 (1:250) cells were first permeabilized with 0.1% TX-100 for 2 min in PEM/sucrose (100 mM Pipes, 1 mM EGTA, 1 mM MgCl₂, pH 6.8 + 8% sucrose) at room temperature and fixed in methanol for 5 min at 4°C. Labeled cells were visualized at RT by epifluorescence on an Olympus BX60 Fluorescence Microscope (OPELCO, Dulles, VA) using an UPlanFl 60x/NA 1.3, phase 1, oil immersion objective. Images were taken using a SPOT digital camera and software (Diagnostic Instruments, Sterling Heights, MI) or a HQ2 CoolSnap digital camera (Roper Scientific, Germany) and IP Labs software v4.04 (BD Biosciences, Rockville, MD). Adobe Photoshop (Adobe Systems Inc, Mountain View, CA) was used to further process images and to compile figures.

Antibody labeling of live cells. Clone 9 cells were continuously labeled for 1 h with antibodies specific for 5'NT, pIgA-R or DPPIV (all 1:100) or endolyn (1:25). After washing three times for 2 minutes each with prechilled medium, cells were fixed and stained with secondary antibodies as described above. WIF-B cells were labeled for 30 min at 4°C with anti-pIgA-R or –DPPIV antibodies. After washing three times for 2 minutes each with prechilled medium, cells were incubated at 37°C for 1 h. Cells were fixed and stained with secondary antibodies as described above.

Recycling assays in Clone 9 cells. Apical antigens were labeled and chased as described above. To strip antibodies from their surface antigens, cells were rinsed briefly with prewarmed PBS and incubated in isoglycine (200 mM glycine, 150 mM NaCl, pH 2.5) for 5 min at RT. The cells were rinsed with PBS, placed in prewarmed complete medium and incubated at 37°C for the desired times. The total population of antibody-antigen complexes was detected with secondary antibodies in cells fixed as described above whereas the cell surface population was detected in cells fixed with 4% PFA in PBS for 30 min at RT.

Immunoblotting. In general, samples were mixed with Laemmli sample buffer (Laemmli, 1970) and boiled for 3 min. Because boiling abolished MAL2 immunoreactivity (data not shown), samples to be immunoblotted for MAL2 were incubated in Laemmli sample buffer for 20 min at RT before loading. Proteins were electrophoretically separated using SDS-PAGE and transferred to nitrocellulose and immunoblotted with the indicated antibodies. HRP-conjugated secondary antibodies

were used at 5 ng/ml, and immunoreactivity was detected with enhanced chemiluminescence. Relative protein levels were determined by densitometric analysis of immunoreactive bands.

Immunoprecipitations. WIB cells were lysed in 0.5 ml lysis buffer (150 mM sodium chloride, 25 mM HEPES, 1% TX-100, pH 7.4) or Kahane's buffer (300 mM sodium chloride, 250 mM sodium phosphate, 20 mM octylglucoside and 0.5% TX-100, pH 7.4) or RIPA buffer (150 mM sodium chloride, 50 mM Tris, 1% NP-40, 0.5% DOC and 1% SDS, pH 8.0) with protease inhibitors (1 µg/ml each of leupeptin, antipain, PMSF and benzamidine) and incubated on ice for 30 min. Lysates were cleared by centrifugation at 120,000 x g for 30 min at 4°C. Samples were incubated with affinity-purified MAL2, STK16, or V5-tag antibodies at 0.8 µg/µL overnight at 4°C for 16 h. Protein-A or Protein G-Sepharose (50 µL of a 50% v/v slurry) was added for 2 h and samples processed as described (Bartles et al., 1987). Immunoprecipitates were separated by SDS-PAGE and transferred to nitrocellulose and immunoblotted for the indicated proteins. HRP-conjugated secondary antibodies were used at 5 ng/ml, and immunoreactivity was detected with enhanced chemiluminescence.

Surface biotinylation. Clone 9 cells grown on coverslips were treated in the absence or presence of 50 µg/ml cycloheximide for the indicated times. Cells were cooled on ice for 5 min then incubated twice for 15 min each with prechilled 1 mg/ml NHS-biotin in borate buffer (10 mM borate, 137 mM NaCl, 3.8 mM KCl, 0.9 mM CaCl₂, 0.52 mM MgCl₂ and 0.16 mM MgSO₄, pH 9.0). Cells were quenched with prechilled 50 mM NH₄Cl made

fresh in PBS for 10 min. Cells were lysed and extracted as described above for immunoprecipitations. Cleared lysates were incubated with 50 μ l of a 50% slurry of streptavidin agarose for 2 h at 4°C. Samples were further collected and washed as described (Bartles et al. 1987). Unbound and bound fractions were separated by SDS-PAGE and transferred to nitrocellulose and immunoblotted for the indicated proteins. The percent surface associated pIgA-R or DPPIV was determined from densitometric analysis of immunoreactive species.

Secretion assays in WIF-B cells. Cells were infected with recombinant AS MAL2 or AS STK16 adenoviruses for 48 h or WT STK16 or KD-STK16 for 20 h. Cells were rinsed five times with prewarmed serum-free medium and then reincubated in serum-free medium. At 0, 15, 30 and 60 min after reincubation, aliquots of media were collected and analyzed for albumin secretion by immunoblotting. The cell lysates were also collected by solubilization directly into SDS-PAGE sample buffer. Samples were processed for Western blotting and densitometry as described above. For each time point, the percent albumin secreted was determined and plotted. A rate of albumin secretion (percent albumin secreted/min) was calculated for each experiment and compared.

Differential centrifugation. Liver was Dounce-homogenized in 20% (w/v) of 0.25 M sucrose containing 10 mM Tris and protease inhibitors (2 μ g/ml each of leupeptin, antipain, PMSF, and benzamidine). Homogenates were centrifuged at $900 \times g$ at 4°C for 5 minutes. The supernatant was centrifuged at $150,000 \times g$ at 4°C for 60 minutes to prepare the cytosolic and total membrane fractions. The nuclear pellet was washed by

resuspending to volume and centrifuged at $14,200 \times g$ at 4°C for 10 minutes. Samples were mixed with 2X Laemmli sample buffer and boiled for 3 minutes.

Construction of bait yeast 2-hybrid (Y2H) plasmid. Full-length human MAL2 with an *SfiI* linker at both the 5' and 3' ends was generated by PCR from primers 5'-GGAACAGGCCATTACGGCCGGCAGCATGTCTG and 5'-GCTTCAGGCCGAGGCGGCCACGGACGGTCGCCATCT. The resulting PCR product was cloned in frame into the pBT3-STE vector (Y2H Membrane Protein System, MoBiTec, Göttingen, Germany) in the x-Cub orientation and the pBT3-N vector (MoBiTec) in the Cub-x orientation. The bait vectors contained the selectable marker *LEU2* and the LexA-VP16 DNA binding and transactivation domains.

Split-ubiquitin Y2H screening. Split-ubiquitin Y2H assays were performed with the Y2H Membrane Protein System (MoBiTec). An adult human liver cDNA library in the x-NubG orientation (MoBiTec) or NubG-x orientation (Dualsystems Biotech AG, Schlieren, Switzerland) was transformed into the bait yeast strain (*S. cerevisiae* NMY51 transformed with the bait-expressing vector). Clones were selected on –leucine-histidine-tryptophan triple selection plates supplemented with 7.5 mM 3-aminotriazole (Sigma-Aldrich). Plasmids were isolated from positive yeast colonies using Zymoprep Yeast Plasmid Miniprep II (Zymo Research, Orange, CA) and transformed into *E. coli* strain XL10-Gold (Agilent, Santa Clara, CA). Plasmids were re-isolated from *E. coli* colonies with the QIAprep Spin Miniprep Kit (Qiagen, Valencia, CA) and sequenced

(Retrogen, San Diego, CA). Sequences were characterized by input into the NCBI protein BLAST database.

Part I: MAL2 selectively regulates polymeric IgA receptor delivery from the Golgi to the plasma membrane in WIF-B cells

Summary

We initiated studies to examine whether the MAL2 is a good candidate for mediating the lipid-dependent transcytotic step we previously described (Nyasae *et al.* 2003). To begin our studies on MAL2, we generated specific antibodies, and determined that MAL2 was mainly localized to the apical membrane and SAC in WIF-B cells, mostly consistent with reports from others (de Marco *et al.* 2002, 2006; Marazuela *et al.* 2004a,b,c). We further discovered that overexpression of pIgA-R, but not the single spanning apical residents, dipeptidyl peptidase IV (DPPIV) or hemagglutinin (HA), led to the remarkable redistribution of MAL2 from the apical membrane into the biosynthetic and transcytotic intermediates also occupied by the receptor. Knockdown of MAL2 restricted transcytotic delivery of DPPIV at the BL EE, similar to previous reports (de Marco *et al.* 2002). However, delivery of pIgA-R was restricted at the Golgi. In Clone9 cells, nonpolarized hepatic cells that lack endogenous MAL2, we found that DPPIV trafficked from the Golgi to the surface before internalization and delivery to a primordial apical compartment, while pIgA-R was retained in the Golgi. Exogenous MAL2 rescued pIgA-R traffic. From the studies reported here, we conclude that in addition to its proposed role in the regulation of transcytosis from early endosomes to the SAC, MAL2 also selectively regulates pIgA-R delivery from the Golgi to the basolateral plasma membrane.

RESULTS

MAL2 is an itinerant protein in WIF-B cells

To begin our studies, we generated anti-MAL2 polyclonal peptide antibodies against a divergent and specific 11 amino acid N-terminal span in rat MAL2 (Wilson *et al.* 2001). On immunoblots in WIF-B cells, our antibodies detected a 19 kDa species (the predicted MAL2 molecular weight), a band at 25 kDa (marked by an asterisk) and a diffuse set of bands ranging from 30 –38 kDa (Figure 6A). The 25 kDa band and the diffuse bands have been detected by others using different custom antibodies and have been postulated to be glycosylated forms of MAL2 (de Marco *et al.* 2002; Marazuela *et al.* 2004c). To further confirm specificity of our antibody, we blotted lysates from control or MAL2-overexpressing Clone 9 cells. Importantly, these hepatic-derived, nonpolarized cells lack endogenous MAL2 expression. As shown in Figure 6A, MAL2 was detected only in Clone 9 cells that were overexpressing MAL2 confirming antibody specificity. As for WIF-B cells, a 19 kDa band, a 25 kDa band and the higher molecular weight cluster were detected, although the latter two species were less abundant suggesting differential protein processing in the two cell types.

In WIF-B cells, the MAL2 antibodies labeled structures at or near the bile canaliculi (BC), and this labeling was lost after preabsorption with the N-terminal MAL2 peptide used to generate the antibodies (Figure 6B). Importantly, canalicular staining of the GPI-anchored apical resident, 5'NT, was not changed when preabsorbed with the peptide further indicating our reagent is specific (Figure 6B). Moreover, labeling was

detected only in Clone 9 cells infected with recombinant MAL2 adenovirus. Staining at both the plasma membrane and in intracellular puncta was observed (Figure 6C and see Figure 11).

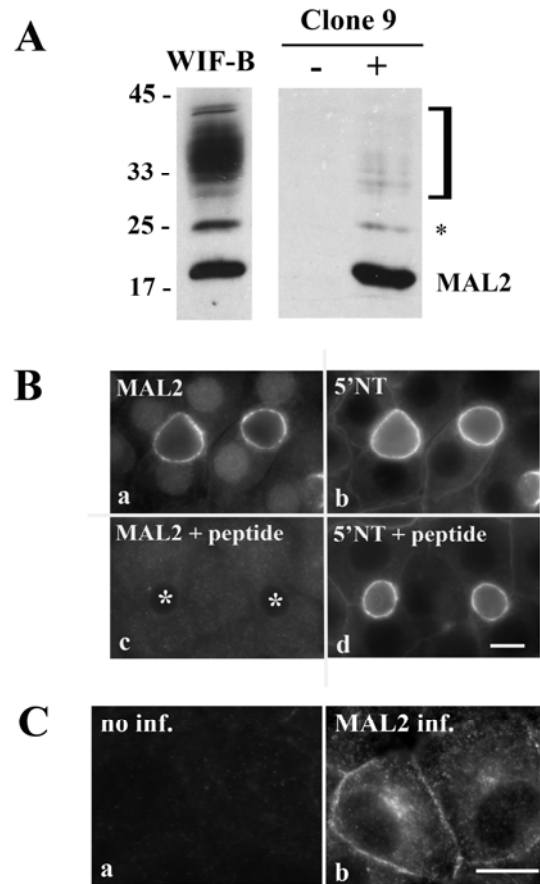


Figure 6. The peptide antibody specifically detects MAL2. (A) WIF-B or Clone 9 (control or exogenously expressing MAL2) cell lysates were immunoblotted for MAL2. The bracket highlights a 30-38 kDa diffuse set of bands that has been described by others and the asterisk indicates a 25 kDa species also detected by others (see text). (B) WIF-B cells were immunolabeled with MAL2 antibodies that were preabsorbed in the absence (a) or presence (c) of a 10-fold molar excess of peptide against which the MAL2 antibodies were generated. Cells were double labeled for 5'NT (b and d). Preabsorption specifically abolished MAL2 apical labeling. Asterisks are marking selected BCs. (C) Clone 9 cells were infected with recombinant adenovirus expressing MAL2 (b). Control and infected cells were labeled with MAL2 antibodies. Only infected cells were stained further confirming the specificity of our antibodies. Bar, 10 μ M

Although MAL2 labeling at the apical pole has been reported by others (de Marco *et al.* 2002, 2006; Marazuela *et al.* 2004a,b,c), this location is not necessarily predicted based on MAL2's proposed role in transcytotic sorting from the basolateral early endosome to the SAC. One explanation is that MAL2 is an itinerant protein cycling among the transcytotic intermediates, a possibility that has been confirmed by live cell imaging in HepG2 cells overexpressing GFP-tagged MAL2 (de Marco *et al.* 2006). To confirm that *endogenous, untagged* MAL2 is itinerant in WIF-B cells, we chose a pharmacological approach to stage MAL2 in various transcytotic intermediates. First, we treated cells for 1 h with 5 mM m β CD, conditions that deplete 80% of cholesterol in WIF-B cells and block transcytotic efflux of apical proteins from early endosomes (Nyasaie *et al.* 2003). As for the apical residents in cholesterol-depleted cells (Nyasaie *et al.* 2003), MAL2 staining was no longer restricted to the apical pole; basolateral labeling was also observed (Figure 7b).

We next used two manipulations that have been shown to alter SAC function and/or morphology in HepG2 cells. The first was an 18°C temperature block that has been reported to impair transport from the SAC (van Ijzendoorn and Hoekstra, 1998), and the second was adding nocodazole that is reported to vesiculate the SAC (Hemery *et al.* 1996). As shown in Figure 7c, after the temperature block, MAL2 staining was found primarily in structures just adjacent to the apical membrane with a reciprocal decrease in apical labeling suggesting it redistributed to the SAC. In nocodazole-treated cells, MAL2 was observed in vesiculated structures emanating from the apical surface with decreased labeling at the BC (Figure 7d) also suggesting MAL2 is present in the SAC.

To further confirm that MAL2 traverses the SAC, we determined the distribution of trafficked endolyn relative to that of MAL2 at steady state. Basolaterally internalized endolyn is delivered to the SAC before its transport to lysosomes providing a useful marker for this transcytotic intermediate (Ihrke *et al.* 1998). The basolateral pool of endolyn was continuously labeled with antibodies for 1 h and then visualized with secondary antibodies. As shown in Figure 7f, a substantial proportion of the endolyn population was present near the apical surface in the SAC (Ihrke *et al.* 1998). MAL2 steady state labeling significantly overlapped with the sub-apically located endolyn indicating that a subpopulation of MAL2 resides in the SAC. Similarly, MAL2 colocalized with basolaterally labeled 5'NT present in the SAC after 1 h of uptake (Figure 7 g and h). Together these results indicate that like overexpressed, GFP-tagged MAL2 in HepG2 cells (de Marco *et al.* 2006), endogenous MAL2 in WIF-B cells is itinerant and can be staged in various transcytotic compartments (basolateral membrane, SAC and apical membrane).

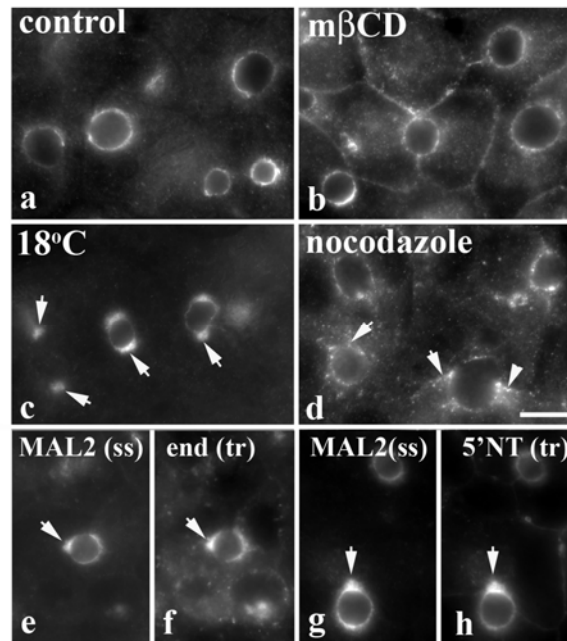


Figure 7. Endogenous, untagged MAL2 is an itinerant protein, traversing the transcytotic pathway. WIF-B cells were immunostained for MAL2 in the absence (a) or presence of 5 mM mβCD for 1 h (b), an 18°C block for 2 h (c), or 33 μM nocodazole for 1h (d). Basolateral populations of endolyn (e and f) or 5'NT (g and h) were labeled with specific antibodies and chased for 1 h at 37°C. Cells were fixed and labeled for steady state (ss) distributions of MAL2 (e and g) and transcytosed (tr) endolyn (f) or 5'NT (h). Arrows are marking MAL2, 5'NT or endolyn labeling in the SAC. Bar, 10 μM

MAL2 and overexpressed pIgA-R selectively colocalize and coimmunoprecipitate

We next examined MAL2 distributions in WIF-B cells overexpressing pIgA-R and other single spanning apical residents. Surprisingly, overexpression of pIgA-R led to the remarkable redistribution of MAL2 into nearly all of the compartments occupied by the receptor (Figure 8A, a-c). Only the diffuse ER-like pIgA-R staining pattern was not observed for MAL2. When cells were treated with nocodazole and focused above the nuclear plane, near perfect colocalization was seen in peripherally located structures (Figure 8A, d-f). Interestingly, overexpression of the single spanning apical ectoenzyme,

DPPIV, did not lead to MAL2 redistribution despite its presence in the same compartments as pIgA-R (albeit with higher levels of diffuse ER-like staining) (Figure 8A, g-i). Similarly, MAL2 and DPPIV did not colocalize in peripheral structures in nocodazole-treated cells (Figure 8A, j-l). When quantitated, we determined that almost 88% of polarized cells positive for intracellular populations of pIgA-R were also positive for MAL2 intracellular labeling whereas only ~12% of polarized cells positive for intracellular DPPIV were also positive for intracellular MAL2 (Figure 8B). Similarly, HA overexpression did not alter MAL2 distributions (data not shown) suggesting selective interactions between MAL2 and pIgA-R.

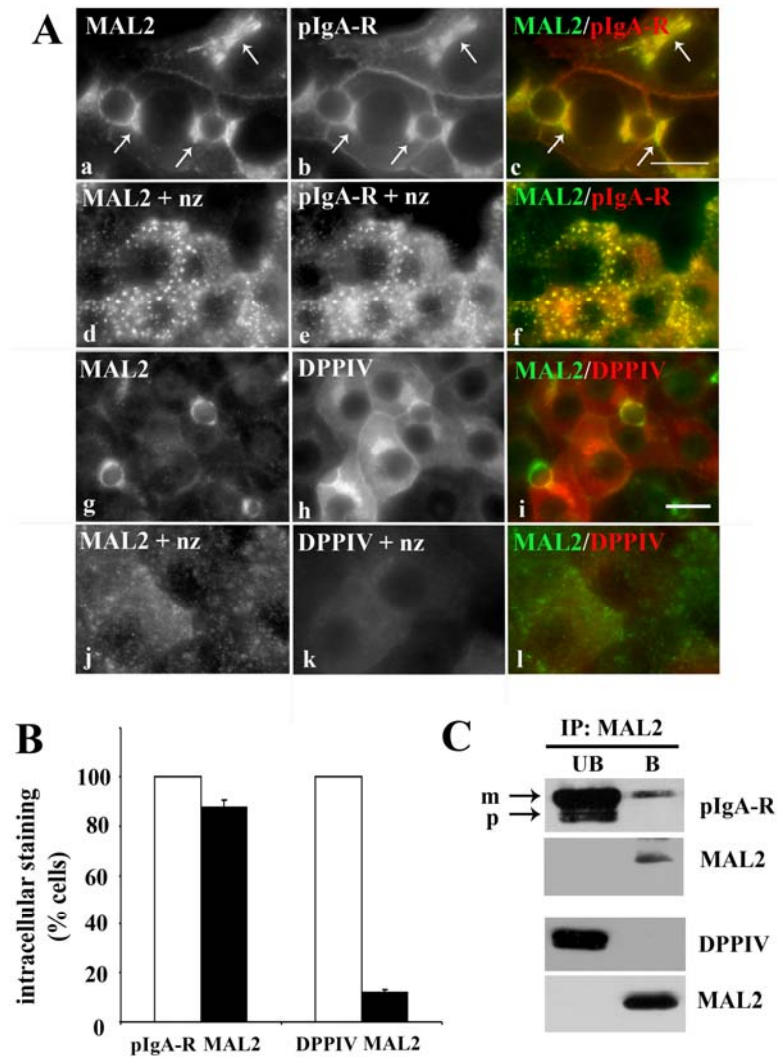


Figure 8. MAL2 co-distributes with exogenously expressed pIgA-R, but not DPPIV. (A) Cells were infected with recombinant adenovirus expressing pIgA-R (a-f) or DPPIV (g-l). After 20 h of expression, cells were immunolabeled for MAL2 (a, d, g) and pIgA-R (b and e) or DPPIV (h and k). In d –f and j-l, cells were treated for 60 min with 33 μ M nocodazole (nz) and images were focused at the cell periphery. Merged images are shown (c, f, i and l). Bar, 10 μ M. (B) pIgA-R or DPPIV overexpressing WIF-B cells were scored for the presence of intracellular puncta positive for the indicated protein. Values are expressed as the mean \pm SEM. Measurements were performed on at least three independent experiments. (C) WIF-B lysates from cells overexpressing pIgA-R or DPPIV were co-immunoprecipitated with 1 μ g affinity-purified MAL2 antibodies. Unbound (UB) and bound (B) fractions were immunoblotted for MAL2 or pIgA-R and DPPIV as indicated. Arrows are pointing to the mature (m) and precursor (p) forms of pIgA-R

The near perfect colocalization of pIgA-R and MAL2 at steady state suggested the proteins were directly interacting. To test this possibility, we performed coimmunoprecipitations. We first tested our antibodies for specific MAL2 immunoprecipitation. As shown in Figure 9A, the affinity purified antibodies specifically immunoprecipitated a 19 kDa protein from WIF-B whole cell extracts (WCE). There was no immunoreactive 19 kDa species in samples incubated without addition of cell extract, and addition of the N-terminal peptide used to generate our antibodies specifically blocked MAL2 immunoprecipitation. We also determined that 1 μ g of affinity purified MAL2 antibodies quantitatively recovered MAL2 from lysates; no additional binding was achieved with 5 μ g (Figure 9B). As shown in Figure 8C, pIgA-R coimmunoprecipitated with anti-MAL2. Importantly, no pIgA-R was detected in immunoprecipitations using preimmune MAL2 sera even on overexposed immunoblots (Figure 9C). Interestingly, only the higher molecular weight, mature form of the receptor was detected in the MAL2 bound fractions (Figure 8C), even upon prolonged exposure (Figure 9D), consistent with the lack of MAL2 colocalization with pIgA-R in the diffuse, ER-like staining pattern (Figure 8A, a-c). This result further indicates that MAL2-pIgA-R interactions are occurring in a late- or post-Golgi compartment. Consistent with the lack of MAL2 redistribution in DPPIV overexpressing cells, no DPPIV was recovered in MAL2 immunoprecipitates (Figure 8C).

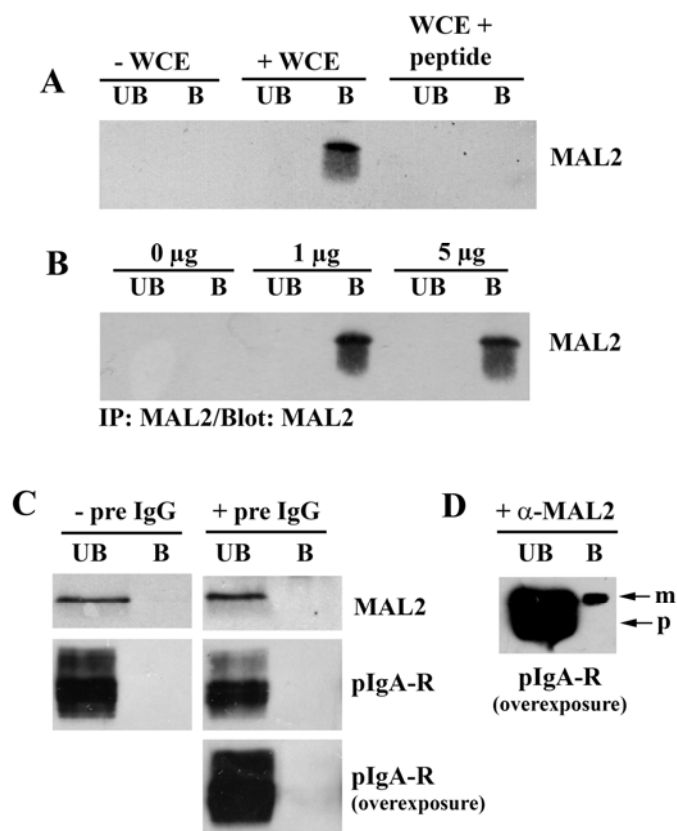


Figure 9. Immunoprecipitation controls. (A) WIF-B lysates were immunoprecipitated with 1 µg affinity-purified MAL2 antibodies and immunoblotted for MAL2 with the same antibodies. MAL2 was detected in the bound fraction (B). No MAL2 was detected in mixtures incubated in the absence of whole cell extract (- WCE) or when a 10-fold molar excess of the MAL2 peptide used to generate the antibodies was added (+ peptide). (B) WIF-B cell lysates were immunoprecipitated with 0, 1 or 5 µg affinity-purified MAL2 antibodies and immunoblotted with the same MAL2 antibodies. Quantitative recovery was obtained with 1 µg/ml antibody. (C) Lysates from WIF-B cells overexpressing pIgA-R were immunoprecipitated with 1 µl MAL2 preimmune serum (pre IgG). Neither MAL2 nor pIgA-R was detected in the bound fractions indicating the results shown in Figure 8C are specific. Overexposure of the bound and unbound fractions confirm that the pIgA-R coimmunoprecipitation shown in Figure 8C is not the result of contaminating pIgA-R detected upon overexposure.

A population of the intracellular structures occupied by pIgA-R and MAL2 appeared Golgi-like. To confirm this, we double labeled pIgA-R overexpressing cells with albumin, a hepatic Golgi marker. As shown in Figure 10A, there was significant overlap of staining in the intracellular structures confirming their Golgi identity. To

further confirm that MAL2 and pIgA-R were present in biosynthetic organelles, we treated cells with cycloheximide. In cells treated for 30 min, the Golgi staining of both MAL2 and pIgA-R was diminished and sub-apical structures were observed (Figure 10B, d-f), and by 60 min, only apical labeling was detected (Figure 10B, g-i). This “chase” from the intracellular structures to the apical membrane suggests that MAL2 and pIgA-R were interacting along the transcytotic route including transport from the Golgi to the basolateral membrane.

We quantitated cells positive for intracellular staining of MAL2 and pIgA-R to confirm these observations. At 0 min, 100% of infected polarized cells contained intracellular pIgA-R populations and ~80% of these cells were also positive for intracellular MAL2. After 30 min, ~50% cells contained intracellular MAL2 and pIgA-R, and by 60 min, only ~35% cells had intracellular MAL2 populations (Figure 10C). Because cells were scored “negative” or “positive” only, the high pIgA-R expression levels prevented complete loss of intracellular labeling after 60 min. Nonetheless, we conclude that pIgA-R and MAL2 traverse the transcytotic pathway together starting at the Golgi. To determine whether pIgA-R overexpression induced MAL2 biosynthesis, and thus its appearance in the Golgi, we immunoblotted control and overexpressing cell lysates. No changes in MAL2 protein levels were detected indicating that the MAL2 Golgi reflects a redistribution, not an induction, in pIgA-R overexpressing cells (Figure 10D).

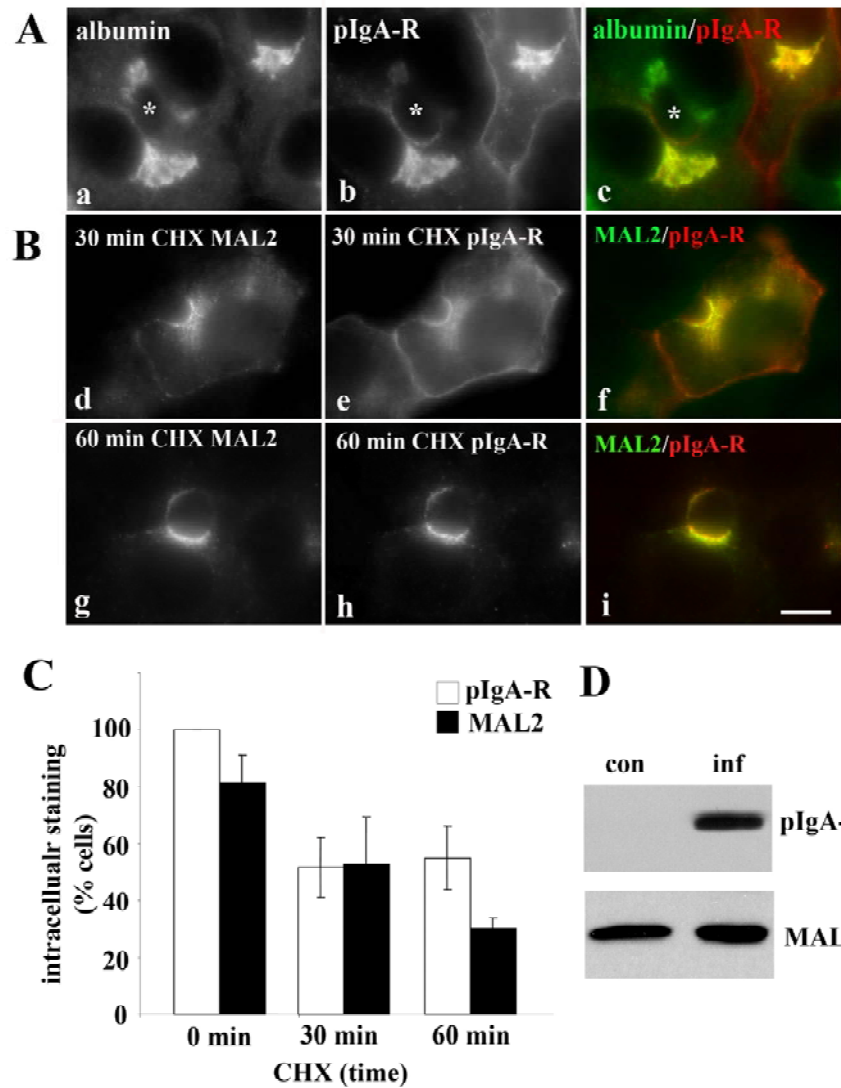


Figure 10. MAL2 and overexpressed pIgA-R are present in the biosynthetic pathway. (A) WIF-B cells were infected with recombinant adenovirus expressing pIgA-R for 20 h. Cells were labeled for albumin (a) and pIgA-R (b). The merged image shows overlapping staining at the Golgi (c). (B) WIF-B cells exogenously expressing pIgA-R were incubated for the indicated times with 50 μ g/ml cycloheximide (CHX). Cells were fixed and stained for MAL2 (d and g) and pIgA-R (e and h). Merged images are shown (f and i). Asterisks are marking selected BCs. Bar, 10 μ M. (C) WIF-B cells overexpressing pIgA-R were treated with 50 μ g/ml CHX for the indicated times and scored for the presence of intracellular puncta positive for pIgA-R or MAL2. Values are expressed as the mean \pm SEM. Measurements were performed on at least three independent experiments. (D) WIF-B (control or exogenously expressing pIgA-R) cell lysates were immunoblotted for pIgA-R (top panel) or MAL2 (bottom panel).

MAL2 regulates delivery from the Golgi to the plasma membrane

The unexpected redistribution of MAL2 into the Golgi in pIgA-R overexpressing cells and the “chase” of both the receptor and MAL2 from the Golgi in cycloheximide-treated cells suggested that MAL2 was regulating pIgA-R delivery from the TGN to the basolateral membrane. To test this possibility, we first examined pIgA-R and DPPIV dynamics in nonpolarized WIF-B cells and nonpolarized, hepatic Clone 9 cells. Importantly, the nonpolarized WIF-B cells express endogenous MAL2 and apical proteins whereas Clone 9 cells do not.

In nonpolarized WIF-B cells, apical proteins distribute to an intracellular compartment that contains only other apical residents (Nyasae *et al.* 2003; Tuma *et al.* 2002). We have rigorously characterized this compartment and determined that it contains only other apical proteins. So far, GPI-anchored apical residents, single spanning ectoenzymes, the polytopic transporter, MRP2, and pIgA-R have been shown to reside in this apical compartment (Nyasae *et al.* 2003; Tuma *et al.* 2002). In contrast, markers for recycling endosomes, early endosomes, lysosomes, late endosomes, Golgi and the basolateral surface are known to be excluded from this compartment (Nyasae *et al.* 2003; Tuma *et al.* 2002). As predicted by its apical location in WIF-B cells, MAL2 was also present in this so-called “apical compartment” in nonpolarized WIF-B cells (Figure 11). Our previous studies have also shown that apical proteins in nonpolarized hepatic cells rapidly recycle between the apical compartment and the cell surface (Nyasae *et al.* 2003; Tuma *et al.* 2002). By monitoring the trafficking of antibody-labeled DPPIV and pIgA-R to the intracellular structures, we further determined that MAL2 localized to

the same compartment to which the apical proteins are delivered (Figure 11).

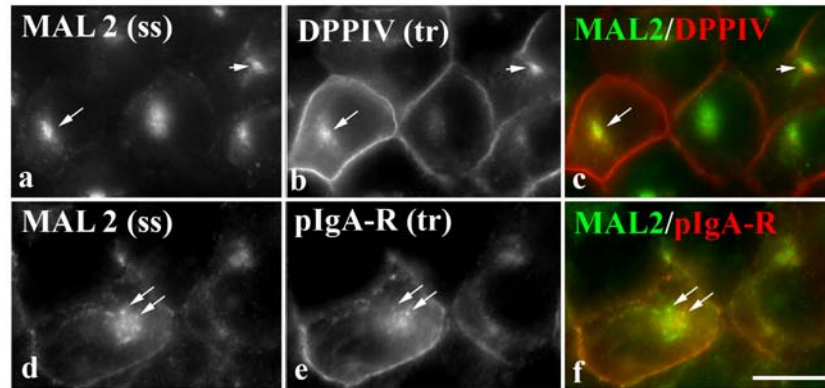


Figure 11. Endogenous MAL2 is present in the “apical compartment” in nonpolarized WIF-B cells. Nonpolarized WIF-B cells overexpressing DPPIV or pIgA-R were continuously labeled with anti-DPPIV (a-c) or anti-pIgA-R antibodies (d-f) for 1 h at 37°C. Cells were fixed and permeabilized and labeled to detect steady state (ss) MAL2 distributions and trafficked (tr) DPPIV or pIgA-R. The merged images are shown in c and e. Arrows are pointing to selected structures that contain both MAL2 and DPPIV or MAL2 and pIgA-R. Bar, 10 μ m

We next examined the distributions of exogenously expressed DPPIV and pIgA-R in Clone 9 cells that lack endogenous expression of apical proteins and MAL2.

Previously, we determined that overexpressed DPPIV distributed to an analogous “apical compartment” in Clone 9 cells (Nyasae *et al.* 2003; Tuma *et al.* 2002) in the absence of MAL2. To confirm that this apical compartment also received apical proteins internalized from the cell surface, we antibody labeled DPPIV present at the plasma membrane at 4°C and chased the antibody-antigen complexes for 1 h at 37°C. As shown in Figure 12A (a), internalized DPPIV was detected at intracellular structures. To determine whether DPPIV recycled between this compartment and the plasma membrane, we first staged DPPIV in the compartment. The remaining plasma membrane-associated antibodies were stripped with isoglycine and only the internalized

antibody-antigen complexes were protected and thus, detected (Figure 12A, b). After an additional hour at 37°C, DPPIV was detected at the plasma membrane indicating that it recycled to the surface (Figure 12A, c). Staining of nonpermeabilized cells processed in parallel (Figure 12A, d-f) verified these observations.

Unlike DPPIV, pIgA-R distributed mainly to the Golgi in Clone 9 cells (Figure 12B, a and b). To determine whether a subpopulation of pIgA-R was delivered to the plasma membrane and then delivered to the apical compartment, we continuously labeled Clone 9 cells with anti-pIgA-R antibodies for 1 h. However, no intracellular staining was observed (Figure 12B, c). To confirm that pIgA-R was not present at the plasma membrane in Clone 9 cells, we surface labeled cells with biotin at 4°C. Only DPPIV was recovered with streptavidin agarose; no pIgA-R was detected in the bound fractions (Figure 12C) even after prolonged exposure of the immunoblots (data not shown). These results indicate that pIgA-R is retained in the Golgi in the absence of MAL2 in Clone 9 cells.

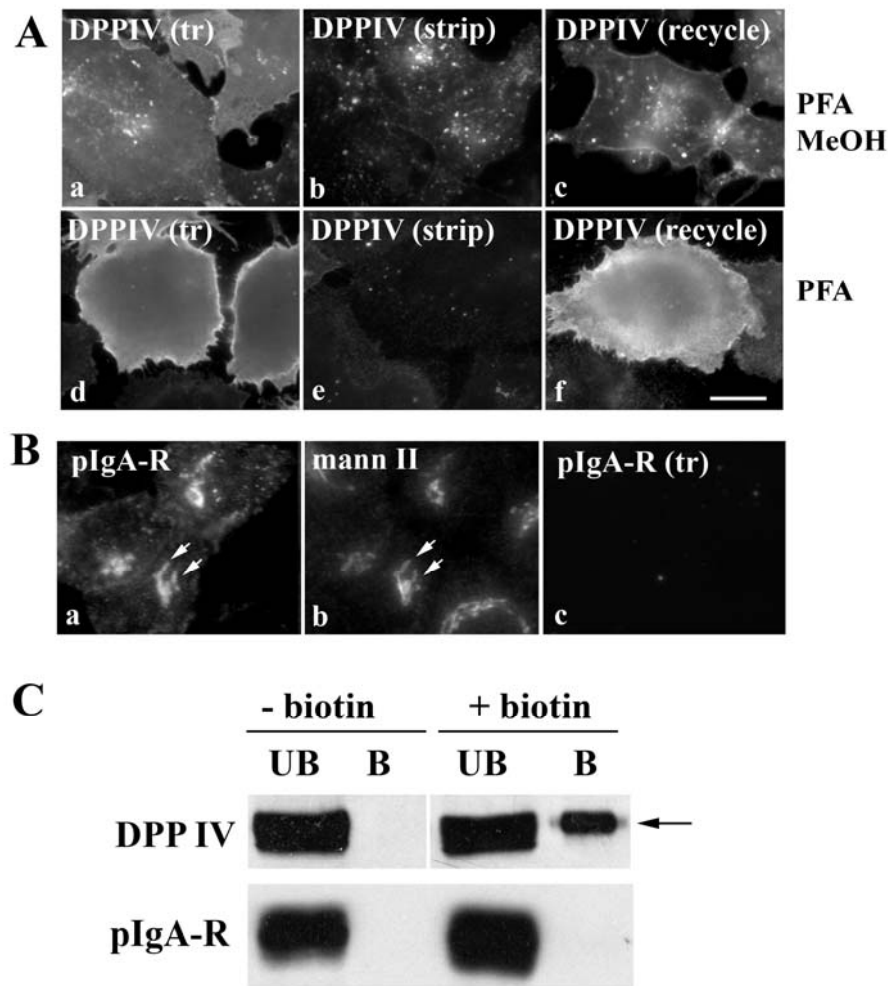


Figure 12. In the absence of MAL2, DPPIV, but not pIgA-R, reaches the plasma membrane in Clone 9 cells. (A) Clone 9 cells expressing exogenous DPPIV were surface-labeled with anti-DPPIV antibodies, and the antibody-antigen complexes trafficked (tr) for 1 h at 37°C (a and d). The remaining membrane-associated antibodies were stripped with isoglycine for 5 min at RT (b and e). Only internalized DPPIV-antibody complexes were detected (b). Cells were incubated an additional hour at 37°C (c and f) to allow recycling. To detect the entire population of trafficked antibodies, cells were fixed and permeabilized (PFA/MeOH) (a-c). To detect only the antigens present at the cell surface, cells were fixed in 4% PFA for 30 min at RT (d-f). Bar, 10 μ m. (B) Clone 9 cells exogenously expressing pIgA-R were double labeled for steady state (ss) distributions of pIgA-R (a) and mannosidase II (mann II) (b). Arrows are pointing to Golgi structures containing pIgA-R. In c, cells were continuously labeled with anti-pIgA-R antibodies for 60 min for 37°C. Cells were fixed and permeabilized and labeled to detect the trafficked (tr) antibody. No pIgA-R was detected. (C) Clone 9 cells overexpressing DPPIV and pIgA-R were treated in the absence or presence of 1 mg/ml biotin as indicated (see Materials and Methods). The unbound (UB) and bound (B) samples were immunoblotted for DPPIV and pIgA-R as indicated. The arrow is marking the mature form of DPPIV

In contrast, when MAL2 was coexpressed in Clone 9 cells, pIgA-R distributed to the MAL2-positive apical compartment and the plasma membrane (Figure 13A, a-c). Double labeling with mannosidase II further confirmed that the intracellular puncta were not the Golgi (Figure 13A, d-f). To confirm that pIgA-R was delivered to the plasma membrane in MAL2 expressing cells, we surface labeled cells with biotin as described for Figure 12. Virtually no pIgA-R (~0.6% of total) was detected at the plasma membrane in cells without MAL2 (Figure 13B). In striking contrast, surface delivery of pIgA-R was greatly enhanced (> 9-fold) in MAL2 coexpressing cells (Figure 13B). For comparison, we monitored DPPIV delivery in singly infected cells or in cells coexpressing MAL2. As shown in Figure 13B, no change in plasma membrane association was observed indicating that DPPIV distributions are MAL2 independent. To determine whether pIgA-R was delivered from the cell surface to the apical compartment, we continuously labeled MAL2 coexpressing cells with anti-pIgA-R as described above. As shown in Figure 13C, pIgA-R was robustly internalized and delivered to intracellular structures. Double labeling further revealed that the internalized pIgA-R was delivered to structures that were also positive for MAL2 (Figure 13C, a-c). Thus, in MAL2 coexpressing cells, pIgA-R distributed to the apical compartment and recycled between it and the cell surface.

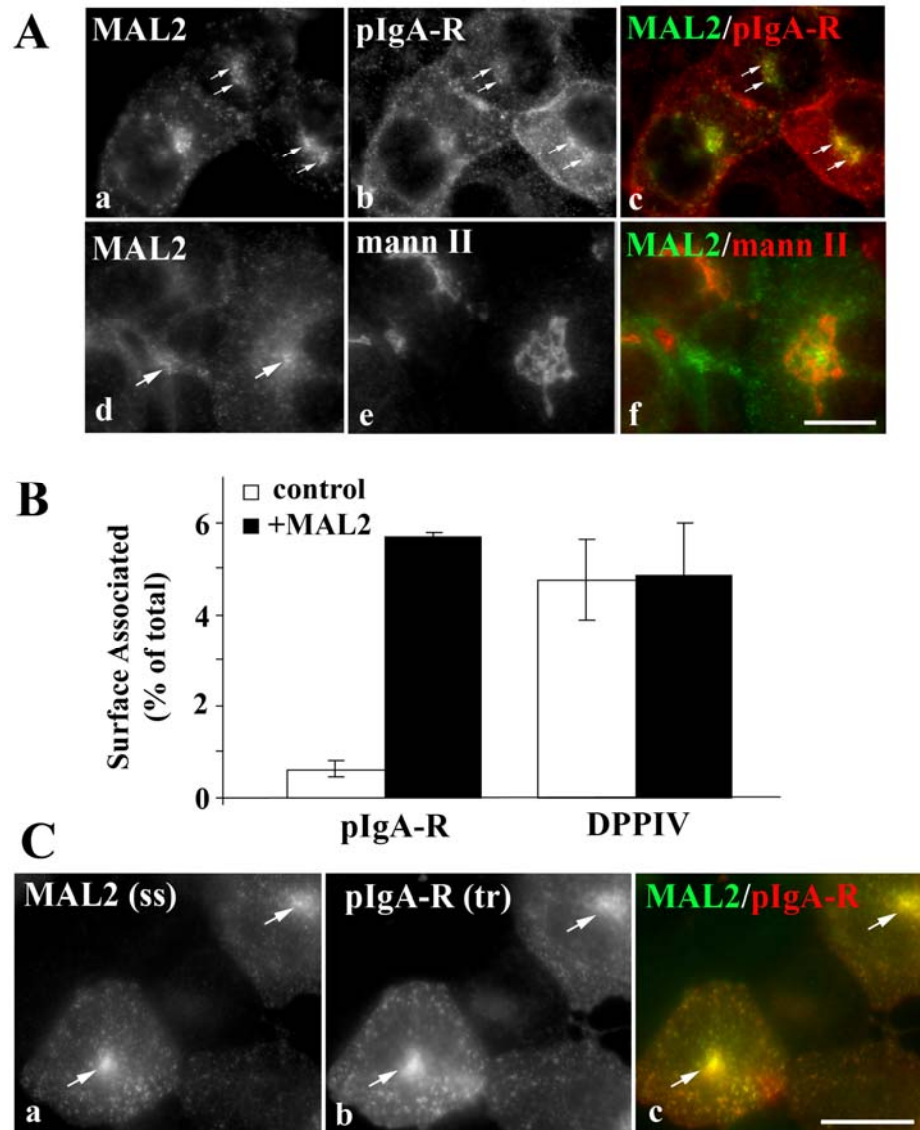


Figure 13. MAL2 expression in Clone 9 cells redistributes pIgA-R to the plasma membrane. (A) Clone 9 cells were infected with both pIgA-R and MAL2 recombinant adenoviruses (a-f). After 20 h of expression, cells were stained for the steady state (ss) distributions of MAL2 and pIgA-R (a-c) or MAL2 and mannosidase II (mann II) (d-f). Arrows are pointing to puncta that contain both MAL2 and pIgA-R (a-c) or only contain MAL2 (d-f). (B) Clone 9 cells were infected with DPPIV or pIgA-R recombinant adenovirus alone (open bars) or with MAL2 (black bars). After 20 h of expression, cells were surface biotinylated (see Materials and Methods). The unbound and bound samples were immunoblotted for pIgA-R or DPPIV and the percent surface association was determined by densitometric analysis of immunoreactive bands. Values are expressed as the mean \pm SEM. Measurements were done on at least three independent experiments. (C) Cells were continuously labeled with anti-pIgA-R antibodies for 60 min for 37°C. Cells were fixed and permeabilized and labeled to detect steady state (ss) MAL2 distributions and the trafficked (tr) pIgA-R. Bar, 10 μ M

To monitor Golgi to plasma membrane delivery directly, we measured plasma membrane association of a pIgA-R cohort in cycloheximide-treated Clone 9 cells using surface biotinylation. In cells overexpressing only pIgA-R, there was virtually no receptor detected at the plasma membrane for any time point indicating very low levels of surface expression consistent with our morphological observations (Figure 14A). In contrast, significant plasma membrane labeling was observed in cells expressing MAL2 (Figure 14A) that decreased after prolonged exposure in cycloheximide (Figure 14B). After 90 min of chase, only 68% of pIgA-R remained at the cell surface indicating the newly synthesized pIgA-R had traversed the plasma membrane and was delivered to the intracellular “apical” structures. In comparison, DPPIV surface association did not change in cells expressing MAL2 (Figure 14B). In both cases, decreased DPPIV was detected in the plasma membrane in cycloheximide-treated cells (Figure 14B and data not shown). Thus, we conclude that MAL2 selectively regulates delivery of pIgA-R from the Golgi to the plasma membrane.

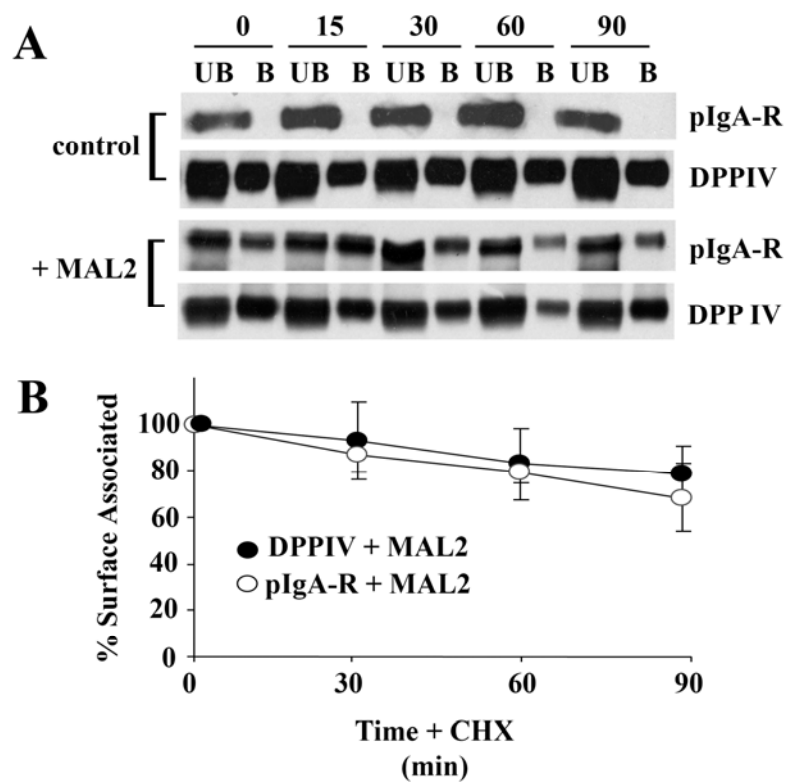


Figure 14. MAL2 expression is required for pIgA-R delivery from the Golgi to the plasma membrane in Clone 9 cells. (A) Clone 9 cells were infected with DPPIV or pIgA-R recombinant adenovirus alone or with MAL2 as indicated. After 20 h of expression, cells were treated with 50 μ g/ml cycloheximide for the indicated times. Cells were chilled on ice and surface biotinylated (see Materials and Methods). The unbound (UB) and bound (B) samples were immunoblotted for pIgA-R or DPPIV as indicated. Representative immunoblots are shown from at least three independent experiments. (B) The percent surface association of DPPIV and MAL2 was calculated from densitometric analysis of immunoreactive bands as shown in A. The 0 min values were set to 100% and the percent of pIgA-R or DPP IV that remained surface associated was calculated. Values are expressed as the mean \pm SEM. Measurements were done on at least three independent experiments

We confirmed these results in WIF-B cells where MAL2 expression was knocked down. Because WIF-B cells are recalcitrant to transfection with conventional reagents to introduce oligonucleotides or siRNA, we chose an anti-sense approach using recombinant adenovirus. After 20 h of infection, MAL2 levels were decreased to 38% of control (Figure 15A). Although this incomplete knockdown precluded quantitative biochemical

analysis, morphological examination of MAL2 knockdown cells was performed. In control cells, pIgA-R was detected in the same biosynthetic and transcytotic structures as was described previously in Figure 8 (Figure 15C, a). However, in cells where MAL2 expression was knocked down, pIgA-R was detected only in the Golgi. Two examples are shown in Figure 15C (b-e). The percent cells exhibiting basolateral populations of pIgA-R was calculated for cells where MAL2 expression was not detected (-), somewhat visible (-/+) or present at normal levels (+) (Figure 15B). In cells with complete MAL2 knockdown, no basolateral receptor populations were observed whereas in cells expressing endogenous MAL2 levels, almost 100% of cells were positive for basolateral pIgA-R staining. In contrast, DPPIV distributions were not changed in MAL2 knockdown cells (Figure 15D). In both control and knockdown cells, intracellular and apical membrane distributions of DPPIV were observed. When quantitated, 100% of cells in all three MAL2 expression level categories were positive for basolateral DPPIV labeling (Figure 15B).

We next examined transcytosis of DPPIV and pIgA-R in MAL2 knockdown cells. Cells were antibody labeled at 4°C and the antibody-antigen complexes chased for 1 h at 37°C. Basolateral labeling at 4°C of both DPPIV (Figure 16A, a) and pIgA-R (Figure 16B, a) was observed in control cells, and after 1 h of chase, both proteins were delivered to the apical membrane with a reciprocal decrease in basolateral labeling (Figures 16A, f and 16B, h). In MAL2 knockdown cells, DPPIV basolateral labeling at 4°C was not changed (two examples are shown in Figure 16A) indicating its TGN to surface delivery is MAL2 independent.

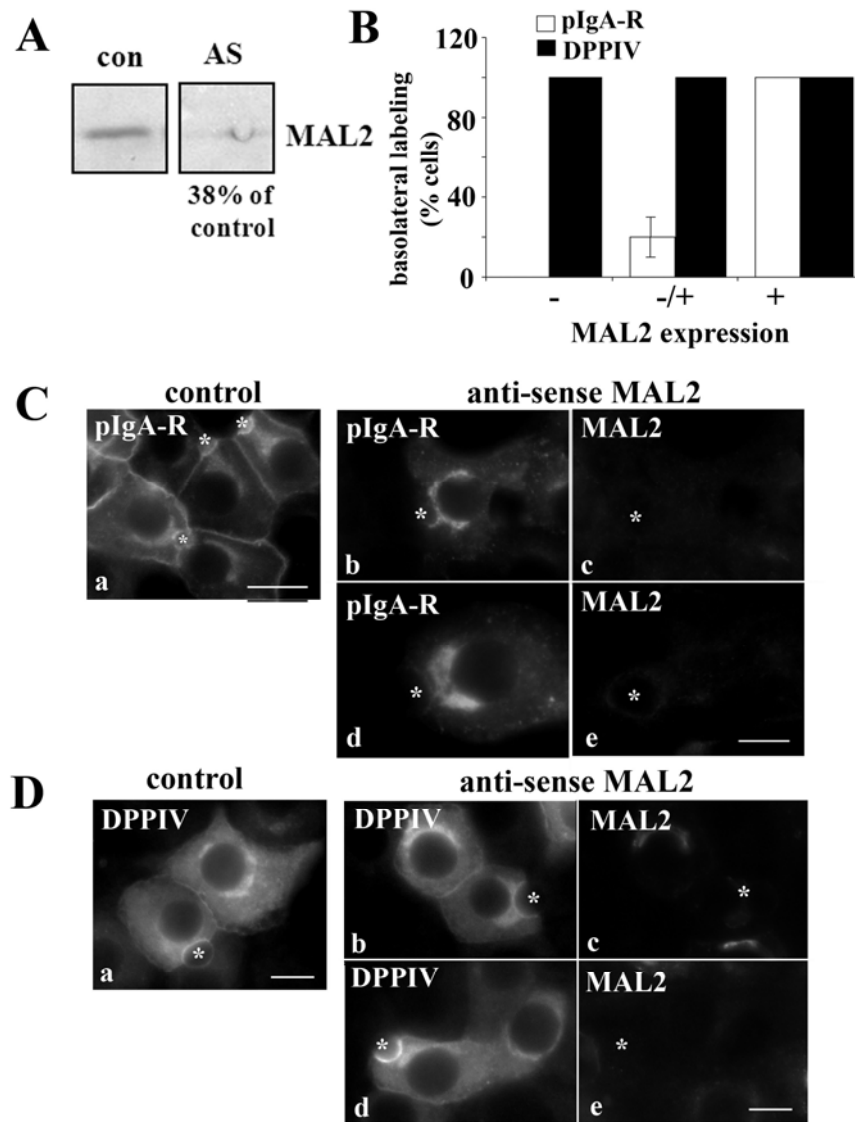


Figure 15. In WIF-B cells with MAL2 expression knocked down, pIgA-R, but not DPPIV, is present only in the Golgi. (A) Lysates from control (con) or MAL2 antisense virus (AS) expressing cells were immunoblotted for MAL2. WIF-B cells were infected with pIgA-R (C) or DPPIV (D) alone or with MAL2 anti-sense adenoviruses (B-D) for 60 min as indicated. After 20 h, cells were fixed and labeled for pIgA-R, DPPIV or MAL2 as indicated. Asterisks are marking selected BCs. Bar, 10 μ m. In B, The percent cells positive for pIgA-R or DPPIV basolateral labeling was determined for cells expressing no (-), low (-/+) and normal (+) levels of MAL2. The calculations for pIgA-R were performed on three independent experiments. Values are expressed as the mean \pm SEM. The calculations for DPPIV were performed on two independent experiments. Values represent the average

Consistent with MAL2's known role in transcytosis from early endosomes to the SAC (de Marco *et al.* 2002), the apical delivery of DPPIV was impaired in MAL2 knockdown cells (Figure 16A, g and h) and intracellular puncta were observed (Figure 16A, g, marked with arrows).

In contrast, no pIgA-R labeling was detected in MAL2 knockdown cells (Figure 16B, d) consistent with impaired basolateral delivery. However, some surface labeling was detected in cells where MAL2 expression was only partially knocked down. Two examples are shown in Figure 16B (b and c). The percent cells with basolateral pIgA-R populations was calculated as described for Figure 15. In cells with complete MAL2 knockdown, no basolateral receptor populations were observed whereas in cells expressing low or endogenous MAL2 levels, basolateral pIgA-R labeling was observed (Figure 16C). After 1 h of chase, no pIgA-R was detected in cells with complete MAL2 knockdown consistent with a lack of surface labeling at 4°C. However, in cells with partial MAL2 knockdown, pIgA-R apical delivery was impaired and the receptor was detected in intracellular puncta (Figure 16B, i; marked with arrows) confirming that MAL2 regulates pIgA-R transcytosis (de Marco *et al.* 2002).

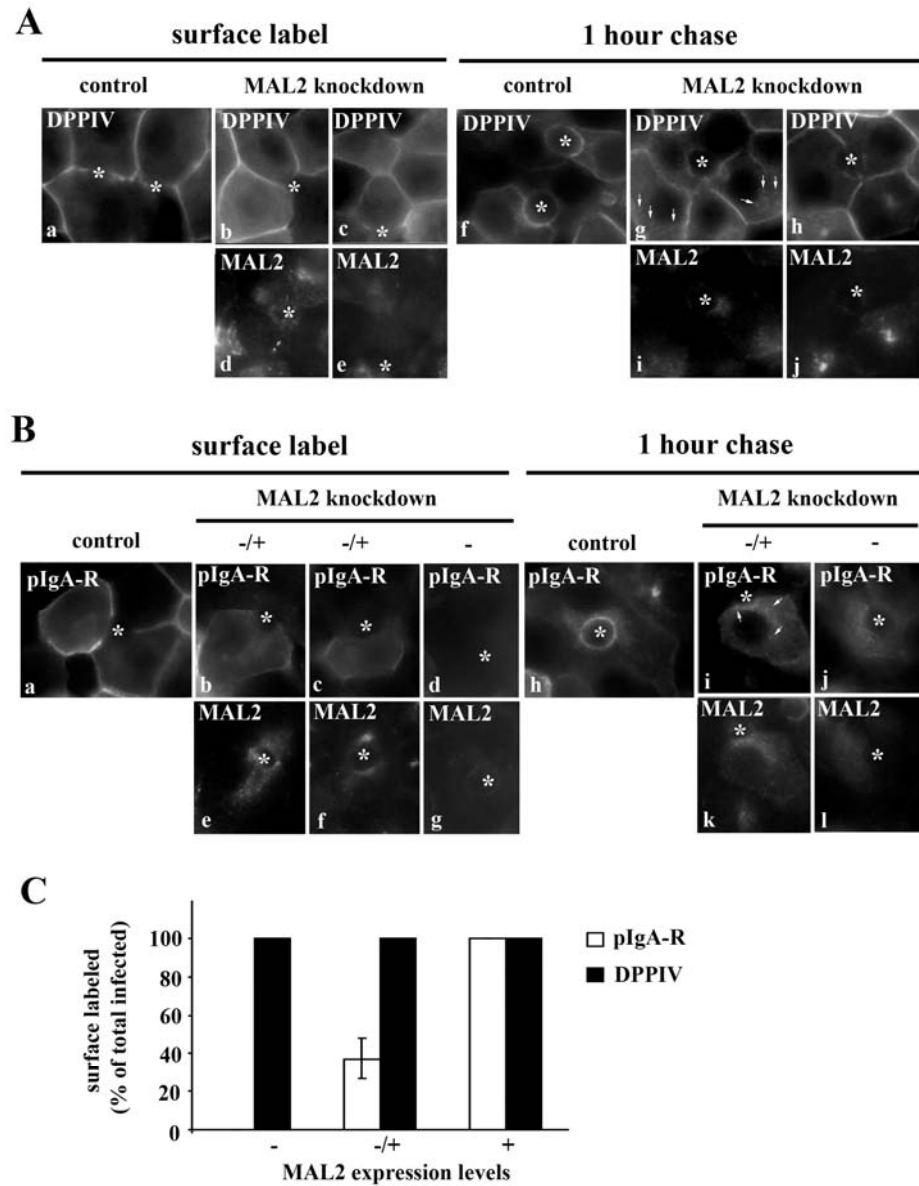


Figure 16. MAL2 knockdown in WIF-B cells inhibits basolateral delivery of pIgA-R, but not DPPIV, yet DPPIV transcytosis is impaired. WIF-B cells were infected with DPPIV (A) or pIgA-R (B) alone or with MAL2 anti-sense adenoviruses for 60 min as indicated. After 20 h, DPPIV or pIgA-R were surface-labeled for 30 min at 4°C (A, a-c; B, a-d) with specific antibodies. Antibody-antigen complexes were chased for 1 h at 37°C (A, f-h; B, h-j). Cells were fixed and permeabilized and labeled to detect the trafficked antibody. Arrows are marking intracellular puncta in MAL2 knockdown cells. Asterisks are marking selected BCs. Bar, 10 μ M. In C, the percent cells positive for pIgA-R or DPPIV basolateral labeling was determined for cells expressing no (-), low (-/+) and normal (+) levels of MAL2. The calculations were performed on at least three independent experiments. Values are expressed as the mean \pm SEM

CONCLUSIONS

We began these studies with the intention of studying the role of MAL2 in lipid-dependent transcytotic sorting at the early endosome. However, the observation that endogenous MAL2 redistributed to the Golgi in pIgA-R overexpressing cells and was “chased” to the apical membrane along with the receptor led us to examine whether MAL2 also functions in plasma membrane delivery from the Golgi. Our studies in Clone 9 cells and WIF-B cells with MAL2 expression knocked down revealed that MAL2 selectively mediates transport of pIgA-R from the Golgi to the plasma membrane. Thus, MAL2 regulates multiple steps of pIgA-R’s cellular itinerary.

Part II: Characterization of STK16, a novel MAL2 interactor, in WIF-B hepatic cells

Summary

Previously, we found that MAL2 functioned in the basolateral targeting of newly synthesized pIgA-R, giving it an additional function to its known role in basolateral to apical transcytosis. Recent characterization of various known MAL2 interactors, such as, informin2, mucin1 and the tumor protein D52 family, have suggested that MAL2 functions in multiple sorting roles in polarized cells. This fact coupled with the complexity of the machineries regulating vesicle budding and targeting further suggest that there are more proteins yet to be identified. To identify other MAL2 binding partners, we initiated a split-ubiquitin Y2H screen of human liver cDNA. We identified 19 novel interactors, including serine/threonine kinase 16 (STK16), an atypical lipid-anchored kinase previously found to be enriched in liver. Co-immunoprecipitations in both rat liver and polarized, hepatic WIF-B cells confirmed the interaction between MAL2 and STK16. Morphological studies found that when overexpressed, STK16 localized mainly to the Golgi with a smaller amount at the basolateral membrane. However, kinase-dead STK16 (KD-STK16) localized to large, bright puncta in the cell periphery. In overexpressing cells, the Golgi remained intact and KD-STK16 was found to be directed to the proteosome for degradation. Interestingly, KD-STK16 overexpressing cells had decreased levels of the secretory proteins, albumin and haptoglobin. Knockdown of endogenous MAL2 also resulted in decreased levels of albumin. Immunoblots revealed that the secretion and overall levels of albumin were

reduced in these cells. However, when treated with ammonium chloride to deacidify lysosomes, intracellular albumin levels were increased, indicating that without regulation imparted by STK16, secretory proteins are directed to lysosomes. Interestingly, treatment with brefeldin A (which inhibits ER to Golgi protein transport and induces retrograde transport of Golgi proteins to the ER) had no effect on the KD-STK16 puncta. The lack of redistribution indicated that KD-STK16 is residing in post-Golgi structures. In cells held at 19°C for 4 h to stop post-TGN trafficking, KD-STK16 surprisingly redistributed to the Golgi. Removal of the temperature block led to a very quick redistribution of KD-STK16 into the large peripheral puncta, further indicating that they are in post-Golgi structures. In contrast to KD-STK16, brefeldin A treatment led to the redistribution of STK16 to the ER (as expected) but also to the basolateral membrane, an unexpected result. Together, these results suggest that STK16 cycles between the Golgi and basolateral membrane. Thus, we conclude that not only does MAL2 selectively regulate the basolateral delivery of pIgA-R from the *trans*-Golgi, it also regulates basolateral constitutive secretion with the help of STK16.

RESULTS

A split-ubiquitin yeast 2-hybrid screen reveals 19 novel MAL2 interactors

To identify novel MAL2 interactors that function in hepatic trafficking, a split ubiquitin Y2H screen of a human liver cDNA library was performed with a full-length human MAL2 as bait. Although other known interactors of MAL2 have been found using a traditional Y2H screen, we chose to use a split-ubiquitin Y2H as it is optimized to detect protein interactions between membrane-bound proteins.

In yeast, ubiquitin can be ‘split’ and expressed as the N-terminal half (known as Nub) or the C-terminal half (known as Cub). Nub and Cub have a natural high affinity for each other and will spontaneously reassemble to ‘split-ubiquitin.’ The bait protein is fused with the Cub motif which is followed by a reporter protein. In our system, the reporter protein is a fusion of the LexA DNA-binding domain and the Herpes simplex VP16 transactivator complex. Upon the formation of the split-ubiquitin, the entirety of the split-ubiquitin and the reporter protein are cleaved by ubiquitin proteases. This allows the translocation of the reporter to the nucleus and the transcription of specific reporter genes in the auxotrophic yeast for growth on minimal media. The prey library is fused with the Nub motif. A point mutation (Ile13 → Gly13) in Nub (now called NubG) prevents the spontaneous reassembly of Nub and Cub. Only when the bait and prey interact will Cub and NubG come into close enough proximity to allow for reassembly into split-ubiquitin. The yeast strain NMY51, which contains most essential genetic markers, was used. For selection of transformants, colonies should grow efficiently on

SD –Leu-Trp-His-Ade media. In the absence of protein-protein interactions, colonies can grow on SD –Ade media, but will express a red color. In the presence of protein-protein interactions, the ADE2 gene is transcribed and the colonies will express a white color.

The limitation of this system is that both Cub and NubG must face the cytosolic side of the membrane. Since both the C- and N-terminal tails of MAL2 are cytosolic, we constructed two baits: MAL2-Cub (Cub fused to the C-terminal tail of MAL2) and Cub-MAL2 (Cub fused to the N-terminal tail of MAL2). To be complete, we screened two liver libraries; X-NubG (Type I membrane proteins where NubG is fused at the cytosolic C-terminus) and NubG-X (Type II membrane proteins where NubG is fused at the cytosolic N-terminus). The different combinations of bait and prey screens as well as the number of clones found are listed in Table 1.

Table 1. Yeast 2-hybrid screens.

Bait	Library	Putative Interactors
MAL2-Cub	x-NubG library (Type I)	STK16
MAL2-Cub	NubG-x library (Type II)	31 clones, 4 false positives
Cub-MAL2	x-NubG library (Type I)	7 clones, all false positives
Cub-MAL2	NubG-x library (Type II)	15 clones, 8 false positives

Y2H assays were performed with two baits; C-ubiquitin on the C-terminal tail of MAL2 (MAL2-Cub) and the N-terminal tail of MAL2 (Cub-MAL2). Type I (x-NubG) and type II membrane protein (NubG-x) libraries were used as preys.

Screening of all colony forming units resulted in 54 clones that remained viable on SD –Leu-Trp-His-Ade media (Table 1). Sequencing of all viable clones identified 19 novel interactors and 35 false positives (of which ubiquitin was the most frequent, a common false positive in split-ubiquitin Y2H screens). The known functions of the novel interactors are briefly described in Table 2. Interestingly, a number of polytopic, twelve-transmembrane (12-TM) spanning transporters were identified. In general, these types of transporters are directly delivered to their resident plasma membrane domain. The identification of these 12-TM spanning transporters suggests a potential novel role for MAL2 in direct delivery from the Golgi to the apical or basolateral membrane. In addition, MAL2 was found to interact with several ER resident proteins. Although there is no evidence of MAL2 function at the ER, others have shown that MAL2 has a strong interaction with the ER localized formin, informin2 (Madrid *et al.* 2010).

The Y2H also pulled down a predicted interactor, Rab17. The Rab GTPase family is composed of peripheral membrane proteins which likely regulate every step in membrane trafficking. Unlike most of the other Rab family members which have a more ubiquitous expression, Rab17 is only expressed in polarized epithelial cells of the kidney, liver and intestine (Lutcke *et al.* 1993). Since it was previously shown that Rab17 is an essential component of the transcytotic pathway in polarized cells (Hunziker and Peters, 1998; Zacchi *et al.* 1998), we predicted it would interact with MAL2, also a known regulator in the transcytotic pathway (de Marco *et al.* 2002; de Marco *et al.* 2006; In and Tuma, 2010). We are currently examining Rab17 and MAL2 interactions and the mechanism(s) by which they regulate transcytosis.

Table 2. Novel MAL2 interactors.

Protein	Number of Clones	Accession number	Putative function
Anti-1 antitrypsin	2	NP_000286.3	Secreted serine protease inhibitor
CD63 antigen	3	NP_001771.1	Tetraspanin involved in protein trafficking (lysosome to PM?)
Cytochrome P450 2E1	2	NP_000764.1	ER membrane monooxygenase
Fibrinogen-like 1	1	NP_004458.3	Golgi-localized member of the fibrinogen family
HIV-1 Tat interactive protein 2	1	NP_006401.3	Cytosolic enhancer of Tat-mediated transcription
Major facilitator superfamily member	1	NP_116182.2	ER membrane transporter
Monocarboxylate transporter 4	1	NP_004198.1	proton-linked 12-TM monocarboxylate transporter
NADH dehydrogenase subunit 4	1	ACA22107.1	mitochondrial membrane respiration
PRA1 family protein 3	1	NP_006398.1	Unknown
Protein disulfide isomerase	1	NP_005733.1	ER lumen protein involved in protein folding
Rab 17	1	NP_071894.1	Regulates transcytosis
Receptor expression-enhancing 6	1	NP_612402.1	Unknown
Retinol binding protein 4	2	NP_006735.2	Retinol carrier protein
Serine/threonine kinase 16	1	NP_001008910.1	Unknown
Transferrin (Tf)	1	NP_001054.1	Secreted iron-binding protein
Solute carrier family 22	1	NP_003048.1	organic cation transporter
Sterol-4-a-carboxylate 3-dehydrogenase	1	NP_057006.1	ER membrane protein involved in cholesterol biosynthesis
Translocon-associated protein b	1	NP_003136.1	Regulates the retention of ER residents
Transmembrane protein 59	1	NP_004863.2	Unknown

Nineteen novel MAL2 interactors were found in the Y2H assay. Numbers of clones found, NCBI accession numbers and known functions of each are listed.

I chose to focus my studies on a lesser known protein, serine/threonine kinase 16 (STK16). First identified in the liver of a 12 day old mouse, STK16 is highly expressed in the liver, kidney and testis and has been shown to be a constitutively active kinase (Ligos *et al.* 1998; Eswaran *et al.* 2008). Sequence analysis of the 305-amino acid STK16 found consensus sequences for N-terminal myristoylation followed by palmitoylation at cysteines 6 and 8 (Figure 17, depicted in red). Structural analysis revealed a protein kinase C (PKC) catalytic domain spanning residues 26-290. Within the PKC domain is an atypical activation segment consisting of an extended β -sheet in the loop region followed by an α -helix. Though most kinases begin their activation segment with a conserved DFG motif; the activation segment of STK16 begins with the variant DLG, a semi-conserved initiation motif found in less than 6% of protein kinases (Eswaran *et al.* 2008).

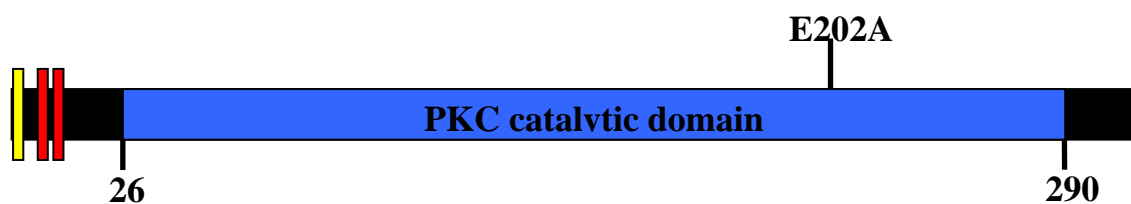


Figure 17. Schematic of full-length STK16. Based on structural analyses predictions, N-terminal membrane anchors include myristoylation at glycine 2 (depicted in yellow) and palmitoylation at cysteines 6 and 8 (depicted in red). Predicted PKC catalytic domain spanning positions 26-290 is depicted in blue. The kinase-dead point mutation is at position 202, from glutamic acid to alanine.

In normal rat kidney (NRK) cells, STK16 localized to the Golgi (Guinea *et al.* 2006). To date, the specific function of STK16 is not known. Interestingly, it was found that a minimal overexpression of STK16 in murine mammary glands during puberty

induced the formation of multiple buds at the terminal endbud axis of the mammary ducts (Stairs *et al.* 2005). This is in stark contrast to wild-type mice, in which a single bud forms at the mammary ducts, with no further bud formation at the terminal endbud axis. Given the effect STK16 overexpression had on mammary development, these authors suggested that STK16 may play a role in vesicular trafficking and secretion (Stairs *et al.* 2005). In addition, biochemical analyses of overexpressed STK16 *in vitro* indicated that it is possibly a subunit of a larger regulatory complex (Guinea *et al.* 2006).

MAL2 and STK16 selectively coimmunoprecipitate

To begin our studies, we examined the endogenous distribution of STK16 in rat liver after differential centrifugation. Both MAL2 and STK16 distributed to the total membrane fraction (high speed pellet, HSP) and were not found in the cytosolic fraction (high speed supernatant, HSS), suggesting they may be present on the same organelles (Figure 18A).

To further our studies on STK16, we created recombinant adenoviruses expressing a V5 epitope tag on the C-terminal end of the full-length wild type STK16 and on the kinase-dead STK16 (KD-STK16) for use in our hepatic cell line, WIF-B. The kinase activity of STK16 was ablated by a point mutation at position 202 from glutamic acid to alanine, creating the KD-STK16 mutant (Guinea *et al.* 2006). Although STK16 was shown to be a constitutively active kinase; its exact enzymatic activity and substrates are unknown (Eswaran *et al.* 2008). On immunoblots in WIF-B cells, anti-V5 tag antibodies detected a specific 35 kDa band, the molecular weight of STK16 and KD-

STK16 (Figure 18B), only in cells which had been infected with STK16 or KD-STK16. Importantly, there was no immunoreactivity in uninfected WIF-B cells. The infection efficiency of KD-STK16 was consistently ~65% less than the infection efficiency of STK16, represented in immunoblots (Figure 18B) and immunostaining (data not shown).

To examine whether the proteins are interacting, we performed coimmunoprecipitations (co-IP) in hepatic WIF-B cells. MAL2 coimmunoprecipitated with anti-V5 antibodies when WT STK16 was expressed, but not when the kinase-dead form was expressed (Figure 18C, left panel). In a reciprocal immunoprecipitation, ~1.25% of total STK16 coimmunoprecipitated with anti-MAL2, but KD-STK16 did not, suggesting MAL2 does not interact with KD-STK16. The addition of the MAL2 peptide specifically blocked MAL2 coimmunoprecipitation with STK16 (Figure 18C, right panel), further indicating that the interaction between MAL2 and STK16 is specific. The low percentage of coimmunoprecipitated STK16 is consistent with the results from pIgA-R co-IP with MAL2 (see part I results). To ensure this interaction is not due to overexpression of proteins, we performed a co-IP in rat liver of endogenous STK16 and MAL2. Endogenous STK16 was coimmunoprecipitated with MAL2 from rat liver (data not shown). This co-IP was prevented when the liver lysate was preincubated with the MAL2 peptide against which the MAL2 antibody was made indicating that the interaction is not due to overexpression of exogenous protein.

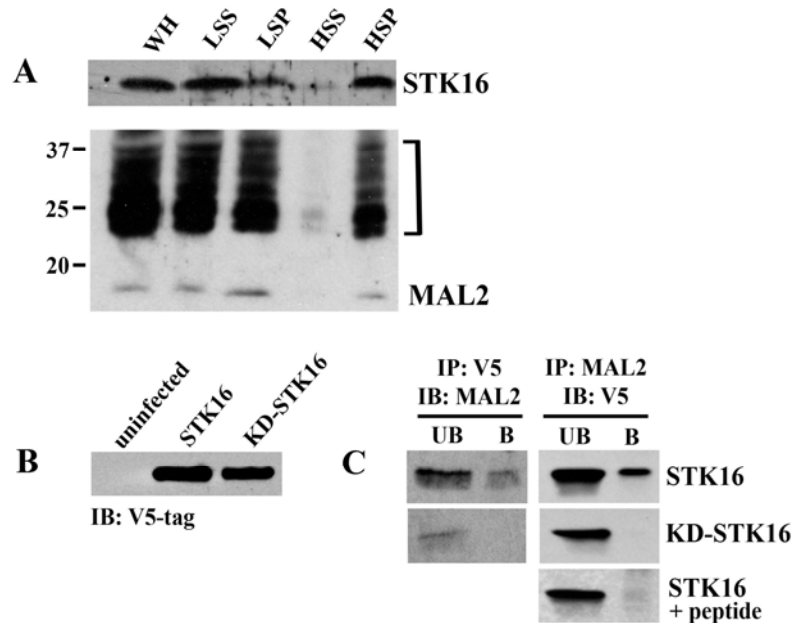


Figure 18. MAL2 specifically immunoprecipitates STK16, but not KD-STK16. (A) Rat liver fractions were immunoblotted for endogenous STK16 and MAL2. Represented fractions are the whole homogenate (WH), post-nuclear supernatant (low speed supernatant, LSS), nuclear pellet (low speed pellet, LSP), cytosol (high speed supernatant, HSS) and total membrane (high speed pellet, HSP). The diffuse MAL2 bands are bracketed. (B) WIF-B cells (uninfected or exogenously expressing V5-tagged STK16 or KD-STK16) were immunoblotted for the V5-tag. (C) WIF-B lysates from cells overexpressing V5-tagged STK16 or KD-STK16 were coimmunoprecipitated with 1 μ g affinity-purified V5-tag (left panel) or MAL2 antibodies (right panel). Unbound (UB) and bound (B) fractions were immunoblotted for MAL2 or V5-tagged STK16 or KD-STK16 as indicated.

The distribution of overexpressed STK16 and KD-STK16 was examined in both polarized WIF-B and nonpolarized hepatic Clone9 cells. In WIF-B cells, STK16 showed minimal staining at the basolateral with the majority of the intracellular staining appearing Golgi-like (Figure 19A, a). To confirm this, we double labeled STK16 overexpressing cells with mannosidase II (mann II), a Golgi marker. There was near perfect overlap of staining in the intracellular structures with mann II, confirming their Golgi identity (Figure 19A, b and c). The Golgi distribution of STK16 was also observed

when overexpressed in Clone9 cells, and confirmed by double labeling with mann II (Figure 19c, a-c). This distribution is consistent with the staining pattern seen in other nonpolarized cells (Guinea *et al.* 2006).

In contrast, KD-STK16 localized to bright puncta in the cell periphery in both WIF-B (Figure 19A, d) and Clone9 cells (Figure 19C, d). To test whether the Golgi was still intact, we double-labeled with mann II, AP-1, Vti1a and syntaxin 6 (Figure 19A, e and Table 3) in WIF-B cells and Clone9 cells (Figure 19C, e). AP-1, Vti1a and syntaxin 6 are *trans*-Golgi markers. All the Golgi markers showed normal distribution in KD-STK16 overexpressing cells, confirming that the Golgi is still intact. The bright puncta did not colocalize with any of the Golgi markers, further indicating that the puncta are not dispersed Golgi vesicles.

Interestingly, the distribution of MAL2 at the apical membrane was not changed upon overexpression of either protein. However, high levels of STK16 expression led to localization of MAL2 at the basolateral membrane (Figure 19B, a), similar to the colocalization of MAL2 and exogenously expressed pIgA-R (described in part I of results). Therefore, the co-IP between MAL2 and STK16 correlates with the expression of MAL2 at the basolateral membrane in STK16 overexpressing cells and MAL2's known itinerary through the Golgi. Additionally, the lack of colocalization between MAL2 and KD-STK16 in the peripheral puncta is consistent with no co-IP between them (Figure 19B, b).

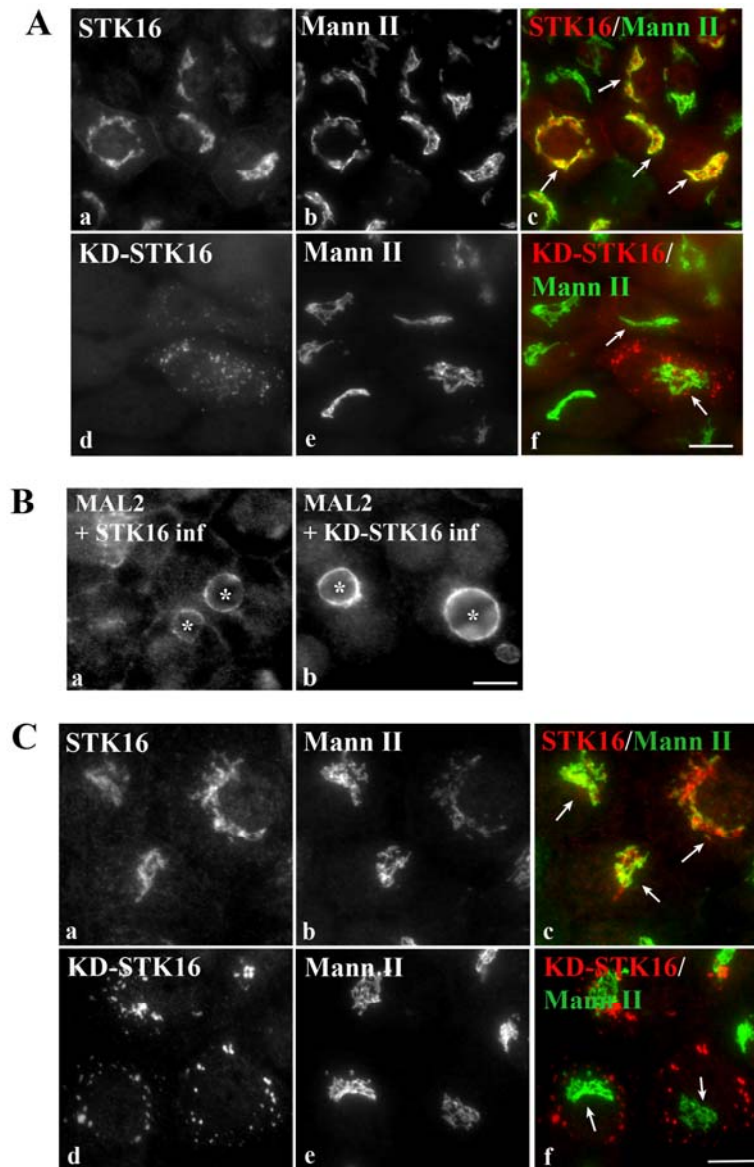


Figure 19. MAL2 minimally codistributes with STK16, but not KD-STK16.

(A) WIF-B cells were infected with recombinant adenovirus expressing STK16 (a-c) or KD-STK16 (d-f). Immunolabeling with mannosidase II confirms Golgi distribution of STK16 (b, c) and intact Golgi in KD-STK16 overexpressing cells (e, f). (B) MAL2 minimally distributes to the basolateral membrane in STK16 overexpressing cells (a) but does not change in KD-STK16 expressing cells (b). (C) Clone 9 cells were infected with recombinant adenovirus expressing STK16 (a-c) or KD-STK16 (d-f). Immunolabeling with mannosidase II confirms Golgi distribution of STK16 (b, c) and intact Golgi in KD-STK16 overexpressing cells (e, f). Arrows indicate Golgi in infected cells. Asterisks label selected BCs. Bar, 10 μ m.

KD-STK16 is present in an unidentified, post-Golgi compartment

To identify the bright KD-STK16 puncta, we double-labeled KD-STK16 overexpressing cells for various organellar markers. The markers and their subcellular locations are listed in Table 3. The endosomal and lysosomal markers tested were early endosomal antigen 1 (EEA1), endolyn-78, transferrin receptor (TfR), mannose 6-phosphate receptor (M6PR) and lysosomal glycoprotein 120 (LGP120). These markers represent the early endosome, endosomal and lysosomal membranes, recycling endosome, late endosome, and lysosome, respectively. The individual distributions of the markers did not change in KD-STK16 overexpressing cells compared to noninfected cells. In each case, the KD-STK16 puncta did not colocalize with any of the endosomal markers. Together these results indicate that KD-STK16 is not present on an endosomal compartment and on lysosomes.

Since the MAL2 Y2H pulled down a surprising number of ER resident proteins, coupled with the large size of the KD-STK16 puncta, we predicted that the puncta represented vesicles of the ER-Golgi intermediate compartment (ERGIC). To test if the bright KD-STK16 containing puncta are ERGIC vesicles, we immunolabeled KD-STK16 overexpressing cells with the ERGIC marker, ERGIC 53. As listed in Table 3, KD-STK16 did not colocalize with ERGIC 53, indicating the puncta are not ERGIC vesicles. Because the puncta resembled lipid droplets, we also stained the KD-STK16 overexpressing cells with oil red O, a dye that stains neutral lipids and fatty acids. As listed in Table 3, the KD-STK16 puncta did not colocalize with the oil red O-stained lipid droplets.

Table 3. Organelle markers for KD-STK16 colocalization.

Protein/Marker	Location	Co-localization?
Mannosidase II	<i>Cis, medial</i> Golgi	No
AP-1	<i>Trans</i> Golgi	No
Vtila	<i>Trans</i> Golgi	No
Syntaxin 6	<i>Trans</i> Golgi	No*
EEA1	Early endosome	No
Endolyn-78	Endosomal and lysosomal membranes	No
Transferrin receptor	Recycling endosome	No
Mannose 6-phosphate receptor	Late endosome	No
Lysosomal membrane glycoprotein 120	Lysosome	No
ER-Golgi intermediate compartment 53	ER-Golgi intermediate compartment	No
Oil Red O	Lipid droplet	No

Various protein markers and dyes were tested for colocalization with KD-STK16. Locations of each marker and colocalization results are listed.

It was previously found that brefeldin A (BFA) disrupts the Golgi and the TGN (Donaldson *et al.* 1992). BFA is a potent inhibitor of protein transport from the ER to the Golgi and causes proteins to redistribute to the endoplasmic reticulum (ER) since it promotes retrograde transport from the Golgi. To test if the KD-STK16 puncta

represented TGN subdomains, we treated KD-STK16 overexpressing cells with BFA. Interestingly, BFA treatment had no effect on KD-STK16 distribution (Figure 20A, a and b). The lack of redistribution identified the KD-STK16 puncta as post-Golgi vesicles, separate from the TGN. Additionally, KD-STK16 overexpressing cells were blocked at 19°C for 4 hours, a known temperature block shown to accumulate proteins at the Golgi. There was a total redistribution of KD-STK16 to the Golgi (Figure 20A, c and d). Subsequent release from 19°C, followed by a 37°C chase led to a rapid redistribution of KD-STK16 to the bright puncta. This redistribution was seen as early as 15 minutes post-chase, with complete punctate staining seen 60 minutes post-chase (data not shown). These results further confirm that KD-STK16 is in a post-Golgi vesicle.

STK16 is itinerant from the Golgi to the basolateral PM

From the previous results, we determined that STK16 is localized mainly to the Golgi and KD-STK16 is in a post-Golgi vesicle. Interestingly, higher levels of STK16 overexpression results in some basolateral staining as well. However, when STK16 overexpressing cells were treated with BFA, only a small proportion of STK16 distributed to the ER, as seen by the diffuse background staining. Interestingly, STK16 staining was mostly seen at the basolateral membrane (Figure 20B, a and b) indicating a pool of STK16 may be in post-Golgi structures at steady state. This result shows that STK16 is an itinerant protein, as it can be localized to the Golgi and the basolateral membrane.

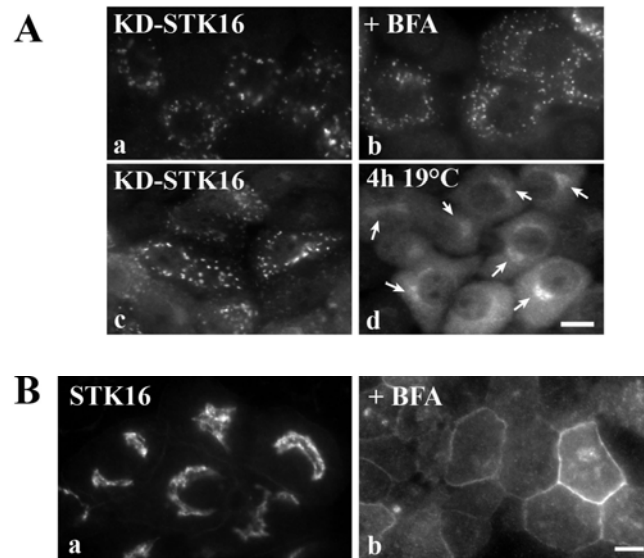


Figure 20. KD-STK16 is present in a post-Golgi compartment. (A) WIF-B cells were infected with recombinant adenovirus expressing KD-STK16. After 20 h of expression, cells were incubated with 10 µg/ml brefeldin A for 1 h (b) or a 19°C block for 4 h (d). Cells were immunolabeled for V5-KD-STK16. Arrows are indicating the accumulation of KD-STK16 in the Golgi. (B) WIF-B cells exogenously expressing STK16 were incubated with 10 µg/ml brefeldin A for 1 h (b). Cells were immunolabeled for V5-STK16. Bar, 10 µm.

KD-STK16 expression results in a decrease of albumin secretion

Because others hypothesized that STK16 may be function in regulating secretion (Stairs *et al*, 2005; Guinea *et al*, 2006), we examined the localization and secretion of albumin and haptoglobin, two abundant secreted serum proteins synthesized by the liver and often used as markers to assess overall liver health. Upon overexpression of STK16, both albumin and haptoglobin showed no change in distribution. Both albumin and haptoglobin showed overlapping localization with overexpressed STK16 at the Golgi (Figure 21A a-d). Soluble forms of both secretory proteins were also visible throughout the biosynthetic pathway, including the ER. In contrast, the overall stain of albumin and

haptoglobin was sharply decreased in KD-STK16 overexpressing cells. As seen in Figure 21B, albumin and haptoglobin mainly localized to the Golgi in cells which were not expressing KD-STK16. However, neighboring infected cells showed a large decrease in albumin and haptoglobin staining (Figure 21B, b and d). During a 19°C temperature block, albumin began to accumulate in the Golgi in KD-STK16 overexpressing cells (Figure 21C). A slight increase in albumin staining at the Golgi was seen at 2h at 19°C (Figure 21C, a) with comparable levels of albumin compared to uninfected cells at 4h at 19°C (Figure 21C, b). This suggests KD-STK16 expression is not causing defects in the synthesis of the secretory proteins. Additionally, whole cell extract lysates of KD-STK16 overexpressing cells showed a marked decrease of expression of the mature form of albumin and haptoglobin, whereas there was no change in expression in STK16 overexpressing cells (Figure 21D). Furthermore, there was no change in expression of the two immature forms of albumin (preproalbumin and proalbumin) in KD-STK16 overexpressing cells. These immature forms are found in the ER and Golgi, respectively. The decrease in expression of only the mature albumin further confirms that the block caused by KD-STK16 occurs after ER processing and at a later post-Golgi step.

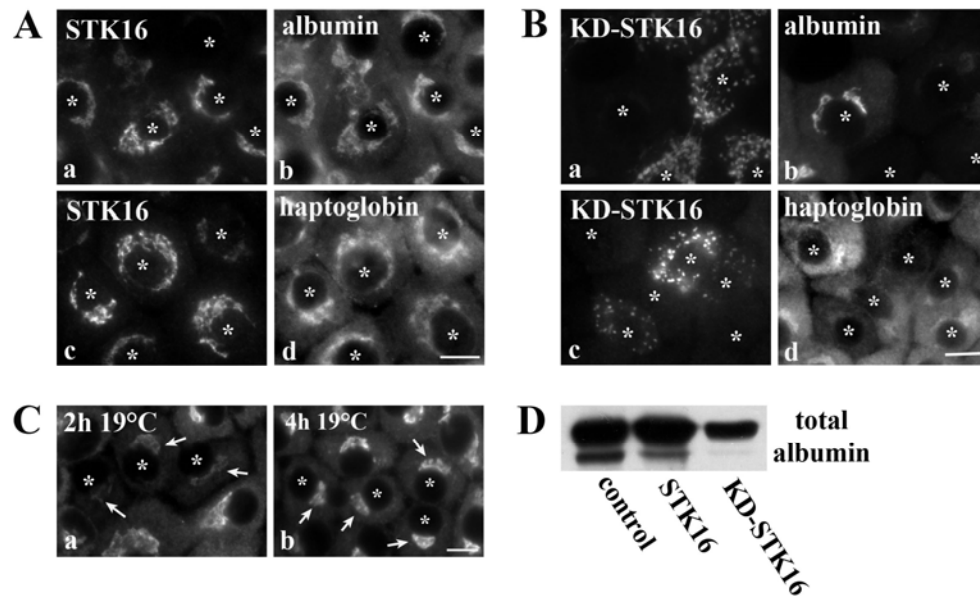


Figure 21. Albumin and haptoglobin expression is decreased in KD-STK16 overexpressing cells. (A) Cells exogenously expressing STK16 were immunolabeled for V5-STK16 (a, c), albumin (b) and haptoglobin (d). (B) Cells exogenously expressing KD-STK16 were immunolabeled for V5-KD-STK16 (a, c), albumin (b) and haptoglobin (d). (C) KD-STK16 overexpressing cells were incubated at 19°C for 2 (a) or 4h (b). Cells were immunolabeled for albumin. Arrows indicate the Golgi in cells exogenously expressing KD-STK16. Asterisks are marking nuclei of individual cells. Bar, 10 μ m. (D) WIF-B cell lysates (control, STK16 or KD-STK16 overexpressing) were immunoblotted for albumin. Note the presence of the immature pre- and pro- forms of albumin in all lysates.

The decrease in staining of both albumin and haptoglobin can be explained by two reasons: the expression of KD-STK16 is causing the secretory proteins to be 1) hypersecreted or 2) degraded. For the first possibility, a lack of regulation due to KD-STK16 expression results in *en masse* secretion, thus emptying the pipeline. The overall lack of secretory protein staining, even at the ER, is consistent with this hypothesis. Alternatively, for the second possibility, the lack of regulation caused by overexpression of KD-STK16 results in rerouting of the secretory proteins for degradation in lysosomes, due to improper sorting at the Golgi.

To test whether the proteins were hypersecreted upon KD-STK16 overexpression, we measured levels of albumin and haptoglobin in the cell medium from control, STK16 overexpressing, and KD-STK16 overexpressing cells. The cells were washed with complete serum-free medium to remove all previously secreted proteins. One mL of complete serum-free medium was added to the cells and aliquots were collected at various timepoints and the amount of secretion was measured via immunoblotting. As seen in Figure 22A and B, in control (noninfected) and STK16 overexpressing cells, the levels of albumin steadily increased in the medium over the hour. However, in KD-STK16 overexpressing cells, while the rate of albumin secretion was the same, the levels of secretion were markedly decreased for each timepoint. Whole cell lysates of each condition were collected post-secretion to assess the levels of intracellular albumin (Figure 22A, left panels). Control and STK16 overexpressing cells had comparably high levels of albumin whereas the levels of albumin in KD-STK16 overexpressing cells were decreased by ~48% after 60 min of secretion. The decrease in albumin levels both intracellularly and in the medium likely reflects the infection levels of KD-STK16. That is, the uninfected cells on the coverslip continue to secrete normally, while secretion in the KD-STK16 expressing cells is impaired. In general, the infection efficiency of the KD-STK16 is ~40%, which is consistent with a ~45% decrease in intracellular albumin, as seen by immunoblotting.

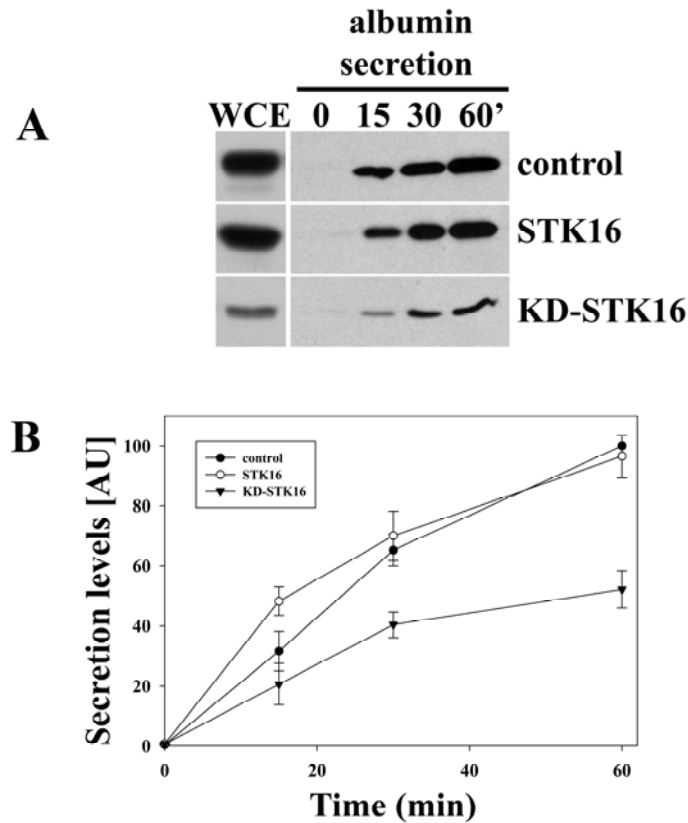


Figure 22. KD-STK16 expression results in decrease in albumin secretion. (A) WIF-B cells were uninfected (control) or infected with recombinant adenovirus expressing STK16 or KD-STK16. After 20 h of expression, cells were washed and reincubated in serum-free medium. At 0, 15, 30 and 60 minutes after reincubation, aliquots of media were collected and analyzed for albumin secretion by immunoblotting. Post-secretion whole cell lysates (left panels) were immunoblotted for intracellular albumin. (B) Arbitrary units of secretion levels were calculated by densitometric analysis of immunoreactive bands as shown in (A). Values are expressed as the mean \pm SEM. Measurements were done on at least three independent experiments.

KD-STK16 expression results in albumin redirection to lysosomes

To test if albumin was redirected to the lysosomes and degraded, KD-STK16 overexpressing cells were treated with 50 mM NH_4Cl for various timepoints. NH_4Cl , a weak base, increases the lysosomal pH, therefore inhibiting lysosomal degradation and

allowing for protein accumulation and detection. As shown in Figure 23A, a-f, albumin staining gradually increased in KD-STK16 expressing cells after a prolonged NH_4Cl treatment. This was confirmed via immunoblots (Figure 23B). For comparison, the levels of MAL2, albumin and STK16 were not changed in STK16 overexpressing cells where treated with NH_4Cl (Figure 23C). To further confirm specific lysosomal degradation, cells overexpressing KD-STK16 were treated with lactacystin (LAC), a potent, irreversible inhibitor of proteosomal degradation (Figure 24B). Unlike in NH_4Cl treated cells, albumin levels remained low, indicating KD-STK16 did not lead to redirection of secretory proteins to the proteosome.

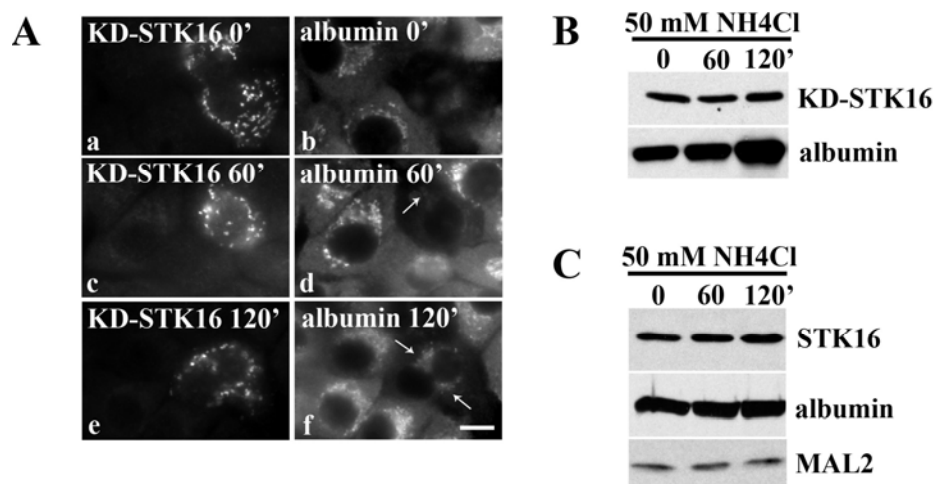


Figure 23. Albumin is rerouted to the lysosomes in KD-STK16 overexpressing cells. (A) Cells were infected with recombinant adenovirus expressing KD-STK16. After 20 h of expression, cells were incubated with 50 mM ammonium chloride (NH_4Cl) for the indicated times. Cells were fixed and stained for V5-KD-STK16 (a, c, e) and albumin (b, d, f). Arrows are pointing to the population of albumin after NH_4Cl treatment. Bar, 10 μm . (B) Whole cell lysates from cells exogenously expressing KD-STK16 after incubation with NH_4Cl were immunoblotted for V5-KD-STK16 and albumin. (C) Whole cell lysates from cells exogenously expressing STK16 after incubation with NH_4Cl were immunoblotted for V5-STK16, albumin and MAL2.

However, an unexpected observation was that KD-STK16 expression was increased and in nearly every cell with LAC treatment. In Figure 24A (a-b), cells are exogenously expressing KD-STK16 with ~40% infection efficiency. However, upon LAC treatment, the infection efficiency increased to ~90% (Figure 24A, c) while albumin staining was markedly decreased in nearly every cell (Figure 24A, d). This was further confirmed via immunoblot. With prolonged LAC treatment, expression levels of KD-STK16 increased and inversely, expression levels of albumin decreased. As a control, expression levels of MAL2, which is not known to undergo proteosomal degradation, did not change in the cell lysates (Figure 24B). Levels of albumin secretion post-LAC treatment were decreased by ~86% compared to control cells and by ~38% compared to KD-STK16 (no LAC treatment) expressing cells. Again, this likely reflects the infection levels of KD-STK16 (Figure 24C and D). Since KD-STK16 cannot be degraded via the proteasome, it remains in nearly every cell, resulting in increased albumin rerouting to lysosomal degradation.

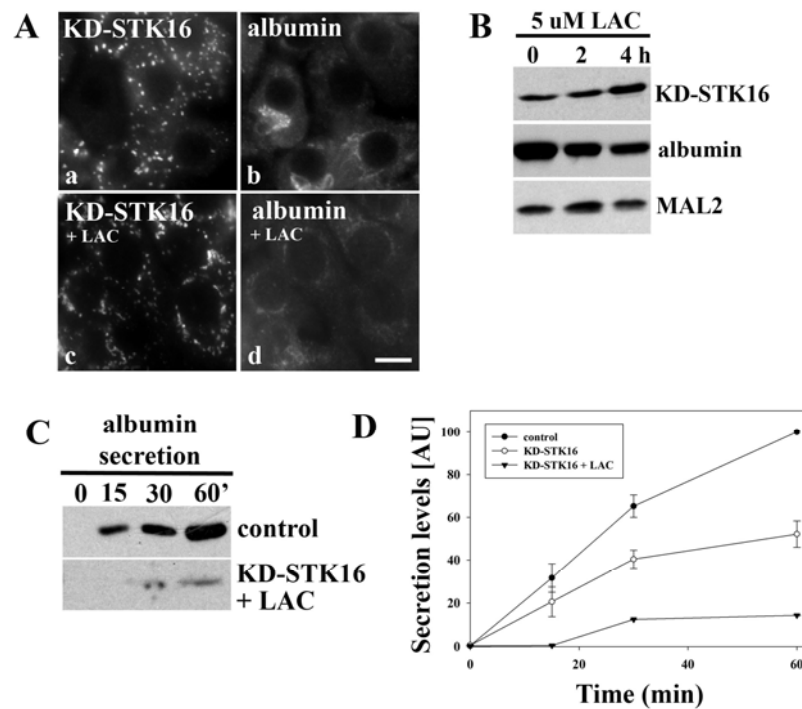


Figure 24. Lactacystin prevents KD-STK16 degradation, but promotes albumin degradation. (A) Cells were infected with recombinant adenovirus expressing KD-STK16. After 20 h of expression, cells were incubated with 5 μ M lactacystin (LAC) for 4 h. Control and LAC-treated cells were fixed and stained for V5-KD-STK16 (a, c) and albumin (b, d). Bar, 10 μ m. (B) Whole cell lysates from cells exogenously expressing KD-STK16 were incubated with LAC for the indicated times. The lysates were then immunoblotted for V5-KD-STK16, albumin and MAL2. (C) Uninfected (control) or KD-STK16 expressing cells were incubated with LAC for 4 h. Cells were then washed and reincubated in serum-free medium in the continued presence of LAC. After reincubation, albumin secretion was analyzed by immunoblotting. (D) Secretion levels were calculated by densitometric analysis of immunoreactive bands shown in (C). Values are expressed as the mean \pm SEM. Measurements were done on at least two independent experiments.

MAL2 regulates albumin secretion

If STK16 and MAL2 are bona fide binding partners, the prediction is that MAL2 also regulates constitutive secretion. To test this possibility, cells were infected with an adenovirus expressing antisense MAL2 for 48h to knock down endogenous MAL2. As

seen in Figure 25A, MAL2 levels were decreased to 47.6% of control. Interestingly, the higher and lower molecular weight bands surrounding the 30-38 kDa set of diffuse bands (Figure 25A, in brackets) on a MAL2 immunoblot also decreased, indicating they may represent different post-translational forms of MAL2.

As seen in KD-STK16 expressing cells, the rate of albumin secretion remained the same but the levels of secretion were markedly decreased in MAL2 knockdown cells (Figure 25B, C). Similarly, the intracellular albumin levels were decreased in cells with MAL2 knockdown (Figure 25 B, left panel). As for KD-STK16 overexpressing cells, the decrease in albumin levels both intracellularly and in the medium likely reflects the infection levels. The uninfected cells, or MAL2 expressing cells, continue to secrete, while the infected, or cells with knocked down MAL2 expression, display impaired secretion. This result not only finds yet another functional role for MAL2 but also implies that secretion is reliant on both MAL2 and STK16.

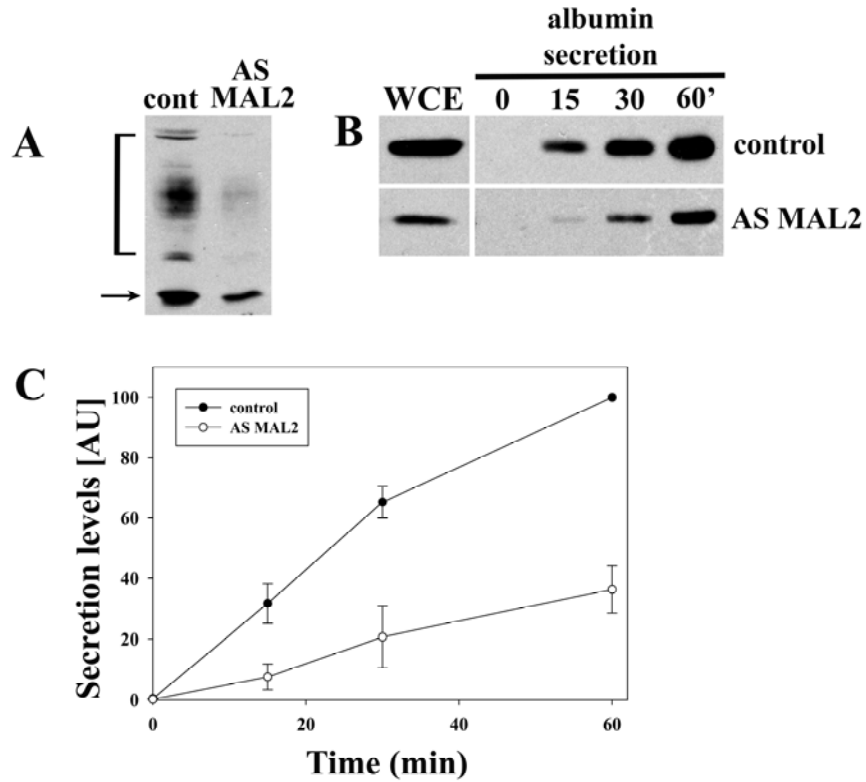


Figure 25. MAL2 regulates albumin secretion. A) WIF-B cells were uninfected (control) or infected with a recombinant adenovirus expressing anti-sense (AS) MAL2. After 48 h of expression, lysates were immunoblotted for MAL2. The bracket highlights the diffuse set of bands and the arrow indicates the 19 kDa MAL2. B) Control and AS MAL2 expressing cells were washed and reincubated in serum-free medium. After reincubation, aliquots of media were collected at the indicated times and analyzed for albumin secretion by immunoblotting. Post-secretion whole cell lysates (left panels) were immunoblotted for intracellular albumin. C) Secretion levels were calculated by densitometric analysis of immunoreactive bands as shown in (B). Values are expressed as the mean \pm SEM. Measurements were done on at least three independent experiments.

CONCLUSIONS

We began these studies with the intention of further characterizing and determining the functions of MAL2 in polarized hepatic trafficking with the use of a split-ubiquitin Y2H screen. However, the unique distribution and proposed functions of MAL2's novel binding partner, STK16, led us to examine the role of STK16 in basolateral secretion. Our studies in WIF-B cells confirmed that STK16 resides in the Golgi while its kinase-dead mutant, KD-STK16, is on post-Golgi vesicles. Further studies into KD-STK16 revealed a complex role in regulation of basolaterally secreted proteins with a not-yet understood mechanism. These studies indicate that MAL2 functions in various pathways as a general regulator of protein sorting, and provides novel proof of MAL2's involvement in the secretory pathway.

DISCUSSION

We began the studies in part I with the intention of studying the role of MAL2 in lipid-dependent transcytotic sorting at the early endosome. However, the observation that endogenous MAL2 redistributed to the Golgi in pIgA-R overexpressing cells and was “chased” to the apical membrane along with the receptor led us to examine whether MAL2 also functions in plasma membrane delivery from the Golgi. Our studies in Clone 9 cells and WIF-B cells with MAL2 expression knocked down revealed that MAL2 selectively mediates transport of pIgA-R from the Golgi to the plasma membrane. Thus, MAL2 regulates multiple steps of pIgA-R’s cellular itinerary.

MAL2 and overexpressed pIgA-R selectively colocalize and coimmunoprecipitate

Overexpression of pIgA-R led to the remarkable redistribution of MAL2 into nearly all of the compartments occupied by the receptor, only the diffuse ER-like pIgA-R staining pattern was not observed for MAL2. This near perfect colocalization at steady state and during “chase” with cycloheximide suggests the proteins interact directly, and this was confirmed with coimmunoprecipitations. Only the mature form of pIgA-R coimmunoprecipitated with MAL2; DPPIV was not recovered. We determined that ~1% of total pIgA-R coimmunoprecipitated with MAL2 consistent with results from MDCK cells where only 0.7-2% of MAL coimmunoprecipitated with overexpressed HA (Tall *et al.* 2003). These results suggest that MAL2-pIgA-R interactions are likely weak, transient or indirect. Because MAL2 has been shown to bind members of the TPD52 family of proteins (Wilson *et al.* 2001; Boutros *et al.* 2004), and because these proteins have been implicated in Ca²⁺-dependent regulation of pancreatic apical secretion

(Grobowski *et al.* 1996, 1999; Kaspar *et al.* 2003), we favor the latter possibility.

We are currently identifying MAL2 binding partners to further examine MAL2 interactions with pIgA-R and other apical proteins.

A new role for MAL2: selective regulation at the TGN

To test whether MAL2 selectively regulated transport from the TGN to the Golgi, we examined pIgA-R and DPPIV dynamics in nonpolarized WIF-B cells, Clone 9 cells, and in polarized WIF-B cells where MAL2 expression was knocked down. In nonpolarized WIF-B cells, apical proteins recycle between the plasma membrane and an intracellular compartment that contains only other apical residents. We have rigorously characterized this so-called “apical compartment” and determined that it contains only other apical proteins; markers for recycling endosomes, early endosomes, lysosomes, late endosomes, Golgi and basolateral membranes are excluded (Nyasae *et al.* 2003; Tuma *et al.* 2002). In this study, we further determined that MAL2 is present in this apical compartment.

In Clone 9 cells, we previously determined that DPPIV is present in an analogous “apical compartment” and displays similar recycling properties (Nyasae *et al.* 2003; Tuma *et al.* 2002). Surprisingly, and unlike DPPIV, pIgA-R distributed only to the Golgi in Clone 9 cells in the absence of MAL2 expression. Similarly, in WIF-B cells where MAL2 expression was knocked down, pIgA-R distributed predominantly to the Golgi. In contrast, when MAL2 was coexpressed in Clone 9 cells, pIgA-R distributed from the Golgi into the MAL2 positive apical compartment after traversing the plasma membrane.

Thus, in MAL2 coexpressing cells, pIgA-R was delivered to the apical compartment and recycled between it and the cell surface. When surface delivery was measured in cycloheximide-treated cells, we further determined that MAL2 coexpression was required for pIgA-R delivery from the Golgi to the plasma membrane. These results were confirmed in polarized WIF-B cells where MAL2 expression was knocked down. Together these results indicate that MAL2 selectively regulates pIgA-R Golgi exit.

In 2002, de Marco and colleagues established that MAL2 is a regulator of hepatic transcytosis (de Marco *et al.* 2002). By using antisense oligonucleotides, they showed that MAL2 knockdown resulted in a block in transport from early endosomes to SAC of both pIgA and the GPI-anchored protein, CD59. Similarly, transcytosis of DPPIV in WIF-B cells lacking MAL2 expression was impaired. However, our finding that pIgA-R basolateral delivery is impaired in complete MAL2 knockdown WIF-B cells is not consistent with the HepG2 studies. If MAL2 knockdown also impairs pIgA-R basolateral delivery in HepG2 cells, the expectation is that there would be no receptor present to internalize the added ligand. One possible explanation is that the block in Golgi exit was not complete in the MAL2 knockdown HepG2 cells allowing some pIgA-R basolateral delivery. This is consistent with our findings that in cells with partial MAL2 knockdown, some pIgA-R is basolaterally delivered and internalized. Differences in approach i.e., monitoring the receptor directly (in WIF-B cells) vs. the ligand (in HepG2 cells) may also explain these disparate results. Another possibility is that there are cell type differences in MAL2 regulation of pIgA-R trafficking. Clearly, further research is needed to define

the role(s) of MAL2 in apical targeting not only in hepatic cells, but also in other polarized epithelial cell types.

Our results together with results from HepG2 cells (de Marco *et al.* 2002) suggest that MAL2 can regulate at least two steps in the itinerary of pIgA-R: transcytotic delivery from the early endosome to the SAC and delivery from the TGN to the basolateral membrane. Interestingly, a highly related family member, MAL, has been found to regulate the itineraries of apical proteins at two transport steps in MDCK cells: direct delivery from the TGN to the apical membrane and apical internalization (Martin-Belmonte *et al.* 2000, 2003). Thus, MAL family members are likely multifunctional proteins, and we predicted at the time that the list of transport steps that these proteins regulate in the itineraries of apical proteins would expand as further study continues. This prediction has been shown to be correct from the studies presented in part II of this dissertation.

Novel MAL2 binding partners: a functional genomic approach

In part II, we assayed for novel MAL2 interactors using a split-ubiquitin yeast-2 hybrid system. As previously detailed, this approach optimizes for protein interactions between membrane bound proteins, providing a more physiologically functional system than a traditional yeast-2 hybrid. The known functions of the novel interactors are briefly described in Table 2 of part II. Interestingly, a number of polytopic, twelve-transmembrane (12-TM) spanning transporters were identified. In general, these types of transporters are directly delivered to their resident plasma membrane domain. Basolateral membrane transporters contain basolateral targeting signals which are

necessary for proper distribution (Gu *et al.* 2001). From our findings with pIgA-R (part I), it is possible that MAL2 mediates interactions with the basolateral targeting signal at the TGN. Apical membrane transporters are not delivered via the transcytotic pathway, like other apical resident proteins. Instead, the apical transporters are delivered directly from the TGN to the apical membrane. The mechanisms of apical transporter delivery are not fully understood. Interactions with PDZ-containing proteins and with radixin (of the ezrin/radixin/moesin family of actin-binding proteins) may play a role in the targeting of apical transporters (Nies and Keppler, 2007). Similar to our understanding of other apical proteins, the targeting motif for apical transporters is not a specific amino acid sequence. Likely, targeting is conferred upon interactions with several regulators. Based on our previous results and the presence of apical transporters in the Y2H screen, MAL2 may play a role in targeting from the TGN to the apical membrane. Confirmation of this hypothesis, along with a specific mechanism for delivery is yet another fertile area of MAL2 research.

MAL2 was also found to interact with several ER resident proteins. Although there is no evidence of MAL2 function at the ER, others have shown that MAL2 interacts with the ER localized formin, informin2 (Madrid *et al.* 2010). These authors proposed that the interaction of MAL2 and informin 2, along with several Ras-related proteins, is needed to regulate apical membrane polarity. Interestingly, this suggests that MAL2 has yet another functional role in polarized membrane trafficking. Although the mechanism for how this may contribute to the establishment and maintenance of polarity is not fully

understood, characterising the ER resident proteins that we found and their relationship with MAL2 may shed light on the current mystery.

The Y2H also pulled down a predicted interactor, Rab17. The Rab GTPase family is composed of peripheral membrane proteins which likely regulate every step in membrane trafficking. Unlike most of the other Rab family members which have a more ubiquitous expression, Rab17 is only expressed in polarized epithelial cells of the kidney, liver and intestine (Lutcke *et al.* 1993). Since it was previously shown that Rab17 is an essential regulator of the transcytotic pathway in polarized cells (Hunziker and Peters, 1998; Zacchi *et al.* 1998), we predicted it would interact with MAL2, also a known regulator in the transcytotic pathway (de Marco *et al.* 2002; de Marco *et al.* 2006; In and Tuma, 2010). We are currently examining Rab17 and MAL2 interactions and the mechanism(s) by which they regulate transcytosis.

Serine/threonine kinase 16: a novel MAL2 interactor

We became interested in a novel interactor of unknown function, serine/threonine kinase 16 (STK16). First identified in 1998, STK16 is the first mammalian member of a new serine/threonine kinase family that is not closely related to other known serine/threonine kinases (Ligos *et al.* 1998; Stairs *et al.* 1998). STK16 belongs to the Numb-associated kinase (NAK) family which also includes family members adaptor-associated kinase 1 (AAK1), cyclin G-associated kinase (GAK) and BMP-2-inducible kinase (BIKE) (Manning *et al.* 2002; Eswaran *et al.* 2008). The NAK family contains a conserved atypical activation segment which includes an alpha-helical segment known as

the activation segment C-terminal helix (ASCH). The physiological function of the ASCH region is not yet understood.

Overexpression of STK16 led to the minimal codistribution of MAL2 at the basolateral membrane. However, MAL2 did not redistribute to the Golgi, where STK16 was most prevalent. The interaction between MAL2 and STK16 was confirmed with coimmunoprecipitations. We found that ~1.25% of STK16 coimmunoprecipitated with MAL2, consistent with our co-IP results from part I. Likely, the low levels of co-IP reflect the minimal codistribution of MAL2 and STK16 at the basolateral membrane. In contrast, KD-STK16 distributed to peripheral puncta. The results using various treatments (brefeldin A, 19°C block and post-block trafficking) suggested that the KD-STK16 puncta are post-Golgi compartments. Overexpression of KD-STK16 did not change MAL2's distribution at the apical membrane. The lack of colocalization was reflected in the lack of co-IP between MAL2 and KD-STK16. A possible explanation is that the interaction between MAL2 and STK16 is dependent on the constitutive kinase activity of STK16.

While testing for various Golgi, endosomal and lysosomal markers in KD-STK16 overexpressing cells to determine the identity of the peripheral puncta, we found that the distribution of syntaxin 6 (a TGN SNARE protein) was altered in the cells expressing KD-STK16. Syntaxin 6 redistributed from the TGN to a disperse post-Golgi pattern. It is not clear why KD-STK16 overexpression changed the distribution of syntaxin 6. However, it has previously been found that syntaxin 6 functions in the retrograde endosome-TGN trafficking. Inhibition of the endosome-TGN trafficking route led to an

accumulation of syntaxin 6 in peripheral puncta that did not contain any known endosomal marker (Otto *et al.* 2010), strikingly similar to the KD-STK16 peripheral puncta. Further testing on KD-STK16's effect on syntaxin 6 is needed to clarify if syntaxin 6 is involved in regulating the secretory pathway as well.

Though the identity of the KD-STK16 puncta remains elusive, we determined that the wild type form, STK16, is an itinerant protein, traversing the Golgi and the basolateral membrane. Using brefeldin A (BFA), which inhibits anterograde transport from the ER to the Golgi and promotes retrograde protein transport back to the ER (Fujiwara *et al.* 1988), we found that STK16 redistributed to the ER (as expected) but mainly to the basolateral membrane (compared to untreated cells). This suggests that a population of STK16 at steady state resides in a post-Golgi compartment which can traffic to the basolateral membrane.

A new role for MAL2: regulation of the secretory pathway

We initially immunolabeled for albumin (a secretory hepatic protein found at the Golgi) in KD-STK16 overexpressing cells to determine if the Golgi remained intact. Instead we found that the expression of albumin and haptoglobin (a secretory hepatic protein found at the Golgi) was diminished in cells expressing KD-STK16. We hypothesized that KD-STK16 expression was causing either 1) hypersecretion or 2) degradation of the proteins. If the proteins were being hypersecreted, it is possible that STK16 and MAL2 function as brakes to secretion, allowing for regulation at the TGN. Overexpression of STK16 had no effect on secretion compared to control, uninfected

cells. In contrast, KD-STK16 overexpression decreased the secretion levels but did not affect the immature forms of the secretory proteins. We determined that KD-STK16 does not cause hypersecretion and also does not affect the synthesis of the proteins. Interestingly, MAL2 knockdown showed a similar decrease in secretion levels to KD-STK16 expression. This further confirms the interaction between MAL2 and STK16 but also indicates the importance of both proteins in the secretory pathway.

The decrease in secretion suggested that albumin is rerouted for degradation in KD-STK16 expressing cells. In KD-STK16 expressing cells treated with ammonium chloride, albumin expression increased over time, suggesting albumin was rerouted to the lysosomes. However, treatment with lactacystin (LAC), a potent, irreversible proteasome inhibitor, resulted in a further decrease of albumin expression in the cells and in albumin secretion. We found that LAC treatment also resulted in increased KD-STK16 expression. This suggests that KD-STK16 undergoes proteasomal degradation. It is possible that KD-STK16 is misfolded or that the presence of the mutant protein is detrimental to the cell. Either possibility would result in removal of the protein in order to ensure cellular integrity. Inhibition of the proteasome results in the increased expression of KD-STK16, causing rerouting of albumin from the secretory to the lysosomal degradative pathway.

Our results indicate that MAL2 regulates yet another pathway in polarized hepatic cells: secretory delivery from the TGN to the basolateral membrane. While this suggests a novel function for MAL2, it has been a previously suggested function for STK16. In 2005, Stairs and colleagues found that overexpression of the wild type STK16 in

mammary glands of pubescent female mice led to the aggravated mammary end-bud formation at the ends of primary ducts (Stairs *et al.* 2005). The authors suggested that STK16 may be required for proper secretion and hypothesized that STK16-deficient mice may have a lactation defect. Additionally, an Y2H screen with STK16 as bait found it interacts with N-acetylglucosamine kinase (NAGK). Although *in vitro* kinase assays showed that NAGK is not a direct substrate of STK16, the assays showed that NAGK negatively regulates STK16 activity. Based on previous research, there are three points to emphasise: 1) N-acetylglucosamine (GlcNAc) is phosphorylated by NAGK and functions in the salvage pathway of lysosomal degradation (Berger *et al.* 2002), 2) most GlcNAc-modified proteins are secreted, and 3) STK16 and NAGK were shown to be interactors (Ligos *et al.* 2002). Taken together, Ligos and colleagues suggested that STK16 is involved in the secretory pathway, where it is negatively regulated by NAGK. This suggestion is fully consistent with our results. Taken together with our findings on MAL2-mediated pIgA-R delivery, we predict that MAL2 functions as a general regulator whose specificity in targeting is conferred by the cargo proteins or by an intermediary, such as STK16.

What is the basis of binding selectivity for MAL2?

One possible selective mechanism is that the different cytoplasmic sequences on various apical cargos promote different interactions with MAL2. The 103 amino acid pIgA-R cytoplasmic domain encodes multiple known targeting signals that mediate its delivery to the basolateral membrane and basolateral internalization, that stimulate

transcytosis and prevent lysosomal degradation (Tuma and Hubbard, 2003). In contrast, DPPIV and HA encode short, cytoplasmic tails (6 or 12 amino acids, respectively) that contain no known targeting information. Interestingly, when MAL was overexpressed in WIF-B cells (that lack endogenous MAL), HA and DPPIV were rerouted to the apical membrane via the direct route whereas indirect pIgA-R sorting was not altered (Ramnarayanan *et al.* 2007). We proposed at the time that the basolateral targeting information in the pIgA-R cytoplasmic domain was dominant thereby preventing interactions with MAL and eluding redirection. An exciting possibility is that the basolateral targeting information is dominant because it mediates interactions (directly or indirectly) with MAL2 at the Golgi.

In contrast, constitutively secreted proteins are not thought to contain specific targeting signals. However, there is evidence that constitutive secretion requires a certain level of regulation at the TGN. One theory states that secretory proteins are ‘captured’ or bind to TGN membranes on the luminal face. The association with the TGN sorts these proteins away from regulated secretory proteins (Lara-Lemus *et al.* 2006). Additionally, in 2000, Wang and colleagues found that cholesterol depletion inhibited both regulated and constitutive secretion (Wang *et al.* 2000). They showed that protein synthesis and ER to Golgi transport was not affected, and that the block was occurring at the TGN. Similarly, it was previously found that cholesterol depletion blocked transcytosis of all cohorts of apical proteins (Nyasae *et al.* 2003), which led to the initiation of our studies by proposing MAL2 as a cholesterol-dependent regulator of trafficking. Studies from our lab have shown that MAL2 distribution is cholesterol-dependent, thus, the impaired

secretion (Wang *et al.* 2000) may be explained by loss of MAL2 localization. Taken together, these results suggest that MAL2 may be involved in stabilization or lipid-mediated sorting of constitutively secreted from regulated secretory proteins.

MAL2: one protein, many functions

Our working model for which steps of apical protein trafficking that MAL2 regulates has further expanded. As shown in Figure 26, there are at least 3 pathways in which MAL2 has been suggested to function. Our lab and others established its role in transcytosis (de Marco *et al.* 2002, 2006; In and Tuma, 2010). We further found that MAL2 selectively participates in TGN to basolateral membrane delivery (In and Tuma, 2010). Our most recent results suggest that MAL2 also regulates secretory proteins away from the degradative pathway. How does MAL2 function in so many disparate pathways? As stated above and in Figure 27, it is an exciting possibility that the various accessory factors which interact with MAL2 confer targeting specificity. Further characterisation of the 19 novel MAL2 interactors will help elucidate the mechanisms behind specific sorting and targeting and perhaps will expand the functions of MAL2 beyond our current understanding.

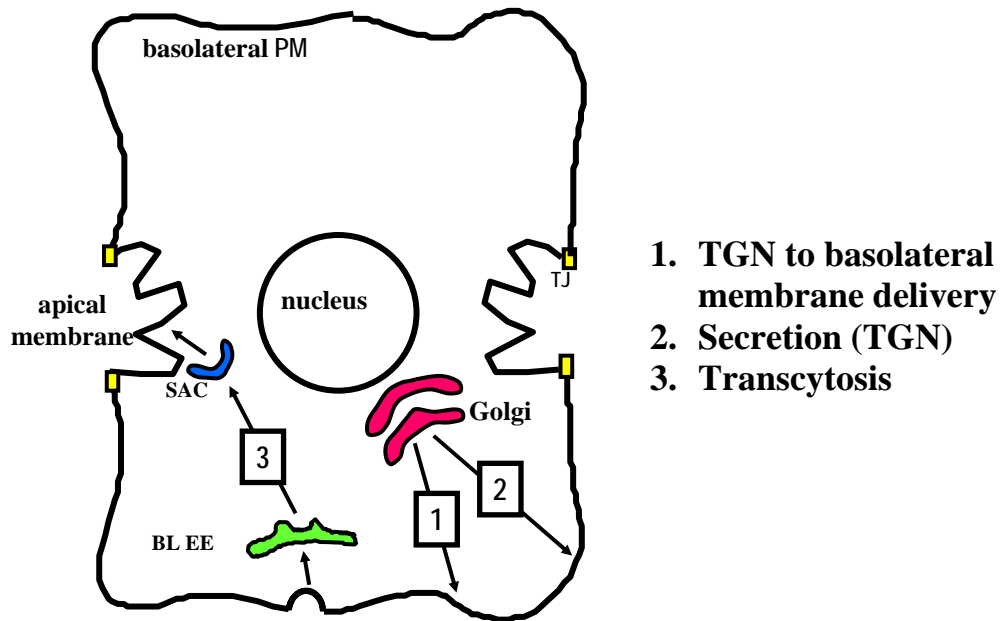


Figure 26. Our working model for MAL2-mediated protein sorting. MAL2 is functioning in at least three pathways: 1) Selective TGN to basolateral membrane delivery (pIgA-R), 2) regulation of the secretory pathway away from the degradative pathway (albumin and haptoglobin), and 3) regulation of the transcytotic pathway (apical cargo proteins).

Possible mechanisms of MAL2-mediated sorting

The mechanisms by which MAL2 specifically sorts various cargo proteins still remain a mystery. As shown in Figure 27, in our predicted model, MAL2 associates with cargo proteins at various organelles. They are then packaged into specific vesicles depending on their location (i.e. TGN, early endosome). Accessory factors and/or coat proteins may be recruited to the vesicles. Since MAL2 can associate with a variety of cargo proteins in various pathways, we believe that the different accessory factors are what confer targeting specificity. Based on our data and others: 1) STK16 is possibly the accessory factor of MAL2 which allows for specific targeting of albumin and haptoglobin to the basolateral membrane for secretion, 2) Rab17 is likely the accessory factor which

confers specific targeting in the transcytotic pathway, and 3) TPD52, which is involved in apical delivery in pancreatic acinar cells (Thomas *et al.* 2004) which is a known interactor of MAL2, may regulate direct delivery of apical proteins. As shown in both parts I and II, removal of MAL2 or its accessory factor results in the loss of targeting specificity and the accumulation of the cargo protein at an earlier step in its trafficking route (pIgA-R) or rerouting to degradation (albumin).

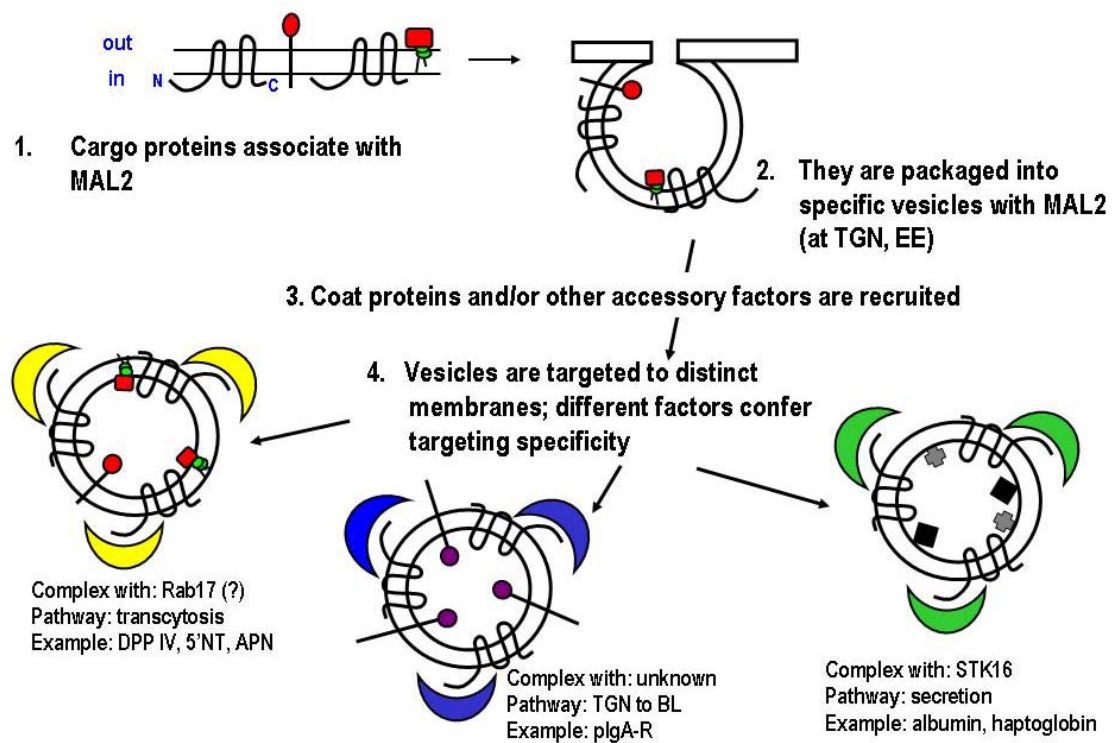


Figure 27. Possible role of MAL2 in protein sorting. MAL2 associates with a variety of cargo proteins and is packaged into specific vesicles. The different accessory factors which interact with MAL2 confer targeting specificity. Removal of MAL2 or its interactor causes the loss of targeting specificity, resulting in accumulation at an earlier step in trafficking or rerouting to degradation.

How does MAL2 interact with the specific accessory factor? Others have suggested that MAL2 is N-glycosylated, perhaps because N-glycosylation is postulated to

be an active apical sorting signal (Vagin *et al.* 2009). But, data from our lab has shown that MAL2 is not N-glycosylated (data not shown), ruling out that possibility. However, O-glycosylation is also suggested to be an important factor for surface delivery (Proszynski *et al.* 2004). It is unknown if MAL2 is O-glycosylated or undergoes other post-translational modifications. For example, since STK16 is a constitutively active kinase, it may be necessary to phosphorylate MAL2. Similarly, TPD52, a known MAL2 binding partner, is only active when phosphorylated. Phosphorylation of TPD52 correlates with increased apical secretion in acinar cells (Kaspar *et al.* 2003; Thomas *et al.* 2004). The mechanisms of interaction and delivery between MAL2, the various factors and the cargo proteins remain an open and quite exciting field of research.

Implications of MAL2 and cancer

The results from parts I and II of this dissertation have shown that knockdown of MAL2 leads to mislocalisation or trafficking defects in various pathways. In contrast, overexpression of MAL2 results in the mislocalisation of MUC1, a known binding partner and a tumour associated protein (Fanayan *et al.* 2009). Although the molecular mechanisms leading to the mislocalisation of the different cargo proteins is not yet understood, it is likely related to aberrant expression of MAL2. MAL2 is likely involved in multiple trafficking pathways, thus, overexpression can lead to random binding of MAL2 to accessory factors at incorrect locations, while knockdown of MAL2 halts regulation and specific trafficking. We hypothesize that MAL2 is an essential component of multiple trafficking pathways in epithelial cells that must be tightly controlled to ensure proper polarity maintenance and growth.

REFERENCES

- Adler AS, Lin M, Horlings H, Nuyten DS, van de Vijver MJ, Chang HY. 2006. Genetic regulators of large-scale transcriptional signatures in cancer. *Nat Genet.* 38:421-430.
- Alberts, B., A. Johnson, J. Lewis, M. Raff, K. Roberts, and P. Walter. 2002. *Molecular Biology of the Cell*. Garland Science, New York, NY.
- Alonso, M.A., and S.M. Weissman. 1987. cDNA cloning and sequence of MAL, a hydrophobic protein associated with human T-cell differentiation. *PNAS.* 84:1997-2001.
- Ang, A.L., Taguchi, T., Francis, S., Fölsch, H., Murrells, L.J., Pypaert, M., Warren, G., and I. Mellman. 2004. Recycling endosomes can serve as intermediates during transport from the Golgi to the plasma membrane of MDCK cells. *J Cell Biol.* 167:531-543.
- Anton, O., Batista, A., Millan, J., Andres-Delgado, L., Puertollano, R., Correas, I., and M.A. Alonso. 2008. An essential role for the MAL protein in targeting Lck to the plasma membrane of human T lymphocytes. *J Exp Med.* 205:3201-3213.
- Apodaca, G., Bomsel, M., Arden, J., Breitfeld, P.P., Tang, K. and K.E. Mostov. 1991. The polymeric immunoglobulin receptor. A model protein to study transcytosis. *J Clin Invest.* 87:1877-1882.
- Apodaca, G., Katz, L.A., and K.E. Mostov. 1994. Receptor-mediated transcytosis of IgA in MDCK cells is via apical recycling endosomes. *J Cell Biol.* 125:67-86.
- Aroeti, B. Kosen, P.A., Kuntz, I.D., Cohen, F.E., and K.E. Mostov. 1993. Mutational and secondary structural analysis of the basolateral sorting signaling of the polymeric immunoglobulin receptor. *J Cell Biol.* 123:1149-1160.
- Arthur, C.P., and M.H. Stowell. 2007. Structure of synaptophysin: a hexameric MARVEL-domain channel protein. *Structure.* 15:707-714.
- Balkovetz, D.F., Pollack, A.L., and K.E. Mostov. 1997. Hepatocyte growth factor alters the polarity of Madin-Darby canine kidney cell monolayers. *J Biol Chem.* 272:3471-3477.
- Barr, V.A., and A.L. Hubbard. 1993. Newly synthesized hepatocyte plasma membrane proteins are transported in transcytotic vesicles in the bile duct-ligated rat. *Gastroenterol.* 105:554-571

- Barr, V.A., Scott, L.J., and A.L. Hubbard. 1995. Immunoadsorption of hepatic vesicles carrying newly synthesized dipeptidyl peptidase IV and polymeric IgA receptor. *J Biol Chem.* 270:27834-27844.
- Bartles, J.R., Braiterman, L.T., and A.L. Hubbard. 1985. Endogenous and exogenous markers of the rat hepatocyte plasma membrane. *J Cell Biol.* 100:1126-1138.
- Bartles, J.R., Feracci, H.M., Stieger, B., and A.L. Hubbard. 1987. Biogenesis of the rat hepatocyte plasma membrane in vivo: comparison of the pathways taken by apical and basolateral proteins using subcellular fractionation. *J Cell Biol.* 105:1241-1251.
- Bello-Morales, R., de Marco, M.C., Aranda, J.F., Matesanz, F., Alcina, A., and J.A. Lopez-Guerrero. 2009. Characterization of the MAL2-positive compartment in oligodendrocytes. *Exp Cell Res.* 315:3453-3465.
- Bender, V., Bravo, P., Decaens, C., and D. Cassio. 1999. The structural and functional polarity of the hepatic human/rat hybrid WIF-B is a stable and dominant trait. *Hepatology.* 30:1002-1010.
- Berger, M., Chen, H., Reutter, W., and S. Hinderlich. 2002. Structure and function of N-acetylglucosamine kinase. Identification of two active site cysteines. *Eur J Biochem.* 269:4212-4218.
- Bosse, F., Hasse, B., Pippirs, U., Greiner-Petter, R., and H.W. Müller. 2003. Proteolipid plasmalipin: localization in polarized cells, regulated expression and lipid raft association in CNS and PNS myelin. *J Neurochem.* 86:508-518.
- Boutros, R., Fanayan, S., Shehata, M., and J.A. Byrne. 2004. The tumor protein D52 family: many pieces, many puzzles. *Biochem Biophys Res Commun.* 325:1115-1121.
- Braet, F., D. Luo, I. Spector, D. vermijlen, and E. Wisse. 2001. Endothelial and Pit Cells. *In The Liver: biology and pathobiology.* I.M. Arias, J.L. Boyer, F.V. Chisari, N. Fausto, D. Schachter, and D.A. Shafritz, editors. Lippincott Williams & Wilkins, Philadelphia, PA.
- Braiterman, L.T., and A.L. Hubbard. 2009. Hepatocyte surface polarity: its dynamic maintenance and establishment. *In The Liver: biology and pathobiology.* I.M. Arias, editor. John Wiley & Sons, Chichester, UK.
- Bravo, P., Bender, V., and D. Cassio. 1998. Efficient in vitro vectorial transport of a fluorescent conjugated bile acid analogue by polarized hepatic hybrid WIF-B and WIF-B9 cells. *Hepatology.* 27:5776-583.

- Brown, D.A., Crise, B., and J.K. Rose. 1989. Mechanism of membrane anchoring affects polarized expression of two proteins in MDCK cells. *Science*. 245:1499-1501.
- Bryant, D.M., and K.E. Mostov. 2008. From cells to organs: building polarized tissue. *Nat Rev Mol Cell Biol*. 9:887-901.
- Bryant, D.M., Datta, A., Rodríguez-Fraticelli, A.E., Peränen, J., Martín-Belmonte, F., and K.E. Mostov. 2010. A molecular network for de novo generation of the apical surface and lumen. *Nat Cell Biol*. 12:1035-1045.
- Byrne, J.A., Mattei, M., and P. Basset. 1996. Definition of the tumor protein D52 (TPD52) gene family through cloning of D52 homologues in human (D53) and mouse (mD52). *Genomics*. 35:523-532.
- Byrne, J.A., Mattei, M., Basset, P., and P. Gunning. 1998. Identification and in situ hybridization mapping of a mouse Tpd52l1 (D53) orthologue to chromosome 10A4-B2. *Cytogen Cell Gen*. 81:199-201.
- Byrne, J.A., Nourse, C., Basset, P., and P. Gunning. 1998. Identification of homo- and heteromeric interactions between members of the breast carcinoma-associated D52 protein family using the yeast two-hybrid system. *Oncogene*. 16:873-881.
- Byrne, J.A., Maleki, S., Hardy, J.R., Gloss, B.S., Murali, R., Scurry, J.P., Fanayan, S., Emmanuel, C., Hacker, N.F., Sutherland, R.L., DeFazio, A., and P.M. O'Brien. 2010. MAL2 and tumor protein D52 (TPD52) are frequently overexpressed in ovarian carcinoma, but differentially associated with histological subtype and patient outcome. *BMC Cancer*. 10:497-507.
- Caduff, J., Sansano, S., Bonnet, A., Suter, U., and N. Schaeren-Wiemers. 2001. Characterization of GFP-MAL expression and incorporation in rafts. *Micros Res Techniq*. 52:645-655.
- Cancino, J., Torrealba, C., Soza, A., Yuseff, M.I., Gravotta, D., Henklein, P., Rodriguez-Boulan, E., and A. González. 2007. Antibody to AP1B adaptor blocks biosynthetic and recycling routes of basolateral proteins at recycling endosomes. *Mol Biol Cell*. 18:4872-4884.
- Carmosino, M., Rizzo, F., Procino, G., Basco, D., Valenti, G., Forbush, B., Schaeren-Wiemers, N., Caplan, M.J., and M. Svelto. 2010. MAL/VIP17, a new player in the regulation of NKCC2 in the kidney. *Mol Biol Cell*. 21:3985-3997.
- Carmosino, M., Valenti, G., Caplan, M.J., and M. Svelto. 2010. Polarized traffic towards the cell surface: how to find the route. *Biol Cell*. 102:75-91.

Casanova, J.E., Breitfeld, P.P., Ross, S.A., and K.E. Mostov. 1990. Phosphorylation of the polymeric immunoglobulin receptor required for its efficient transcytosis. *Science*. 248:742-745.

Casanova, J.E., Apodaca, G., and K.E. Mostov. 1991. An autonomous signal for basolateral sorting in the cytoplasmic domain of the polymeric immunoglobulin receptor. *Cell*. 66:65-75.

Chen, Y., Zheng, B., Robbins, D.H., Lewin, D.N., Mikhitarian, K., Graham, A., Rumpp, L., Glenn, T., Gillanders, W.E., Cole, D.J., Lu, X., Hoffman, B.J., and M. Mitas. 2007. Accurate discrimination of pancreatic ductal adenocarcinoma and chronic pancreatitis using multimarker expression data and samples obtained by minimally invasive fine needle aspiration. *Int J Cancer*. 120:1511-1517.

Cheong, K.H., Zacchetti, D., Schneeberger, E.E., and K. Simons. 1999. VIP17/MAL, a lipid raft-associated protein, is involved in apical transport in MDCK cells. *PNAS*. 96:6241-6248.

Chew, C.S., Chen, X., Zhang, H., Berg, E.A., and H. Zhang. 2008. Calcium/calmodulin-dependent phosphorylation of tumor protein D52 on serine residue 136 may be mediated by CAMK2delta6. *Am J Physiol Gastrointest Liver Physiol*. 295:G1159-G1172.

Cochary, E.F., Bizzozero, O.A., Sapirstein, V.S., Nolan, C.E., and I. Fischer. 1990. Presence of the plasma membrane proteolipid (plasmolipin) in myelin. *J Neurochem*. 55:602-610.

Cresawn, K.O., Potter, B.A., Oztan, A., Guerriero, C.J., Ihrke, G., Goldenring, J.R., Apodaca, G., and O.A. Weisz. 2007. Differential involvement of endocytic compartments in the biosynthetic traffic of apical proteins. *EMBO J*. 26:3737-3748.

De Marco, M.C., Kremer, L., Albar, J.P., Martinez-Menarguez, J.A., Ballesta, J., Garcia-Lopez, M.A., Marazuela, M., Puertollano, R., and M.A. Alonso. 2001. BENE, a novel raft-associated protein of the MAL proteolipid family, interacts with caveolin-1 in human endothelial-like ECV304 cells. *J Biol Chem*. 276:23009-23017.

De Marco, M.C., Martin-Belmonte, F., Kremer, L., Albar, J.P., Correias, I., Vaerman, J.P., Marazuela, M., Byrne, J.A., and M.A. Alonso. 2002. MAL2, a novel raft protein of the MAL family, is an essential component of the machinery for transcytosis in hepatoma HepG2 cells. *J Cell Biol*. 159:37-44.

De Marco, M.C., Puertollano, R., Martinez-Menarguez, J., and M.A. Alonso. 2006. Dynamics of MAL2 during glycosylphosphatidylinositol-anchored protein transcytotic transport to the apical surface of hepatoma HepG2 cells. *Traffic*. 7:61-73.

Deborde, S., Perret, E., Gravotta, D., Deora, A., Salvarezza, S., Schreiner, R., and E. Rodriguez-Boulan. 2008. Clathrin is a key regulator of basolateral polarity. *Nature*. 452:719-723.

Decaens, C., Durand, M., Grosse, B., and D. Cassio. 2008. Which in vitro models could be best used to study hepatocyte polarity? *Biol Cell*. 100: 387-398.

Delacour, D., Gouyer, V., Zanetta, J.P., Drobecq, H., Leteurtre, E., Grard G., Moreau-Hannedouche, O., Maes, E., Pons, A., André, S., Le Bivic, A., Gabius, H.J., Manninen, A., Simons, K., and G. Huet. 2005. Galectin-4 and sulfatides in apical membrane trafficking in enterocyte-like cells. *J Cell Biol*. 169:491-501.

Delacour, D., and R. Jacob. 2006. Apical protein transport. *CMLS*. 63:2491-2505.

Delacour, D., Greb, C., Koch, A., Salomonsson, E., Leffler, H., Le Bivic, A., and R. Jacob. 2007. Apical sorting by galectin-3-dependent glycoprotein clustering. *Traffic*. 8:379-388.

Duncan, S.A. 2003. Mechanisms controlling early development of the liver. *Mech Dev*. 120:19-33.

Enrich, C. Apodaca, G., and K.E. Mostov. 1996. Calmodulin regulates the intracellular trafficking in epithelial cells. *Z Gastroenterol*. 34:83-85.

Estrada, B., Maeland, A.D., Gisselbrecht, S.S., Bloor, J.W., Brown, N.H., and A.M. Michelson. 2007. The MARVEL domain protein, Singles Bar, is required for progression past the pre-fusion complex stage of myoblast fusion. *Dev Biol*. 307:328-339.

Eswaran, J., Bernad, A., Ligos, J.M., Guinea, B., Debreczeni, J.E., Sobott, F., Parker, S.A., Najmanovich, R., Turk, B.E., and S. Knapp. 2008. Structure of the human protein kinase MPSK1 reveals an atypical activation loop architecture. *Structure*. 16:115-124.

Fanayan, S., Shehata, M., Agterof, A.P., McGuckin, M.A., Alonso, M.A., and J.A. Byrne. 2009. Mucin 1 (MUC1) is a novel partner for MAL2 in breast carcinoma cells. *BMC Cell Biol*. 10:7-19.

Feracci, H.M., Connolly, T.P., Margolis, R.N., and A.L. Hubbard. 1987. The establishment of hepatocyte cell surface polarity during fetal liver development. *Developmental Biology*. 123:73-84.

Folgueira, M.A., Carraro, D.M., Brentani, H., Patrão, D.F., Barbosa, E.M., Netto, M.M., Caldeira, J.R., Katayama, M.L., Soares, F.A., Oliveira, C.T., Reis, L.F., Kaiano, J.H., Camargo, L.P., Vêncio, R.Z., Snitcovsky, I.M., Makdissi, F.B., e Silva, P.J., Góes, J.C., and M.M. Brentani. 2005. Gene expression profile associated with response to doxorubicin-based therapy in breast cancer. *Clin Cancer Res.* 11:7434-7443.

Frank, M. 2000. MAL, a proteolipid in glycosphingolipid enriched domains: functional implications in myelin and beyond. *Prog Neurobiol.* 60:531-544.

Frank, M., Atanasoski, S., Sancho, S., Magyar, J.P., Rüllicke, T., Schwab, M.E., and U. Suter. 2000. Progressive segregation of unmyelinated axons in peripheral nerves, myelin alterations in the CNS, and cyst formation in the kidneys of myelin and lymphocyte protein –overexpressing mice. *J Neurochem.* 75:1927-1939.

Fraser, R., Dobbs, B.R., and G. W. Rogers. 1995. Lipoproteins and the liver sieve: the role of the fenestrated sinusoidal endothelium in lipoprotein metabolism, atherosclerosis, and cirrhosis. *Hepatology.* 21:863-874.

Fujiwara, T., Oda, K., Yokota, S., Takatsuki, A., and Y. Ikehara. 1988. Brefeldin A causes disassembly of the Golgi complex and accumulation of secretory proteins in the endoplasmic reticulum. *J Biol Chem.* 263:18545-18552.

Gao, B., Jeong, W., and Z. Tian. 2008. Liver: an organ with predominant innate immunity. *Hepatology.* 47:729-736.

Gillen, C., Gleichmann, M., Greiner-Petter, R., Zoidl, G., Kupfer, S., Bosse, F., Auer, J., and H.W. Müller. 1996. Full-length cloning, expression and cellular localization of rat plasmalogen mRNA, a proteolipid of PNS and CNS. *Eur J Neuro.* 8:405-414.

Golachowska, M.R., Hoekstra, D., and S.C. van Ijzendoorn. 2010. Recycling endosomes in apical plasma membrane domain formation and epithelial cell polarity. *Trends Cell Biol.* 20:618-626.

Gonzalez, A., and E. Rodriguez-Boulán. 2009. Clathrin and AP1B: key roles in basolateral trafficking through trans-endosomal routes. *FEBS Lett.* 583:3784-3795.

Groblewski, G.E., Wishart, M.J., Yoshida, M., and J.A. Williams. 1996. Purification and identification of a 28-kDa calcium-regulated heat-stable protein. A novel secretagogue-regulated phosphoprotein in exocrine pancreas. *J Biol Chem.* 271:31502-31507.

Groblewski, G.E., Yoshida, M., Yao, H., Williams, J.A., and S.A. Ernst. 1999. Immunolocalization of CRHSP28 in exocrine digestive glands and gastrointestinal tissues of the rat. *Am J Physiol.* 276:G219-G226.

Grønberg M, Pavlos NJ, Brunk I, Chua JJ, Münster-Wandowski A, Riedel D, Ahnert-Hilger G, Urlaub H, Jahn R. 2010. Quantitative comparison of glutamatergic and GABAergic synaptic vesicles unveils selectivity for few proteins including MAL2, a novel synaptic vesicle protein. *J Neurosci.* 30:2-12.

Gu, H.H., Wu, X., Giros, B., Caron, M.G., Caplan, M.J., and G. Rudnick. 2001. The NH(2)-terminus of norepinephrine transporter contains a basolateral localization signal for epithelial cells. *Mol Biol Cell.* 12:3797-3807.

Guerriero, C.J., Lai, Y., and O.A. Weisz. 2008. Differential sorting and Golgi export requirements for raft-associated and raft-independent apical proteins along the biosynthetic pathway. *J Biol Chem.* 283:18040-18047.

Guinea, B., Ligos, J.M., Laín de Lera, T., Martín-Caballero, J., Flores, J., Gonzalez de la Peña, M., García-Castro, J., and A. Bernad. 2006. Nucleocytoplasmic shuttling of STK16 (PKL12), a Golgi-resident serine/threonine kinase involved in VEGF expression regulation. *Exp Cell Res.* 312:135-144.

Hatta, M., Nagai, H., Okino, K., Onda, M., Yoneyama, K., Ohta, Y., Nakayama, H., Araki, T., and M. Emi. 2004. Down-regulation of members of glycolipid-enriched membrane raft gene family, MAL and BENE, in cervical squamous cell cancers. *J Obstet Gynaecol Res.* 30:53-58.

Hemery, I., Durand-Schneider, A.M., Feldmann, G., Vaerman, J.P., and M. Maurice. 1996. The transcytotic pathway of an apical plasma membrane protein (B10) in hepatocytes is similar to that of IgA and occurs via a tubular pericentriolar compartment. *J Cell Sci.* 109:1215-1227.

Hoekstra, D., Tyteca, D., and S.C. van Ijzendoorn. 2004. The subapical compartment: a traffic center in membrane polarity development. *J Cell Sci.* 117:2183-2192.

Hollingsworth, M.A., and B.J. Swanson. 2004. Mucins in cancer: protection and control of the cell surface. *Nat Rev Cancer.* 4:45-60.

Horne, H.N., Lee, P.S., Murphy, S.K., Alonso, M.A., Olson, J.A. Jr, and J.R. Marks. 2009. Inactivation of the MAL gene in breast cancer is a common event that predicts benefit from adjuvant chemotherapy. *Mol Cancer Res.* 7:199-209.

Hsi, E.D., Sup, S.J., Alemany, C., Tso, E., Skacel, M., Elson, P., Alonso, M.A., and B. Pohlman. 2006. MAL is expressed in a subset of Hodgkin lymphoma and identifies a population of patients with poor prognosis. *Am J Clin Pathol.* 125:776-782.

Hua, W., Sheff, D., Toomre, D., and I. Mellman. 2006. Vectorial insertion of apical and basolateral membrane proteins in polarized epithelial cells revealed by quantitative 3D live cell imaging. *J Cell Biol.* 172:1035-1044.

Hubbard, A.L., Bartles, J.R., and L.T. Braiterman. 1985. Identification of rat hepatocyte plasma membrane proteins using monoclonal antibodies. *J Cell Biol.* 100:1115-1125.

Hunziker, W., and P.J. Peters. 1998. Rab17 localizes to recycling endosomes and regulates receptor-mediated transcytosis in epithelial cells. *J Biol Chem.* 273:15734-15741.

Ihrke, G., Neufeld, E.B., Meads, T., Shanks, M.R., Cassio, D., Laurent, M., Schroer, T.A., Pagano, R.E., and A.L. Hubbard. 1993. WIF-B cells: an *in vitro* model for studies of hepatocyte polarity. *J Cell Biol.* 123:1761-1775.

Ihrke, G., Martin, G.V., Shanks, M.R., Schrader, M., Schroer, T.A., and A.L. Hubbard. 1998. Apical plasma membrane proteins and endolyn-78 travel through a subapical compartment in polarized WIF-B hepatocytes. *J Cell Biol.* 141:115-133.

Ikonen, E., and K. Simons. 1998. Protein and lipid sorting from the *trans*-Golgi network to the plasma membrane in polarized cells. *Sem Cell Dev Biol.* 9:503-509.

In, J.G., and P.L. Tuma. 2010. MAL2 selectively regulates polymeric IgA receptor delivery from the Golgi to the plasma membrane in WIF-B cells. *Traffic.* 11:1056-1066.

Jacob, R., and H.Y., Naim. 2001. Apical membrane proteins are transported in distinct vesicular carriers. *Curr Biol.* 11:1444-1450.

Kaspar, K.M., Thomas, D.D., Taft, W.B., Takeshita, E., Weng, N., and G.E. Groblewski. 2003. CaM kinase II regulation of CRHSP-28 phosphorylation in cultured mucosal T84 cells. *Am J Physiol Gastrointest Liver Physiol.* 285:G1300-109.

Kim, T., Fiedler, K., Madison, D.L., Krueger, W.H., and S.E. Pfeiffer. 1995. Cloning and characterization of MVP17: a developmentally regulated myelin protein in oligodendrocytes. *J Neurosci Res.* 42:413-422.

Kipp, H., and I.M. Arias. 2002. Trafficking of canalicular ABC transporters in hepatocytes. *Annu Rev Physiol.* 64:595-608.

Kuntz, E., and H.-D. Kuntz. 2008. Hepatology: Textbook and Atlas. Springer-Verlag, New York, NY.

Lara-Lemus, R., Liu, M., Turner, M.D., Scherer, P., Stenbeck, G., Iyengar, P., and P. Arvan. 2006. Lumenal protein sorting to the constitutive secretory pathway of a regulated secretory cell. *J Cell Sci.* 119:1833-1842.

Lazarevich, N.L., Cheremnova, O.A., Varga, E.V., Ovchinnikov, D.A., Kudrjavitseva, E.I., Morozova, O.V., Fleishman, D.I., Engelhardt, N.V., and S.A. Duncan. 2004. Progression of HCC in mice is associated with a downregulation in the expression of hepatocyte nuclear factors. *Hepatology.* 39:1038-1047.

Leyt, J., Melamed-Book, N., Vaerman, J.P., Cohen, S., Weiss, A.M., and B. Aroeti. 2007. Cholesterol-sensitive modulation of transcytosis. *Mol Biol Cell.* 18:2057-2071.

Ligos, J.M., Gerwin, N., Fernández, P., Gutierrez-Ramos, J.C., and A. Bernad. 1998. Cloning, expression analysis, and functional characterization of PKL12, a member of a new subfamily of ser/thr kinases. *Biochem Biophys Res Commun.* 249:380-384.

Ligos, J.M., de Lera, T.L., Hinderlich, S., Guinea, B., Sánchez, L., Roca, R., Valencia, A., and A. Bernad. 2002. Functional interaction between the Ser/Thr kinase PKL12 and N-acetylglucosamine kinase, a prominent enzyme implicated in the salvage pathway for GlcNAc recycling. *J Biol Chem.* 277:6333-6343.

Lind, G.E., Ahlquist, T., Kolberg, M., Berg, M., Eknaes, M., Alonso, M.A., Kallioniemi, A., Meling, G.I., Skotheim, R.I., Rognum, T.O., Thiis-Evensen, E., and R.A. Lothe. 2008. Hypermethylated MAL gene - a silent marker of early colon tumorigenesis. *J Transl Med.* 6:13-23.

Lisanti, M.P., Caras, I.W., Davitz, M.A., and E. Rodriguez-Boulton. 1989. A glycosphospholipid membrane anchor acts as an apical targeting signal in polarized epithelial cells. *J Cell Biol.* 109:2145-2156.

Llorente, A., de Marco, M.C., and M.A. Alonso. 2004. Caveolin-1 and MAL are located on prostasomes secreted by the prostate cancer PC-3 cell line. *J Cell Sci.* 117:5343-5351.

Low, S.H., Miura, M., Roche, P.A., Valdez, A.C., Mostov, K.E., and T. Weimbs. 2000. Intracellular redirection of plasma membrane trafficking after loss of epithelial cell polarity. *Mol Biol Cell.* 11:3045-3060.

Luo, D.Z., Vermijlen D, Ahishali B, Triantis V, Plakoutsi G, Braet F, Vanderkerken K, and E. Wisse. 2000. On the cell biology of pit cells, the liver-specific NK cells. *World J Gastroenterol.* 6:1-11.

Lütcke, A., Jansson, S., Parton, R.G., Chavrier, P., Valencia, A., Huber, L.A., Lehtonen, E., and M. Zerial. 1993. Rab17, a novel small GTPase, is specific for epithelial cells and is induced during cell polarization. *J Cell Biol.* 121:553-564.

Luton, F., Cardone, M.H., Zhang, M., and K.E. Mostov. 1998. Role of tyrosine phosphorylation in ligand-induced regulation of transcytosis of the polymeric Ig receptor. *Mol Biol Cell.* 9:1787-1802.

Luton, F., and K.E. Mostov. 1999. Transduction of basolateral-to-apical signals across epithelial cells: ligand-stimulated transcytosis of the polymeric immunoglobulin receptor requires two signals. *Mol Biol Cell.* 10:1409-1427.

Luton, F., Verges, M., Vaerman, J.P., Sudol, M., and K.E. Mostov. 1999. The SRC family protein tyrosine kinase p62yes controls polymeric IgA transcytosis in vivo. *Mol Biol Cell.* 4:627-632.

Luton, F., Hexham, M.J., Zhang, M., and K.E. Mostov. 2009. Identification of a cytoplasmic signal for apical transcytosis. *Traffic.* 10:1128-1142.

Madrid, R., Aranda, J.F., Rodriguez-Fraticelli, A.E., Ventimiglia, L., Andres-Delgado, L., Shehata, M., Fanayan, S., Shahheydari, H., Gomez, S., Jimenez, A., Martin-Belmonte, F., Byrne, J.A., and M.A. Alonso. 2010. The formin INF2 regulates basolateral-to-apical transcytosis and lumen formation in association with Cdc42 and MAL2. *Dev Cell.* 18:814-827.

Magal, L.G., Yaffe, Y., Shepshelovich, J., Aranda, J.F., de Marco, M.C., Gaus, K., Alonso, M.A., and K. Hirschberg. 2009. Clustering and lateral concentration of raft lipids by the MAL protein. *Mol Biol Cell.* 20:3751-3762.

Magyar, J., Ebensperger, C., Shaeren-Wiemers, N., and U. Suter. 1997. Myelin and lymphocyte protein (MAL/MVP17/VIP17) and plasmolipin are members of an extended gene family. *Gene.* 189:269-275.

Manning, G., Whyte, D.B., Martinez, R., Hunter, T., and S. Sudarsanam. 2002. The protein kinase complement of the human genome. *Science.* 298:1912-1934

Marazuela, M., Acevedo, A., Adrados, M., García-López, M.A., and M.A. Alonso. 2003. Expression of MAL, an integral protein component of the machinery for raft-mediated pical transport, in human epithelia. *J Histochem Cytochem.* 51:665-674.

Marazuela, M. and M.A. Alonso. 2004. Expression of MAL and MAL2, two elements of the protein machinery for raft-mediated transport, in normal and neoplastic human tissue. *Histol Histopathol.* 19:925-933.

Marazuela, M., Acevedo, A., García-López, M.A., Adrados, M., de Marco, M.C., and M.A. Alonso. 2004. Expression of MAL2, an integral protein component of the machinery for basolateral-to-apical transcytosis, in human epithelia. *J Histochem Cytochem.* 52:243-252.

Marazuela, M., Martín-Belmonte, F., García-López, M.A., Aranda, J.F., de Marco, M.C., and M.A. Alonso. 2004. Expression and distribution of MAL2, an essential element of the machinery for basolateral-to-apical transcytosis, in human thyroid epithelial cells. *Endocrinology.* 145:1011-1016.

Martin-Belmonte, F., Kremer, L., Albar, J.P., Marazuela, M., and M.A. Alonso. 1998. Expression of the MAL gene in the thyroid: the MAL proteolipid, a component of glycolipid-enriched membranes, is apically distributed in thyroid follicles. *Endocrinology.* 139:2077-2084.

Martin-Belmonte, F., Puertollano, R., Millan, J., and M.A. Alonso. 2000. The MAL Proteolipid Is Necessary for the Overall Apical Delivery of Membrane Proteins in the Polarized Epithelial Madin–Darby Canine Kidney and Fischer Rat Thyroid Cell Lines. *Mol Biol Cell.* 11:2033-2045.

Martin-Belmonte, F., Arvan, P., and M.A., Alonso. 2001. MAL mediates apical transport of secretory proteins in polarized epithelial Madin-Darby canine kidney cells. *J Biol Chem.* 276:49337-49342.

Martin-Belmonte, F., Martinez-Menarguez, J.A., Aranda, J.F., Ballesta, J., de Marco, M.C., and M.A. Alonso. 2003. MAL regulates clathrin-mediated endocytosis at the apical surface of Madin-Darby canine kidney cells. *J Cell Biol.* 163:155-164.

Martin-Belmonte, F., Gassama, A., Datta, A., Yu, W., Rescher, U., Gerke, V., and K.E. Mostov. 2007. PTEN-mediated apical segregation of phosphoinositides controls epithelial morphogenesis through Cdc42. *Cell.* 128:383-397.

Martin-Belmonte, F., and K.E. Mostov. 2008. Regulation of cell polarity during epithelial morphogenesis. *Curr Opin Cell Biol.* 20:227-234.

Mellman, I., and W.J. Nelson. 2008. Coordinated protein sorting, targeting and distribution in polarized cells. *Nat Rev Mol Cell Biol.* 9:833-845.

McCuskey, R., 2006. Sinusoidal endothelial cells as an early target for hepatic toxicants. *Clinical Hemorheology and Microcirculation.* 34:5-10.

Millan, J., Puertollano, R., Fan, L., Rancano, C., and M.A. Alonso. 1997. The MAL proteolipid is a component of the detergent-insoluble membrane subdomains of human T-lymphocytes. *The Biochem J.* 321:247-252.

- Millan, J., Puertollano, R., Fan, L., and M.A. Alonso. 1997. Caveolin and MAL, two protein components of internal detergent-insoluble membranes, are in distinct lipid microenvironments in MDCK cells. *Biochem Biophys Res Commun.* 233:707-712.
- Millan, J. and M.A. Alonso. 1998. MAL, a novel integral membrane protein of human T lymphocytes, associates with glycosylphosphatidylinositol-anchored proteins and Src-like tyrosine kinases. *Eur J Immuno.* 28:3675-3684.
- Mimori, K., Shiraishi, T., Mashino, K., Sonoda, H., Yamashita, K., Yoshinaga, K., Masuda, T., Utsunomiya, T., Alonso, M.A., Inoue, H., and M. Mori. 2003. MAL gene expression in esophageal cancer suppresses motility, invasion and tumorigenicity and enhances apoptosis through the Fas pathway. *Oncogene.* 22:3463-3471.
- Mostov, K.E., Su, T., and M. ter Beest. 2003. Polarized epithelial membrane traffic: conservation and plasticity. *Nat Cell Biol.* 5:287-293.
- Nejsum, L.N., and W.J. Nelson. 2007. A molecular mechanism directly linking E-cadherin adhesion to initiation of epithelial cell surface polarity. *J Cell Biol.* 178:323-335.
- Nelson, W.J., and C. Yeaman. 2001. Protein trafficking in the exocytic pathway of polarized epithelial cells. *Trends Cell Biol.* 11:483-486.
- Nies, A.T., and D. Keppler. 2007. The apical conjugate efflux pump ABCC2 (MRP2). *Pflugers Arch.* 453:643-659.
- Nyasae, L.K., Hubbard, A.L. and P.L. Tuma. 2003. Transcytotic efflux from early endosomes is dependent on cholesterol and glycosphingolipids in polarized hepatic cells. *Mol Biol Cell.* 14:2689-2705.
- Otto, G.P., Razi, M., Morvan, J., Stenner, F., and S.A. Tooze. 2010. A novel syntaxin 6-interacting protein, SHIP164, regulates syntaxin 6-dependent sorting from early endosomes. *Traffic.* 11:688-705.
- Overmeer, R.M., Henken, F.E., Bierkens, M., Wilting, S.M., Timmerman, I., Meijer, C.J., Snijders, P.J., and R.D. Steenbergen. 2009. Repression of MAL tumour suppressor activity by promoter methylation during cervical carcinogenesis. *J Pathol.* 219:327-336.
- Paladino, S., Sarnataro, D., Pillich, R., Tivodar, S., Nitsch, L., and C. Zurzolo. 2004. Protein oligomerization modulates raft partitioning and apical sorting of GPI-anchored proteins. *J Cell Biol.* 167:699-709.

Paladino, S., Pocard, T., Catino, M.A., and C. Zurzolo. 2006. GPI-anchored proteins are directly targeted to the apical surface in fully polarized MDCK cells. *J Cell Biol.* 172:1023-1034.

Parviz, F., Matullo, C., Garrison, W.D., Savatski, L., Adamson, J.W., Ning, G., Kaestner, K.H., Rossi, J.M., Zaret, K.S., and S.A. Duncan. 2003. Hepatocyte nuclear factor 4alpha controls the development of a hepatic epithelium and liver morphogenesis. *Nat Genet.* 34:292-296.

Perez, P., Puertollano, R., and M.A. Alonso. 1997. Structural and biochemical similarities reveal a family of proteins related to the MAL proteolipid, a component of detergent-insoluble membrane microdomains. *Biochem Biophys Res Commun.* 232:618-621.

Potter, B.A., Ihrke, G., Bruns, J.R., Weixel, K.M., and O.A. Weisz. 2004. Specific N-glycans direct apical delivery of transmembrane, but not soluble or glycosylphosphatidylinositol-anchored forms of endolyn in Madin-Darby canine kidney cells. *Mol Biol Cell.* 15:1407-1416.

Potter, B.A., Hughey, R.P., and O.A. Weisz. 2006. Role of N- and O-glycans in polarized biosynthetic sorting. *Am J Physiol Cell Physiol.* 290:C1-C10.

Potter, B.A., Weixel, K.M., Bruns, J.R., Ihrke, G., and O.A. Weisz. 2006. N-glycans mediate apical recycling of the sialomucin endolyn in polarized MDCK cells. *Traffic.* 7:146-154.

Proszynski, T.J., Simons, K., and M. Bagnat. 2004. O-glycosylation as a sorting determinant for cell surface delivery in yeast. *Mol Biol Cell.* 15:1533-43.

Puertollano, R., Li, S., Lisanti, M.P., and M.A. Alonso. 1997. Recombinant expression of the MAL proteolipid, a component of glycolipid-enriched membrane microdomains, induces the formation of vesicular structures in insect cells. *J Biol Chem.* 272:18311-18315.

Puertollano, R., and M.A. Alonso. 1998. A short peptide motif at the carboxyl terminus is required for incorporation of the integral membrane MAL protein to glycolipid-enriched membranes. *J Biol Chem.* 273:12740-12745.

Puertollano, R., and M.A. Alonso. 1999. MAL, an integral element of the apical sorting machinery, is an itinerant protein that cycles between the *trans*-Golgi network and the plasma membrane. *Mol Biol Cell.* 10:3435-3447.

Puertollano, R., Martin-Belmonte, F., Millan, J., de Marco, M.C., Albar, J.P., Kremer, L., and M.A. Alonso. 1999. The MAL proteolipid is necessary for normal apical transport and accurate sorting of the influenza virus hemagglutinin in Madin-Darby canine kidney cells. *J Cell Biol.* 145:141-151.

Puertollano, R., Martinez-Menarguez, J.A., Batista, A., Ballesta, J., and M.A. Alonso. 2001. An intact dilysine-like motif in the carboxyl terminus of MAL is required for normal apical transport of the influenza virus hemagglutinin cargo protein in epithelial Madin-Darby canine kidney cells. *Mol Biol Cell.* 12:1869-1883.

Raleigh, D.R., Marchiando, A.M., Zhang, Y., Shen, L., Sasaki, H., Wang, Y., Long, M., and J.R. Turner. 2010. Tight junction-associated MARVEL proteins marveld3, tricellulin, and occluding have distinct but overlapping functions. *Mol Biol Cell.* 21:1200-1213.

Ramnarayanan, S.P., Cheng, C., Bastaki, M., and P.L. Tuma. 2007. Exogenous MAL reroutes hepatic apical proteins into the direct pathway in WIF-B cells. *Mol Biol Cell.* 18:2707-2715.

Rancano, C., Rubio, T., Correas, I., and M.A. Alonso. 1994. Genomic structure and subcellular localization of MAL, a human T-cell-specific proteolipid protein. *J Biol Chem.* 269:8159-8164.

Renfranz, P.J., and M.C. Beckerle. 2002. Doing (F/L)PPPPs: EVH1 domains and their proline-rich partners in cell polarity and migration. *Curr Opin Cell Biol.* 14:88-103.

Rodriguez-Boulán, E., and A. Gonzalez. 1999. Glycans in post-Golgi apical targeting: sorting signals or structural props? *Trends Cell Biol.* 9:291-294.

Rodriguez-Boulán, E., Kreitzer, G., and A. Müsch. 2005. Organization of vesicular trafficking in epithelia. *Nat Rev Mol Cell Biol.* 6:233-247.

Rohan, S., Tu JJ, Kao J, Mukherjee P, Campagne F, Zhou XK, Hyjek E, Alonso MA, Chen YT. 2006. Gene expression profiling separates chromophobe renal cell carcinoma from oncocytoma and identifies vesicular transport and cell junction proteins as differentially expressed genes. *Clin Cancer Res.* 12:6937-6945.

Sanchez-Pulido, L., Martin-Belmonte, F., Valencia, A., and M.A. Alonso. 2002. MARVEL: a conserved domain involved in membrane apposition events. *Trends Biochem Sci.* 27:599-601.

Sathasivam, P., Bailey, A.M., Crossley, M., and J.A. Byrne. 2001. The role of the coiled-coil motif in interactions mediated by TPD52. *Biochem Biophys Res Commun.* 288:56-61.

Satohisa, S., Chiba, H., Osanai, M., Ohno, S., Kojima, T., Saito, T., and N. Sawada. 2005. Behavior of tight-junction, adherens-junction and cell polarity proteins during HNF-4alpha-induced epithelial polarization. *Exp Cell Res.* 310:66-78.

Shehata, M., Bièche, I., Boutros, R., Weidenhofer, J., Fanayan, S., Spalding, L., Zeps, N., Byth, K., Bright, R.K., Lidereau, R., and J.A. Byrne. 2008. Nonredundant functions for tumor protein D52-like proteins support specific targeting of TPD52. *Clin Cancer Res.* 14:5050-5060.

Shen, L., and J.R. Turner. 2005. Role of epithelial cells in initiation and propagation of intestinal inflammation. Eliminating the static: tight junction dynamics exposed. *Am J Physiol Gastrointest Liver Physiol.* 290:G577-G582.

Shen, L., Weber, C.R., Raleigh, D.R., Yu, D., and J.R. Turner. 2011. Tight junction pore and leak pathways: a dynamic duo. *Annu Rev Physiol.* 73:283-309.

Shivas, J.M., Morrison, H.A., Bilder, D., and A.R. Skop. 2010. Polarity and endocytosis: reciprocal regulation. *Trends Cell Biol.* 20:445-452.

Shrout, J., Yousefzadeh, M., Dodd, A., Kirven, K., Blum, C., Graham, A., Benjamin, K., Hoda, R., Krishna, M., Romano, M., Wallace, M., Garrett-Mayer, E., and M. Mitas. 2008. Beta(2)microglobulin mRNA expression levels are prognostic for lymph node metastasis in colorectal cancer patients. *Br J Cancer.* 98:1999-2005.

Simons, K., and A. Wandering-Ness. 1990. Polarized sorting in epithelia. *Cell.* 62:207-210.

Simons, K. and E. Ikonen. 1997. Functional rafts in cell membranes. *Nature.* 387:569-572.

Song, W., Bomsel, M., Casanova, J.E., Vaerman, J.P., and K.E. Mostov. 1994. Stimulation of transcytosis of the polymeric immunoglobulin receptor by dimeric IgA. *PNAS.* 91:163-166.

Song, W., Apodaca, G., and K.E. Mostov. 1994. Transcytosis of the polymeric immunoglobulin receptor is regulated in multiple intracellular compartments. *J Biol Chem.* 269:29474-29480.

Soto-Gutierrez, A., Navarro-Alvarez, N., and N. Kobayashi. 2010. Hepatocytes. *In* Molecular Pathology of Liver Diseases. S.P.S. Monga, editor. Springer Science, New York, NY.

Stairs, D.B., Perry Gardner, H., Ha, S.I., Copeland, N.G., Gilbert, D.J., Jenkins, N.A., and L.A. Chodosh. 1998. Cloning and characterization of Krct, a member of a novel subfamily of serine/threonine kinases. *Human Mol Genet.* 7:2157-2166.

Stairs, D.B., Notarfrancesco, K.L., and L.A. Chodosh. 2005. The serine/threonine kinase, Krct, affects endbud morphogenesis during murine mammary gland development. *Transgenic Res.* 14:919-940.

Stauffer, T.P., Ahn, S., and T. Meyer. 1998. Receptor-induced transient reduction in plasma membrane PtdIns(4,5)P₂ concentration monitored in living cells. *Curr Biol.* 8:343-346.

Tall, R.D., Alonso, M.A., and M.G. Roth. 2003. Feature of influenza HA required for apical sorting differ from those required for association with DRMs or MAL. *Traffic.* 4:838-849.

Tanimizu, N., Miyajima, A., and K.E. Mostov. 2009. Liver progenitor cells fold up a cell monolayer into a double-layered structure during tubular morphogenesis. *Mol Biol Cell.* 20:2486-2494.

Thomas, D.D., Weng, N., and G.E. Groblewski. 2004. Secretagogue-induced translocation of CRHSP-28 within an early apical endosomal compartment in acinar cells. *Am J Physiol Gastrointest Liver Physiol.* 287:G253-G263.

Thomas, D.D., Frey, C.L., Messenger, C.W., August, B.K., and G.E. Groblewski. 2010. A role for tumor protein TPD52 phosphorylation in endo-membrane trafficking during cytokinesis. *Biochem Biophys Res Commun.* 462:583-587.

Tracey, L., Villuendas, R., Ortiz, P., Dopazo, A., Spiteri, I., Lombardia, L., Rodríguez-Peralto, J.L., Fernández-Herrera, J., Hernández, A., Fraga, J., Dominguez, O., Herrero, J., Alonso, M.A., Dopazo, J., and M.A. Piris. 2002. Identification of genes involved in resistance to interferon-alpha in cutaneous T-cell lymphoma. *Am J Pathol.* 161:1825-1837.

Tuma, P.L., Finnegan, C.M., Yi, J.H., and A.L. Hubbard. 1999. Evidence for apical endocytosis in polarized hepatic cells: phosphoinositide 3-kinase inhibitors lead to the lysosomal accumulation of resident apical plasma membrane proteins. *J Cell Biol.* 145:1089-1102.

Tuma, P.L., Nyasae, L.K., and A.L. Hubbard. 2002. Nonpolarized cells selectively sort apical proteins from cell surface to a novel compartment, but lack apical retention mechanisms. *Mol Biol Cell.* 13:3400-3415.

Tuma, P.L. and A.L. Hubbard. 2003. Transcytosis: crossing cellular barriers. *Physiol Rev.* 83:871-932.

Tyteca, D., van Ijzendoorn, S.C., and D. Hoekstra. 2005. Calmodulin modulates hepatic membrane polarity by protein kinase C-sensitive steps in the basolateral endocytic pathway. *Exp Cell Res.* 310:293-302.

Vagin, O., Kraut, J.A. and G. Sachs. 2009. Role of N-glycosylation in trafficking of apical membrane proteins in epithelia. *Am J Physiol Renal Physiol.* 296:F459-469.

Van der Wouden, J.M., Maier, O., van Ijzendoorn, S.C., and D. Hoekstra. 2003. Membrane dynamics and the regulation of epithelial cell polarity. *Int Rev Cytol.* 226:127-164.

Van Ijzendoorn, S.C., and D. Hoekstra. 1998. (Glyco)sphingolipids are sorted in sub-apical compartments in HepG2 cells: a role for non-Golgi-related intracellular sites in the polarized distribution of (glyco)sphingolipids. *J Cell Biol.* 142:683-696.

Wang, Y., Thiele, C., and W.B. Huttner. 2000. Cholesterol is required for the formation of regulated and constitutive secretory vesicles from the trans-Golgi network. *Traffic.* 1:952-962.

Wakabayashi, Y., Lippincott-Schwartz, J., and I.M. Arias. 2004. Intracellular trafficking of bile salt export pump (ABCB11) in polarized hepatic cells: constitutive cycling between the canalicular membrane and rab11-positive endosomes. *Mol Biol Cell.* 15:3485-3496.

Weimbs, T., Low, S.H., Chapin, S.J., and K.E. Mostov. 1997. Apical targeting in polarized epithelial cells: there's more afloat than rafts. *Trends Cell Biol.* 7:393-399.

Weimbs, T., Low, S.H., Chapin, S.J., Mostov, K.E., Bucher, P., and K. Hofmann. 1997. A conserved domain is present in different families of vesicular fusion proteins: a new superfamily. *PNAS.* 94:3046-3051.

Wilson, S.H., Bailey, A.M., Nourse, C.R., Mattei, M.G., and J.A. Byrne. 2001. Identification of MAL2, a novel member of the mal proteolipid family, though interactions with TPD52-like proteins in the yeast two-hybrid system. *Genomics.* 76:81-88.

Zacchi, P., Stenmark, H., Parton, R.G., Orioli, D., Lim, F., Giner, A., Mellman, I., Zerial, M., and C. Murphy. 1998. Rab17 regulates membrane trafficking through apical recycling endosomes in polarized epithelial cells. *J Cell Biol.* 140:1039-1053.

Zegers, M.M., and D. Hoekstra. 1998. Mechanisms and functional features of polarized membrane traffic in epithelial and hepatic cells. *The Biochem J.* 336:257-269.

Zegers, M.M., O'Brien, L.E., Yu, W., Datta, A., and K.E. Mostov. 2003. Epithelial polarity and tubulogenesis *in vitro*. *Trends Cell Biol.* 13:169-176.